EROSION RATES AND PATTERNS
INFERRED FROM COSMOGENIC $^{10}$BE
IN THE SUSQUEHANNA RIVER BASIN


A Thesis Presented

by

Joanna M. Reuter

to

The Faculty of the Graduate College

of

The University of Vermont


In Partial Fulfillment of the Requirements
for the Degree of Master of Science
Specializing in Geology


May, 2005

Accepted by the Faculty of the Graduate College, The University of Vermont, in partial fulfillment of the requirements for the degree of Master of Science, specializing in Geology.

Thesis Examination Committee:

_____ Advisor
Paul R. Bierman, Ph.D.


_____
Milan J. Pavich, Ph.D.


_____
Donna M. Rizzo, Ph.D.


_____
Beverley C. Wemple, Ph.D.


_____ Chairperson
W. Cully Hession, Ph.D., P.E.


_____ Vice President for
Frances E. Carr, Ph.D.                              Research and Dean
                                                    of the Graduate College

Date: March 11, 2005

## ABSTRACT

I use cosmogenic $^{10}$Be analyses to address both applied and basic science questions regarding rates and patterns of erosion in the 71,250 km$^2$ Susquehanna River Basin of New York, Pennsylvania, and Maryland. Measurements of in situ-produced $^{10}$Be from 88 fluvial sediment samples constrain basin-scale erosion rates on a $10^4$ to $10^5$ year time scale, and four bedrock samples provide ridge-top erosion rates. Sediment samples are from two groups: (1) 60 samples are from small (0.6 to 25 km$^2$), non-glaciated basins underlain by a single lithology; these were selected through geographic information systems (GIS) analysis; (2) 28 samples are from USGS stream gages and represent complex basins of multiple lithologies and varying degrees of present-day land use; some of the USGS basins were glaciated during the Pleistocene.

Erosion rates range from 4 to 54 m/My in the southern, non-glaciated part of the Susquehanna River Basin. The broadest range of erosion rates occurs among the small, GIS-selected basins, but the average erosion rate of this group (16 ± 10 m/My, mean ± standard deviation) is similar to that of the larger USGS basins (14 ± 4 m/My). The erosion rates from the Susquehanna River Basin are consistent with rates from other regions of relatively low relief and tectonic quiescence, as determined through a comparison with more than 360 other basins for which $^{10}$Be data are available worldwide.

My analysis of erosion rate patterns in the Susquehanna River Basin utilized GIS-selected basins to test for relationships between erosion rate, mean basin slope, lithology, and physiographic province. Overall, erosion rate correlates positively with slope ($R^2 = 0.57$), but correlations vary by physiographic province, with progressively weaker relations in a down-basin direction (Appalachian Plateaus, $R^2 = 0.72$; Valley and Ridge, $R^2 = 0.37$; Piedmont, $R^2 = 0$). After accounting for slope, lithology does not appear to affect basin-scale erosion rates, based on comparisons between sandstone and shale basins in the Valley and Ridge.

The relationships established among the small basins lend confidence that the inferred erosion rates for the lithologically complex and human-impacted USGS basins that are not glaciated are robust. However, samples from glaciated basins yield $^{10}$Be concentrations (0.5-1.2 x $10^5$ atoms g$^{-1}$ quartz) that are consistently lower than those for similarly sized basins south of the glacial margin (1.7-4.9 x $10^5$ atoms g$^{-1}$ quartz). This discrepancy results from violation of the steady-state erosion assumption in previously glaciated basins. Thus, data from these basins are not directly interpretable as erosion rates.

USGS basins have sediment yield records that can be compared with $^{10}$Be erosion rates to assess whether background rates of sediment generation are in equilibrium with contemporary sediment yield. These comparisons indicate that contemporary sediment yields exceed $^{10}$Be sediment generation rates by up to an order of magnitude. Sediment yields are particularly high relative to $^{10}$Be sediment generation rates in the agricultural southeastern part of the Susquehanna River Basin.

Extrapolating the $^{10}$Be data to longer time scales allows for an assessment of geomorphic models of landscape change. I infer that the central Appalachian landscape is dynamic, conforming to the models of neither Davis nor Hack. The $^{10}$Be results imply that on a $10^4$ to $10^5$ year time scale, the topography and relief of the Susquehanna landscape are changing as valleys lower faster than ridges and steep slopes erode more quickly than gentle slopes. The spatial patterns of erosion rates suggest that the basin is not in steady state and may be experiencing a transient response to a drainage network perturbation, perhaps one initiated in the Miocene as suggested by other work. These results lend insight into how relief is maintained in a passive margin setting.

grateful for the work and assistance of Bob Finkel and the rest of the Accelerator Mass Spectrometry team at Lawrence Livermore National Laboratory. They provided around-the-clock assistance throughout my weekend at Livermore.

Data analysis and writing benefited from the input of many people, as well. Allen Gellis provided sediment yield data for the Susquehanna Basin. Elizabeth Safran, Mark Johnsson, and Chris Duncan shared data for the global compilation of $^{10}$Be sediment data. The Spring 2004 Surface Process Seminar provided constructive feedback on an early, early draft of the Susquehanna paper. I received helpful input on drafts from Luke Reusser, Eric Butler, Milan Pavich, Cully Hession, Donna Rizzo, Beverley Wemple, and, most of all, Paul Bierman.

I want to thank the faculty, staff, and students of the UVM Geology Department. I'd especially like to recognize my 434 North Street housemates: Eric Butler, Luke Reusser, and Matt Jungers, as well as the short-term residents of this house who proved it really is possible to finish a thesis: Angelo Antignano, Andi Lord, Rena Ford, and Robert Price. Thanks especially to Matt Jungers and Eric Butler for letting me move my office into the hobby and TV room after I gave up on Delehanty.

Special thanks to my parents, Mary and Frank Reuter, for everything.

And, in the usual tradition of reserving the last paragraph for one's significant other, I give my heartfelt thanks to Eric Butler, my best friend. I do not know how I would have finished this thesis without his friendship, humor, support, and cooking. He also gets credit for introducing me to one form of steady-state topography: the scenery of model railroads.

iv

**Chapter 3**

**Chapter 4**

**Chapter 5**

**Appendix A**

CHAPTER 1: INTRODUCTION

The quest to understand the development of landscapes, including controls on erosion and sediment generation, is fundamental to geomorphology. This is neither a new task, nor a simple one. For many years, researchers have sought correlations between erosion and spatial landscape characteristics. Relationships have been identified or hypothesized, for example, between denudation and relief (Ahnert, 1970), sediment yield, precipitation, and vegetation (Langbein and Schumm, 1958), lithology and topography (Hack, 1960), and climate and tectonics (Montgomery et al., 2001; Molnar, 2003).

The research presented in this thesis continues the quest to understand rates and patterns of erosion, drawing upon two tools: cosmogenic nuclide and geographic information systems (GIS) analysis. Cosmogenic $^{10}$Be in fluvial sediment serves as a proxy for erosion rates that are averaged over multi-millennial time scales, while spatial scales correspond to the size of the sampled drainage basins. GIS analysis complements the $^{10}$Be data by providing a means to quantify the characteristics of the drainage basins. With GIS, metrics can be calculated to characterize topography, climate, vegetation, tectonics, and geology. Using these tools, I explored relationships between long-term erosion rates, as inferred from cosmogenic $^{10}$Be, and GIS-measurable components of the present-day landscape.

### *Background*

Estimates of contemporary erosion rates have been based on sediment yield data (e.g., Dole and Stabler, 1909), reservoir sedimentation (e.g., Langbein and Schumm, 1958), and small-area sediment traps (e.g., Gellis et al., 2004b). Such data are often

limited in length of record (years to decades) and may be confounded by land use signals

and episodic sediment delivery (Meade, 1969; Trimble, 1977; Kirchner et al., 2001).

Thermochronologic methods, such as fission track and (U-Th)/He thermochronometry,

also provide information about exhumation rates, but such results generally address much

longer time scales ($10^6$-$10^8$ years). $^{10}$Be-derived sediment-generation rates provide a

complementary data set for an intermediate ($10^3$-$10^5$ year) time scale (Brown et al., 1995;

Bierman and Steig, 1996; Granger et al., 1996).

$^{10}$Be is produced in quartz near the surface by cosmic-ray bombardment (Lal and

Peters, 1967). In an eroding landscape, grains of quartz function as dosimeters, carrying

isotopic concentrations that reflect their near-surface exposure histories (Bierman et al.,

2001). Rivers collect, transport, and mix grains from various parts of the basin. The

abundance of cosmogenic nuclides in stream sediments reflects the cosmic ray dosing of

rock and soil on slopes and, to varying degrees, dosing during intermittent storage as

material is carried downstream (Bierman and Steig, 1996). The concentration of $^{10}$Be in

river sediment reflects the integrated erosional history of the basin over both space and

time.

Because of their temporal and spatial resolution, erosion rates from $^{10}$Be can be

used to address basic science as well as applied questions. Cosmogenic nuclides are of

particular value in assessing models of landscape evolution, because the erosion rates

inferred from them are averaged over a time scale long enough to be useful for making

inferences about topographic change. From a practical standpoint, $^{10}$Be erosion rates can

be used to put contemporary measurements of sediment yield into perspective (Kirchner

et al., 2001; Schaller et al., 2001; Matmon et al., 2003a); this comparison may reveal the degree to which humans have impacted sediment movement.

### *Motivation and objectives*

The new $^{10}$Be data that are the primary focus of this thesis come from the basin of the Susquehanna River, which drains 71, 250 km$^2$ of New York, Pennsylvania, and Maryland. The Susquehanna River drains the central Appalachians, a decay-phase orogen in a passive margin setting. Developing a better understanding of erosion rates in such a setting can help to address long-standing questions about the longevity of topography after active mountain building has ceased (Ahnert, 1970; Baldwin et al., 2003). The Susquehanna River Basin and the surrounding Appalachian Mountains are also rich in geomorphic history. Both William Morris Davis's geographic cycle and John Hack's dynamic equilibrium have strong ties to the Appalachian landscape, and $^{10}$Be erosion rates can be used to test whether these models of landscape change apply to the mountains where they were proposed (Davis, 1889; Hack, 1960). Finally, there are practical reasons to study the Susquehanna River Basin, which is the largest tributary to Chesapeake Bay. High sediment delivery to the Bay is impacting aquatic ecosystems (Langland and Cronin, 2003). Developing a better understanding of past and present sediment dynamics in the Susquehanna River Basin is important for effective management.

Both the basic science questions regarding models of landscape change and the applied questions regarding Chesapeake Bay sedimentation can be addressed with $^{10}$Be-inferred erosion rates. Motivated by such issues, the objectives of this research were:

- to examine relationships between $^{10}$Be-based erosion rate estimates and landscape characteristics including slope, lithology, and physiographic province;
- to test geomorphic models of landscape change, including Davis's geographical cycle (1899) and Hack's dynamic equilibrium (1960);
- to determine if $^{10}$Be modeled erosion rates for complex basins, including basins with multiple lithologies and basins that have been glaciated, are reasonable and internally consistent;
- to compare long-term rates of sediment generation inferred from $^{10}$Be with short-term rates of sediment yield.

The second component of this thesis is a compilation of $^{10}$Be and GIS data for more than 450 drainage basins from six continents. This analysis was possible because of the accumulation of $^{10}$Be data from sediment over the course of about a decade; indeed, the basins included in this analysis represent all $^{10}$Be measurements from sediment that were available from published and unpublished sources as of summer 2004. GIS analysis provides a consistent approach to an otherwise diverse group of data sets. The objective was to investigate relationships between erosion rates and landscape characteristics within and between geographic regions. This analysis is not the primary focus of my thesis, so results are presented without a great deal of discussion; a paper will be prepared for publication following the completion of this thesis.

*Structure of this thesis*

As this is a journal-style thesis, the core of the thesis consists of two papers to be submitted for publication, and the other chapters provide supporting material. Chapter 2 provides an overview of the methods, though technical details about GIS and data analysis have been relegated to Appendix A. Chapter 3 presents the results of the global data compilation and also serves as the literature review. Chapter 4, the first paper for publication, focuses on the implications of $^{10}$Be results for geomorphic models of landscape change. The second paper, Chapter 5, is longer, contains more detail, and has a more applied focus. It contains a comparison of $^{10}$Be results to sediment yield and an assessment of limitations of $^{10}$Be in a complex drainage basin such as the Susquehanna River Basin. Chapter 6 summarizes the findings of the work in the Susquehanna River Basin, and puts this work in the context of the global data. The final chapter is followed by a comprehensive listing of references cited. Appendix A consists of GIS and data analysis methods in detail; these are written for someone who is trying to repeat the process. Appendix B describes the contents of the accompanying data CD.

This chapter provides an overview of the methods used for the Susquehanna River

Basin research and for the global data compilation. Geographic information systems

(GIS) analysis was integral to all phases of research, from preparing for field work in the

Susquehanna River Basin to analyzing the cosmogenic data for all regions. I also describe

the field and laboratory methods for the Susquehanna River Basin research.

## *GIS analysis*

Spatial analysis with geographic information systems (GIS) is a powerful means

of studying landscapes from a basin-scale perspective. Drainage basin boundaries can be

determined based on digital elevation data. After basins have been delineated, the

characteristics of the basins can be determined. This is accomplished by using the

drainage basin as a cookie cutter on data layers of interest and by obtaining summary

statistics for the data values that fall within the drainage basin. Many types of digital map

data can be summarized. Elevation data can be used to obtain slope and relief grids, for

example, and the mean slope or the total relief can be determined within each drainage

basin. Other examples include lithology, physiography, land cover, and precipitation.

This approach of delineating drainage basins and summarizing characteristics can

be used for both sample selection and data analysis. For the Susquehanna data set, I used

GIS to develop a sampling strategy. I summarized basin characteristics for thousands of

basins, and I developed a sampling strategy based on analysis of the characteristics of

these basins (as explored in more detail in Chapters 4 and 5). For the global compilation

of $^{10}$Be sediment data, I used GIS for data analysis. This allowed for a consistent

approach to basin characterization despite a range of sampling strategies that had been developed and used by different researchers for various reasons.

For detailed information on the GIS procedures, refer to Appendix A.

### *Sample collection*

With Eric Butler as field assistant, I spent approximately two weeks during July and August of 2003 collecting samples in Pennsylvania from the basins that I had selected using GIS. At each site, we acquired a sample of sediment from the active channel. When water was available (as it was in most streams during the wet summer of 2003), we sieved the samples in the field to include the 250-850 micron size fraction. Depending on the quartz content of the sediment, we collected one or two gallon bags of sediment from each basin.

In addition to the sediment samples, we collected four upland bedrock samples, using a hammer and chisel, where opportunities arose. Three of these samples are from a cluster of tors in the Appalachian Plateaus, and one is from a bedrock outcrop in the Valley and Ridge.

### *Lab work*

Standard procedures (http://www.uvm.edu/cosmolab/lab/whatwedo.html; accessed March 2005) were modified slightly for these sediment samples. For each sample, the process involved (at a minimum) wet sieving the samples, drying them, sieving them, etching in 6N hydrochloric acid (two eight-hour etches), etching in 1% hydrofluoric and nitric acid for 8, 14, and 24 hours, performing density separations with LST (a heavy liquid) to sink heavy minerals and float coal, and etching in hydrofluoric

and nitric acid for 48 hours. The wet sieving step involved washing the 250-500 micron fraction in a 250 micron sieve; I added this step to help break up aggregates of grains that remained together during dry sieving. I worked exclusively with the 250-500 micron fraction for sediment samples, largely because this size fraction was the most consistently abundant grain size available in my samples.

Coal was present in many of the samples. Coal is less dense than quartz, so it can be floated off with dilute LST, though sometimes it is difficult to completely eliminate every grain. In some coal rich samples, I did a second LST density separation to adequately clean the samples of coal. One of the earliest samples that I processed (JS19, Susquehanna River at Danville) had more [10]Be than we expected, given that it drains a predominantly glaciated region. My notes indicate that this sample was quite coal rich, and, as it was one of the earliest samples that I processed, I suspect that some residual amount of coal that was not adequately removed from the sample might have contributed to the high [10]Be activity. We will run a replicate of this sample, from which coal has been burned off; however, results are not yet available.

Jennifer Larsen isolated [10]Be according to standard procedures (http://www.uvm.edu/cosmolab/lab/whatwedo.html; accessed March 2005). I traveled to Lawrence Livermore National Laboratory to measure [10]Be using Accelerator Mass Spectrometry. Results were corrected to process blanks run with each batch of 7 samples.

### *Calculation of erosion rates from [10]Be*

I used an accepted interpretative model for calculating erosion rates (Bierman and Steig, 1996) with a sea level, high latitude production rate of 5.2 atoms g$^{-1}$ quartz yr$^{-1}$ and

an attenuation depth of 165 g/cm$^2$. I calculated erosion rates assuming a rock density of 2.7 g/cm$^3$. I did not make minor model corrections for muons, topographic shielding, quartz enrichment (Riebe et al., 2001a), magnetic field variations, or snow cover (Schildgen et al., 2005).

I calculated latitude- and elevation-corrected, basin-wide production rates based on the polynomials from Lal (1991). I applied the polynomials on a pixel-by-pixel basis to calculate the production factor for each pixel according to its elevation and latitude. The basin-wide production factor is a mean of the production factors calculated for each pixel within the basin boundaries. The results are the same as for a hypsometric approach, as commonly applied previously (for example, Matmon et al., 2003b).

For detailed information on the calculation of production rates using GIS, refer to Appendix A.

**CHAPTER 3: GLOBAL COMPILATION OF $^{10}$BE DATA FROM FLUVIAL SEDIMENT**

*Overview*

$^{10}$Be has been measured from sediment from more than 450 drainage basins on six continents (fig. 1). I compiled $^{10}$Be results from published and unpublished sources (table 1) and used GIS analysis, as described in Chapter 2 and Appendix A, to summarize drainage basin characteristics for each sample. The primary goal of this effort is to develop a better understanding of spatial patterns of erosion rates by investigating relationships between $^{10}$Be-derived erosion rates and basin characteristics (topography, climate, tectonics, vegetation, and--to the extent possible--lithology).

The purpose of this chapter is to provide background and to present initial results of this work. In-depth discussion of the results will come when a paper develops out of this work.

*Variables related to erosion*

Over the course of several decades, empirical relationships have been sought between basin-averaged erosion or denudation rates (often based on sediment yield) and variables representing climatic, topographic, vegetative, tectonic, lithologic, pedologic, and anthropogenic factors (e.g., Ahnert, 1970; Walling and Webb, 1983; Summerfield and Hulton, 1994; e.g., Ludwig and Probst, 1998). Broad trends have emerged from these attempts to understand patterns of erosion rates, but there is little consensus regarding the details. Such trends include relationships of erosion rate with topography, climate and hydrology.

Many studies find a topographic variable (such as slope, relief, or elevation) to be either the factor most strongly related to erosion (Ahnert, 1970; Pinet and Souriau, 1988) or one of the most important variables (Jansen and Painter, 1974; Ludwig and Probst, 1998; Syvitski et al., 2003); the cited studies are based on sediment yield data, and they represent broad geographic scales, often incorporating data from several continents. A relationship between erosion rate and relief has also been identified for [10]Be data sets from Europe and the Himalayas (Vance et al., 2003). The nature of the functional relationship is unclear, however. Some results suggest a linear relationship (Ruxton and McDougall, 1967; Ahnert, 1970; Pinet and Souriau, 1988), while other results suggest an exponential relationship (Schumm, 1963; Granger et al., 1996). Complicating matters further, the details of the relationships (such as slope and intercept of regression lines) identified in one study often cannot be compared directly with those of other studies, because the topographic metrics, most commonly relief and slope, have been quantified in a variety of ways. Finally, topographic metrics are not always identified as being among those most strongly related to erosion rates, particularly on intra-regional scales (e.g., Hicks et al., 1996; Bierman et al., in press).

The role of climate, and particularly the role of water, whether the amount of precipitation that enters a basin or the amount that leaves a basin as runoff, remains uncertain. In some cases, relationships have been found between erosion rate and unit runoff (Summerfield and Hulton, 1994; Ludwig and Probst, 1998). Although runoff data are readily available in conjunction with sediment yield measurements, such data are not easily available in general, which makes runoff a less useful variable if the goal is to predict erosion rates from easily obtainable basin characteristics. Although a positive

correlation has been found between erosion rate and unit runoff (Summerfield and Hulton, 1994), relationships between erosion and precipitation tend to be more complex, often showing a peak at moderate amounts of precipitation. Such non-linearity is usually attributed to the protection provided by vegetative cover in regions of higher precipitation (e.g., Fournier, 1949; Langbein and Schumm, 1958). The relationship suggested by Langbein and Schumm has also been called into question, in part because it does not appear to apply within global data sets (Walling and Webb, 1983), and in part because the numerous Langbein and Schumm-style curves that have been fit to various data sets show little overall agreement (Riebe et al., 2001b). Furthermore, some results suggest that seasonality of precipitation matters (Ludwig and Probst, 1998), while others do not (Syvitski et al., 2003).

## *Caveats and limitations regarding the $^{10}$Be data*

The interpretation of $^{10}$Be concentrations as erosion rates relies on a number of assumptions (Bierman and Steig, 1996), and a variety of issues have the potential to reduce the accuracy and precision of the erosion rate interpretations. These include:

- glaciers (Chapter 5, this thesis)

- deep landslides (Riebe et al., 2003; Niemi et al., 2004)

- non-uniform lithology and quartz distribution within basins (Safran et al., in press)

- sediment storage (Clapp et al., 2002)

- grain size (Matmon et al., 2003b)

- quartz enrichment (Riebe et al., 2001a)

- loess deposition (Schaller et al., 2001)

- land use (von Blanckenburg et al., 2004)

- dams (Chapter 5, this thesis)

- samples from small basins representing poorly mixed colluvium rather than alluvium

I recognize that many of these factors substantially impact the quality of the inferred $^{10}$Be erosion rates. Rather than setting an arbitrary cutoff regarding which data give "good" $^{10}$Be erosion rates and which do not, the results that follow present the most complete data set possible, with the exception that some of the smallest basins have been removed for practical, GIS-related reasons.

During the process of compiling these regional data sets, I found a number of inconsistencies and mistakes in various publications. These are documented in Appendix B (data CD). While I have tried my best to minimize the introduction of my own mistakes, these data are still in need of one final, thorough confirmation, so the results presented here should be considered preliminary. Data from the Himalayas (Vance et al., 2003) contain the most substantial remaining discrepancies between published $^{10}$Be erosion rates and the $^{10}$Be erosion rates based on my calculations.

### *Commentary on the figures*

The $^{10}$Be data sets that I compiled (fig. 1, table 1) were collected by numerous researchers who used a variety of different approaches to basin selection. These basins represent a range of spatial scales, with a mean area of about 3,000 km$^2$ and a median of 70 km$^2$ (fig. 2). The diverse approaches to basin selection are reflected in the plots that

show erosion rate against area (fig. 3). Some samples were taken at intervals along a single river's mainstem (e.g., Meuse and Sagavanirktok). Other basin selection strategies placed an emphasis on collecting samples from above and below stream junctions as a way to assess mixing of sediment from tributaries (e.g., Great Smoky Mountains and Rio Puerco). In the Susquehanna River Basin, I selected small basins for desired characteristics (slope, lithology, and physiography) and sampled a set of larger basins based on sediment yield availability.

Many of the plots in figure 3 show that the range of erosion rates decreases with increasing basin area, often such that the average erosion rate of the small basins approximates the large-basin erosion rate. This has been interpreted to mean that sediment mixing is effective (Bierman et al., in press). While not all regions conform exactly to this pattern, in some cases the deviations can be explained. In the data set from Sri Lanka, the larger basins have high apparent erosion rates due to impacts from extreme land use (von Blanckenburg et al., 2004). The points that plot high on the Susquehanna graph were impacted by Pleistocene glaciation, and these $^{10}$Be results do not yield robust erosion rates (Chapter 5, this thesis).

Figures 4 through 10 show relationships between $^{10}$Be erosion rates and basin-scale metrics that represent vegetation, climate, topography, and tectonics. Neither tree cover (fig. 4) nor mean annual precipitation (fig. 5) are correlated with erosion rate. Erosion rate shows a weak correlation with seasonality of precipitation (fig. 6), such that regions with high intra-annual precipitation variability tend to have faster erosion rates than regions in which precipitation is more uniformly distributed during the year. Erosion rate correlates with each of the topographic metrics; these include elevation (fig. 7), relief

14

(fig. 8), and slope (fig. 9). Slope explains less of the variance from the full data set than relief or elevation, but for many regions, slope is the variable that best explains intra-regional variance in erosion rates. Finally, erosion rate correlates with seismic hazard (fig. 10), a proxy for tectonic setting; this relationship explains about half of the variance in the data.

TABLE 1: SUMMARY OF REGIONAL DATA SETS FOR GLOBAL COMPILATION

| Region | Basin or region name | Abbreviation | Source |
|---|---|---|---|
| New Mexico, USA | Rio Puerco | RP | (Bierman et al., in press) |
| Oregon, USA | Oregon Coast Range | OC | (Bierman et al., 2001; Bierman, unpublished data; Heimsath et al., 2001) |
| New York and Pennsylvania, USA | Susquehanna | SQ | (Reuter et al., in preparation) |
| North Carolina and Tennessee, USA | Great Smoky Mountains | SM | (Matmon et al., 2003b) |
| Arizona, USA | Yuma Wash | YU | (Clapp et al., 2002) |
| Texas, USA | Llano Uplift | LL | (Bierman, 1993) |
| Idaho, USA | Idaho | ID | (Kirchner et al., 2001) |
| California, USA | Sierras | SR | (Granger et al., 1996; Riebe et al., 2000) |
| California, USA | California Coast | CA | (Heimsath et al., 1997, 1999) |
| Alaska, USA | Sagavanirktok | AK | (Johnsson, unpublished data) |
| Puerto Rico, USA | Puerto Rico | PR | (Brown et al., 1995; Brown et al., 1998; Riebe et al., 2003) |
| Panama | Panama | PN | (Nichols et al., in press) |
| Venezuela | Apure | VZ | (Johnsson, unpublished data) |
| Namibia | Namibia | NM | (Bierman and Caffee, 2001) |
| Germany | Regen | RG | (Schaller et al., 2001) |
| Germany | Neckar | NC | (Schaller et al., 2001) |
| France, Belgium, Netherlands | Meuse | ME | (Schaller et al., 2001) |
| France | Loire | LO | (Schaller et al., 2001) |
| Germany | Wutach | WU | (Morel et al., 2003) |
| Bhutan | Bhutan | BH | (Duncan, unpublished data) |
| Sri Lanka | Sri Lanka | SL | (Hewawasam et al., 2003) |
| India | Upper Ganges | HM | (Vance et al., 2003) |
| Israel | Nahal Yael | NY | (Clapp et al., 2000) |
| Bolivia | Bolivia | BO | (Safran et al., in press) |
| Australia | Trephina | TR | (Bierman et al., 1998) |
| Australia | Wilpena | WP | (Bierman et al., 1998) |

Figure 1. Location map of regions with basin-scale $^{10}$Be erosion rate estimates.
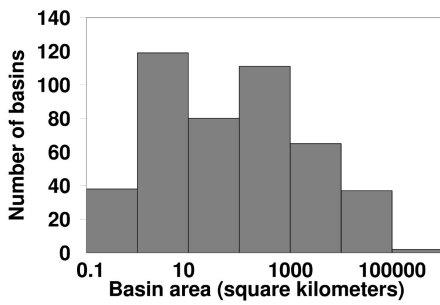


Figure 2. Histogram of basin size for the basins included in the global compilation.

17

18

**Regen**

**Wutach**

**Neckar**

**Meuse**

**Apure**

**Llano Uplift**

**Yuma Wash**

**Oregon Coast Range**

**Sagavanirktok**

19
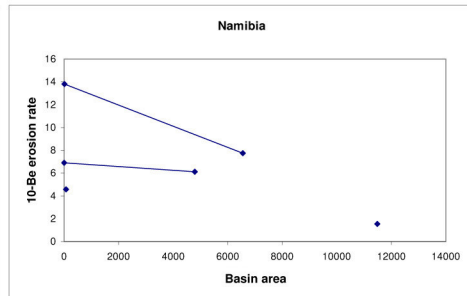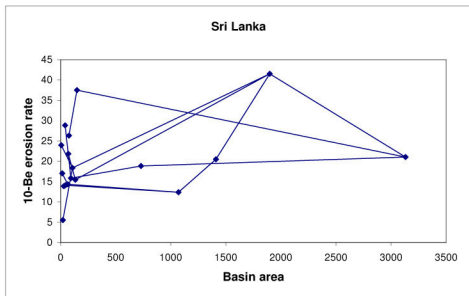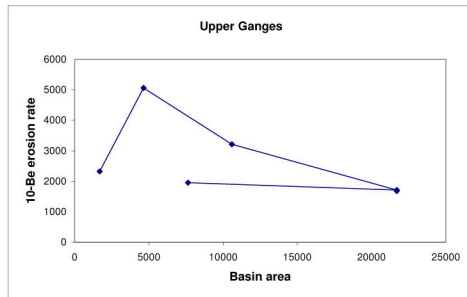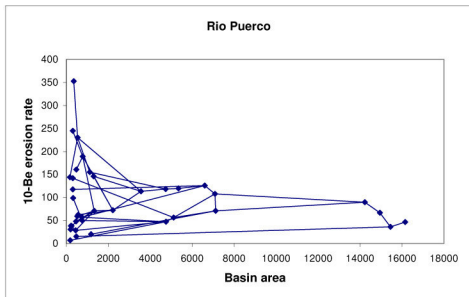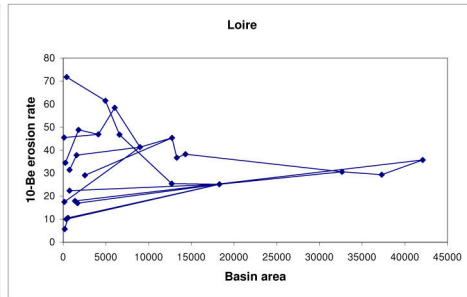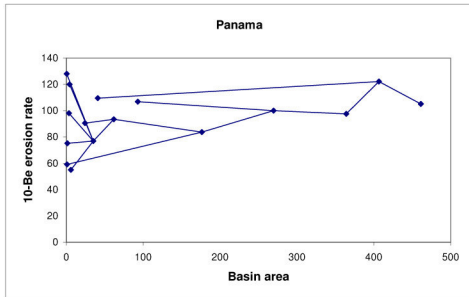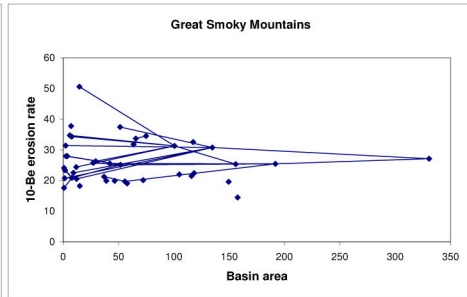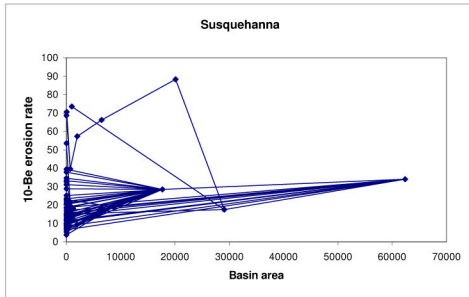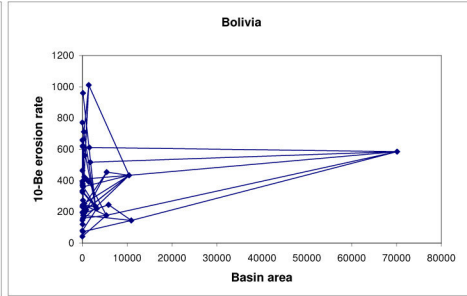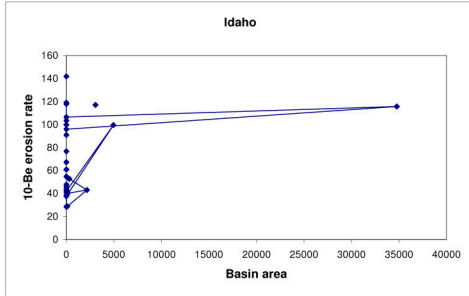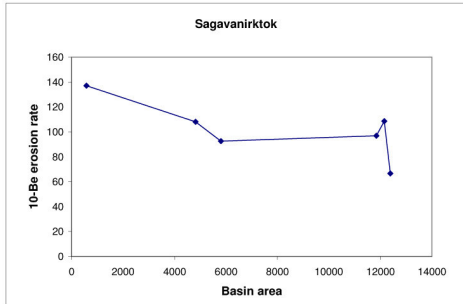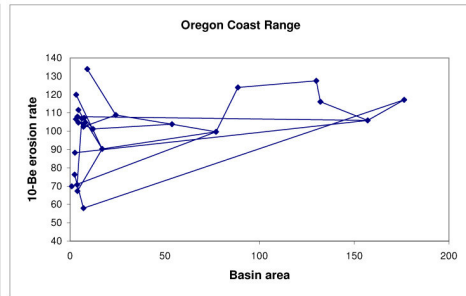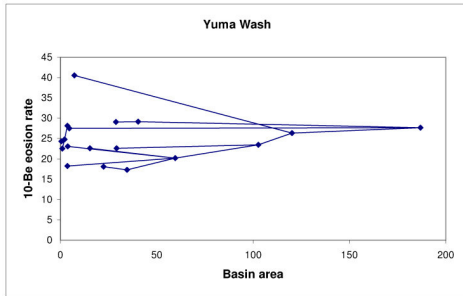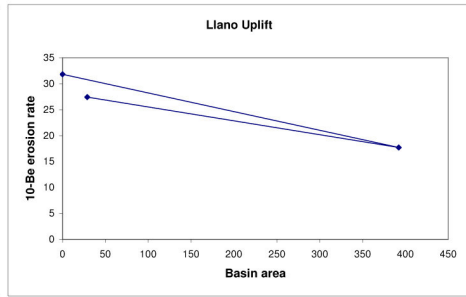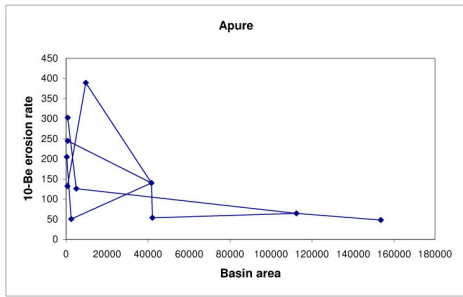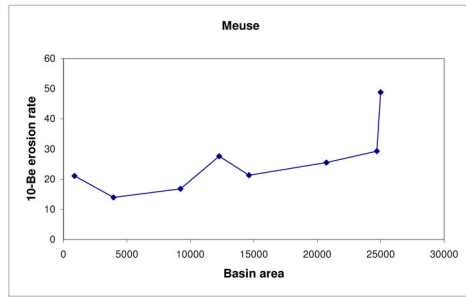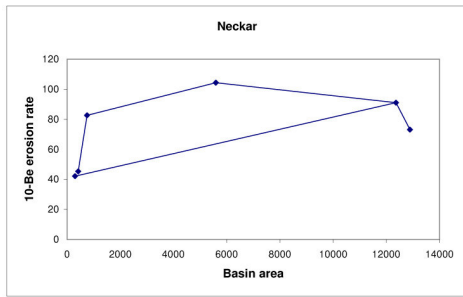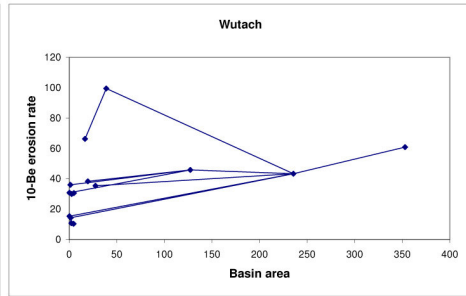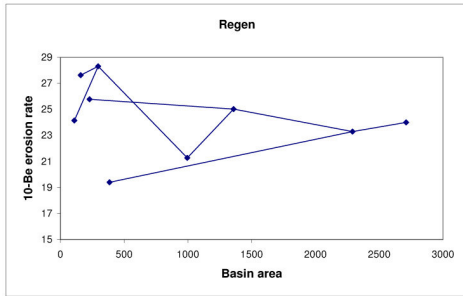
Figure 3. (previous two pages) These figures show the relationship between erosion rate (m/My) and basin area (km$^2$) by region. Points represent basins, and lines represent the stream network connectivity between the sample locations. For many of these regions, the range of erosion rates tends to collapse to an intermediate value as basin scale increases. These plots also serve to highlight the different sampling approaches. (Note that the Susquehanna plot does include the glaciated basins.)
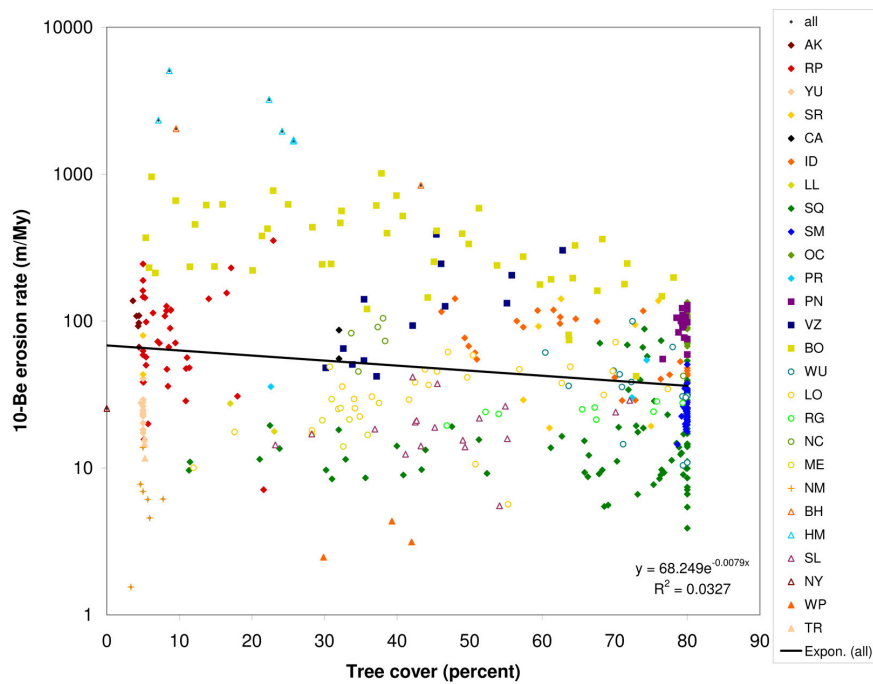


Figure 4. There is no relationship between [10]Be erosion rate and tree cover. Tree cover data are on a 1 km grid, based on 1993 AVHRR remote sensing data (DeFries et al., 2000). Each basin is represented by a single symbol. Colors and shapes of symbols identify regions. Abbreviations identifying areas sampled are listed in table 1.
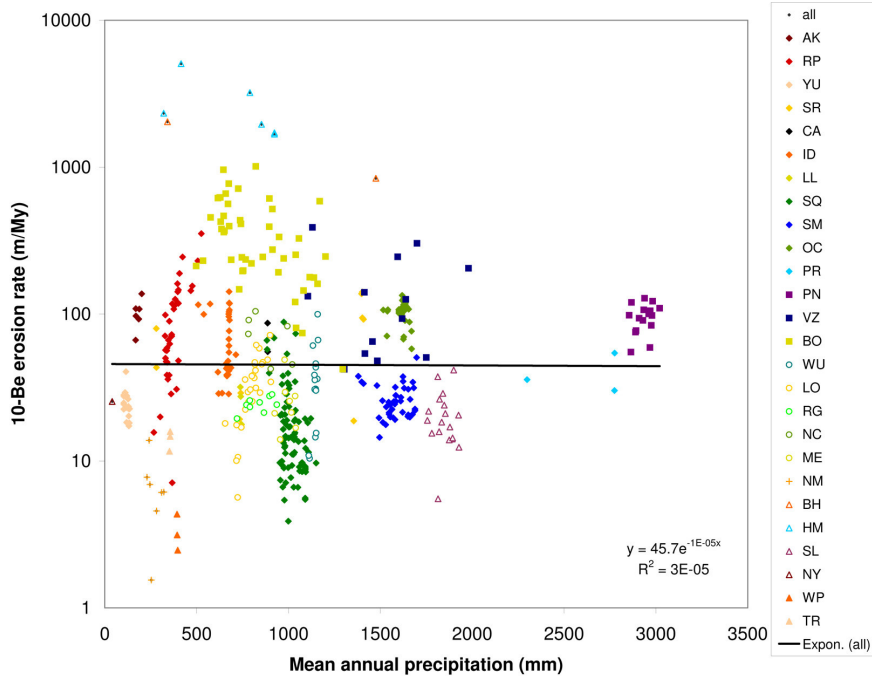
Figure 5. There is no apparent relationship between [10]Be erosion rate and mean annual

precipitation (New et al., 2002).
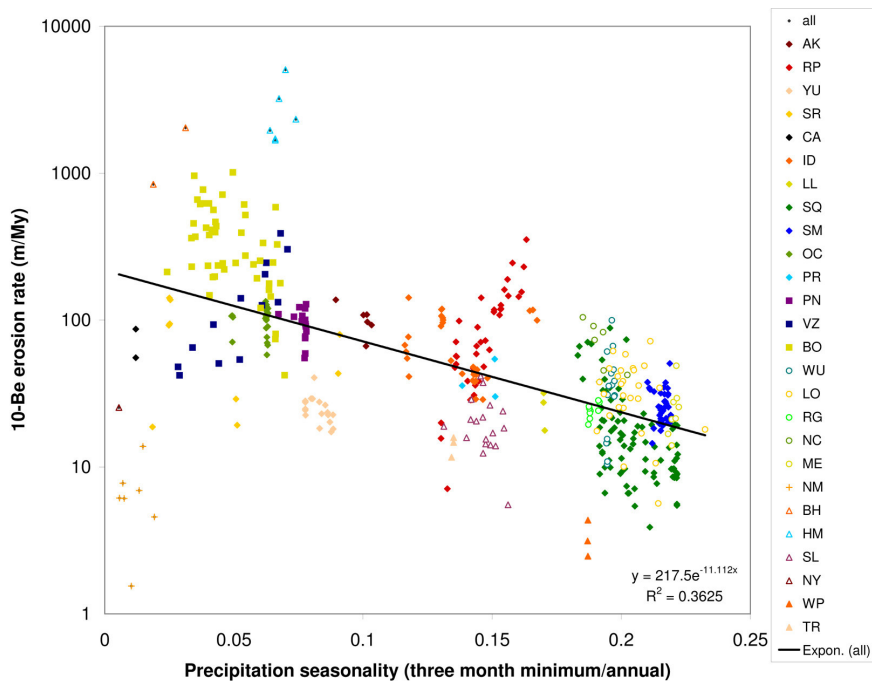


Figure 6. A slight negative correlation exists between [10]Be erosion rate and seasonality of

precipitation; regions with precipitation that is more evenly distributed throughout the

year tend to have lower erosion rates. Seasonality of precipitation was calculated based on average monthly precipitation (New et al., 2002) as the precipitation for the driest three consecutive months divided by total annual precipitation.
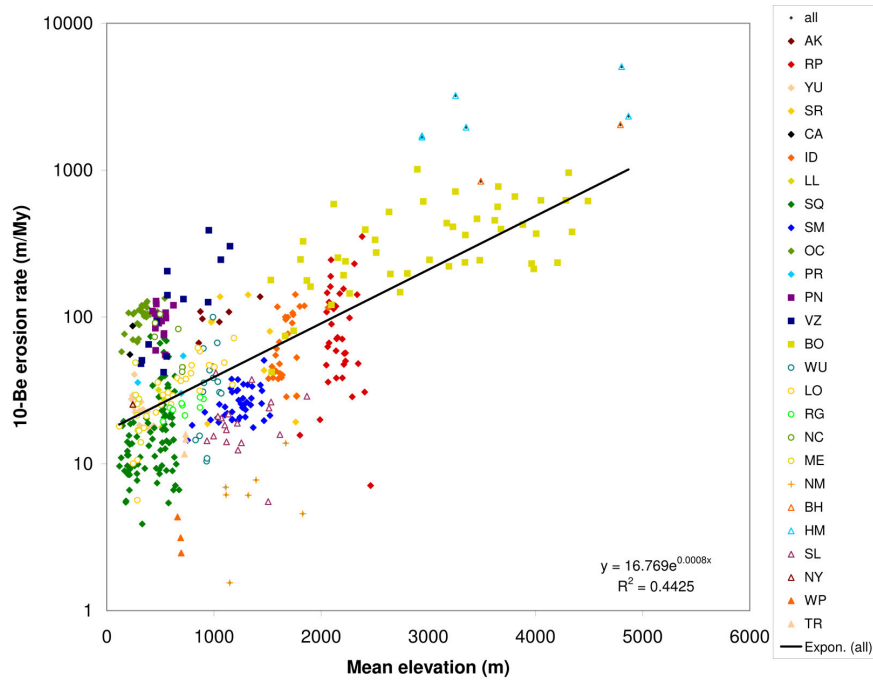


Figure 7. A positive correlation exists between [10]Be erosion rate and mean elevation (NASA et al., 2004).
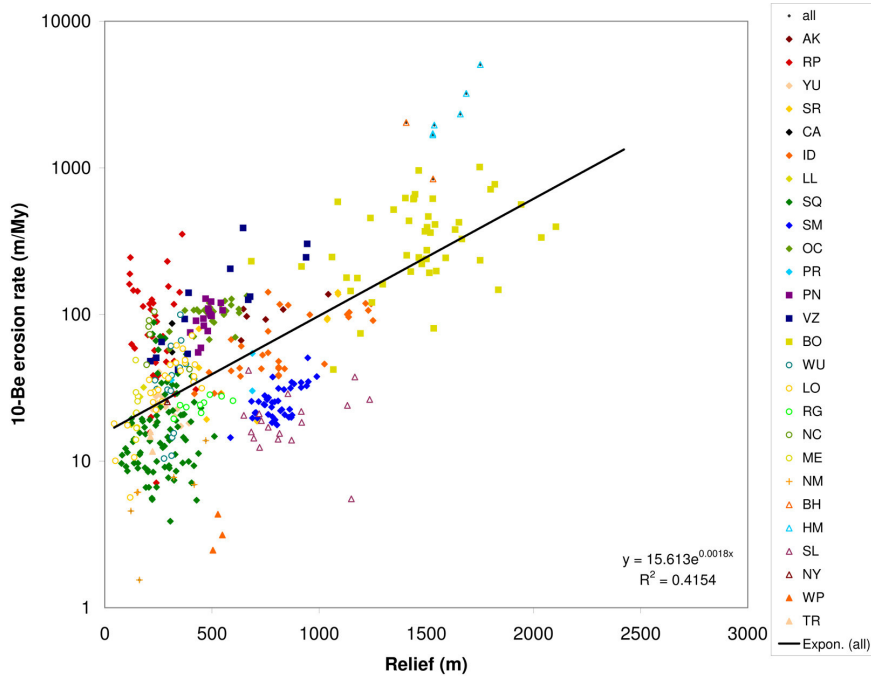
Figure 8. A positive correlation exists between [10]Be erosion rate and relief. Relief was calculated in 25 km[2] grid cells as the maximum minus minimum elevation (NASA et al., 2004); this relief grid was used to calculate the mean relief for each basin.
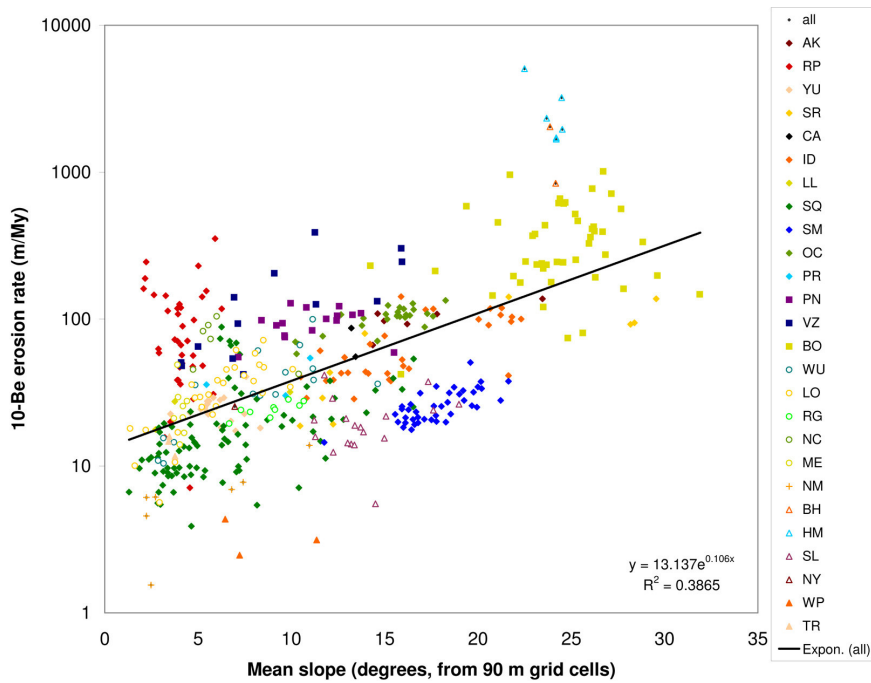


Figure 9. A positive correlation exists between [10]Be erosion rate and slope. Slope is from

SRTM data with 90 m grid cells (NASA et al., 2004). Though the overall correlation is weaker than for relief or mean elevation, slope is commonly the best predictor variable on an intra-regional basis.
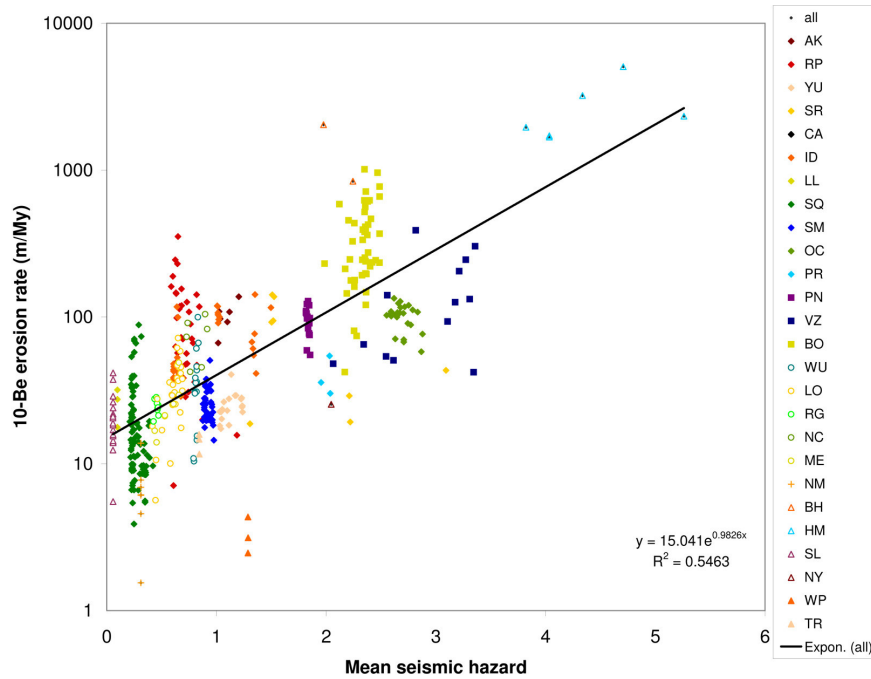


Figure 10. A positive correlation exists between [10]Be erosion rate and the basin mean seismic hazard. Seismic hazard is the peak ground acceleration, in m/s$^2$, with 10% probability of exceedance in 50 years (Giardini et al., 1999).

Testing models of Appalachian Mountain geomorphology with erosion rates inferred from cosmogenic $^{10}$Be

Joanna M. Reuter*, Paul R. Bierman, Jennifer Larsen
Geology Department, University of Vermont, Burlington, Vermont 05405, USA

Milan J. Pavich
U.S. Geological Survey, Reston, Virginia 20192, USA

Robert C. Finkel
Lawrence Livermore National Laboratory, Livermore, California 94550, USA

*Corresponding author. E-mail: joanna.reuter@alumni.carleton.edu

*Abstract*

We use $^{10}$Be-based erosion rates from the 71,250 km$^2$ Susquehanna River Basin in the central Appalachian Mountains to test models that describe topographic change over time. Concentrations of $^{10}$Be in fluvial sediment demonstrate that small sub-basins (0.6 to 25 km$^2$) have been eroding between 4 and 54 m/My during the last $10^4$ to $10^5$ years. Samples are from 59 non-glaciated basins that span a range of mean slopes (2º to 21º) in three physiographic provinces. All sampled basins are mapped as a single lithology: sandstone in the Appalachian Plateaus, sandstone and shale in the Valley and Ridge, and schist in the Piedmont. Overall, erosion rate correlates positively with slope (R$^2$ = 0.57); the strongest relationship is found for the Appalachian Plateaus sandstone basins (R$^2$ = 0.72). After accounting for slope, lithology does not appear to affect basin-scale erosion rates. Samples of exposed sandstone at and near ridge tops are eroding more slowly (2.5 to 4.9 m/My, n = 4) than most sampled basins. The results imply that on a $10^4$ to $10^5$ year time scale, the topography and relief of the Susquehanna landscape is changing as valleys lower faster than ridges and steep slopes erode more quickly than gentle slopes. Erosion rates and the strength of the slope-erosion relationship increase toward the Susquehanna headwaters, from the Piedmont to the Valley and Ridge to the Appalachian Plateaus; this suggests that the Susquehanna Basin is not in steady state and may be experiencing a transient response to a drainage network perturbation.

*Introduction*

The question of how topography changes over time after active mountain building has ceased is fundamental to geomorphology. The Appalachian Mountains, which have

26

been on a passive margin since Triassic/Jurassic rifting (Shultz, 1999), have catalyzed

such geomorphic thought since the mid 1800s (Hitchcock, 1841; Davis, 1889; Hack,

1960; Pazzaglia and Brandon, 1996). Davis drew upon observation from the

Appalachians and the Susquehanna River (Fig. 1) when developing the *Geographical*

*Cycle* (Davis, 1899); this model is arguably the most influential, as well as the most

harshly criticized (Mills et al., 1987), description of how topography changes over time.

According to Davis, if a landscape is unperturbed, relief will diminish until only a flat

peneplain remains. The peneplain concept has largely been abandoned. However, the idea

that relief diminishes over time has credibility, and the duration of topographic decay

continues to stimulate research (Ahnert, 1970; Baldwin et al., 2003).

As an alternative to Davis's cycle, Hack advocated the dynamic equilibrium

model, a uniformitarian hypothesis postulating that topography will develop a steady-

state form, still exhibiting relief, if subjected to uniform conditions over time (Hack,

1960). Furthermore, Hack proposed that slope adjusts to lithology to compensate for

differences in erosion resistance. That is, in a region that is in dynamic equilibrium,

erosion rates should be spatially uniform and independent of slope as well as lithology;

slope and lithology, however, should be related to each other, such that more resistant

lithologies exhibit steeper slopes.

If erosion rates vary across the landscape, a statistical steady state may occur such

that measures of relief remain uniform over time scales of interest (Burbank, 2002;

Willett and Brandon, 2002). The inability to achieve a strict topographic steady state in

physical, scale models under constant forcing (Hasbargen and Paola, 2000; Bonnet and

Crave, 2003) has suggested this alternative, in which ridge and valley positions migrate

over time. The statistical steady state suggests that changing topography need not imply that the landscape is responding to a perturbation; rather, "stable" landscapes may be dynamic.

All of these models recognize that landscapes respond to external forcings, such as changes in climate, tectonism, base level, or drainage network organization (Riebe et al., 2000; Granger et al., 2001; Bonnet and Crave, 2003). Thus, another possibility for any given landscape is that it is in a transient state of change from one form to another; a response may be manifested through either increasing or decreasing relief (Bonnet and Crave, 2003; Gabet et al., 2004).

The models of Davis and Hack, as well as the statistical steady-state model and the case of transient response, differ in predictions regarding if and how topography and relief change over time. Data on erosion and/or erosion rates can be used to make inferences about how topography changes and can therefore be used to test such models. Methods used to measure erosion rates in the Susquehanna Basin integrate over vastly different time frames. Relevant data include fission track thermochronology (Miller and Duddy, 1989; Roden and Miller, 1989; Blackmer et al., 1994), analyses of the offshore sedimentary record (Poag and Sevon, 1989), terrace dating (Pazzaglia and Gardner, 1993; Reusser et al., 2004), and sediment yield (Gellis et al., 2004a). In this paper, we add a new data set (cosmogenic $^{10}$Be) that integrates erosion rates over the $10^4$ to $10^5$ years and allows us to consider relationships between erosion rate, slope, and lithology in the Susquehanna Basin. We use these data to test the three geomorphic models of landscape change presented above and to search for evidence of a transient landscape response to external forcing.

*The Susquehanna River Basin*

Lithology and slope vary substantially within the Susquehanna Basin; other factors considered to be important to erosion, such as climate and tectonics (Molnar, 2003), do not. The limited precipitation gradient at present (Daly and Taylor, 1998) is outweighed by temporal variability of climate in the Susquehanna Basin; the continental ice sheet extended into the northern part of the basin (Braun, 2004). In this passive margin setting, no major recent faulting is known to have caused substantial differential rock uplift (Gardner, 1989). The physiographic provinces of the Susquehanna Basin (Fig. 1) reflect variations in tectonic history across an old and complex mountain range (Shultz, 1999). The Piedmont, which experienced several episodes of Phanerozoic deformation, includes metamorphic rocks. To the west and northwest lies the fold and thrust belt, now the Valley and Ridge province, with sedimentary rocks including sandstone, shale, and carbonate. Farther north and west, the Appalachian Plateaus are composed of relatively undeformed sedimentary rocks, largely sandstone and shale.

*Methods*

Geographic information system (GIS) analysis of the Susquehanna Basin guided the development of our sampling strategy (Fig. 2)[1]. All basins we sampled are south of the glacial margin, range from 0.6 to 25 $km^2$ in size (4.5 ± 3.5 $km^2$, mean ± 1σ), and are spread among the three major physiographic provinces. Each basin is mapped with a single dominant lithology (Pennsylvania Bureau of Topographic and Geologic Survey, 2001), and the basins span a range of mean basin slopes from 2° to 21° (USGS, 1999d).

---

[1] GSA data repository item XXX, Selection of basins for sampling, Figure DR-1, Figure DR-2, Table DR-1, and Table DR-2, is available at www.geosociety.org/pubs/ftXXXX.htm, or on request from editing@geosociety.org or Document Secretary, GSA, P.O.Box 9140, Boulder, CO 80301-9140.

We measured the $^{10}$Be concentration of 59 fluvial sediment samples (including 3 nested

basin pairs, Fig. DR-1), as well as 4 bedrock samples. Samples were prepared according

to standard procedures (Bierman and Caffee, 2001), and $^{10}$Be was measured at Lawrence

Livermore National Laboratory. Erosion rates were calculated using production rates

corrected for latitude and altitude considering neutrons only (Lal, 1991), with production

factors from pixel by pixel calculations.

### *Results*

$^{10}$Be concentrations from sediment in sampled drainage basins range from 0.92 to

9.6 x $10^5$ atoms g$^{-1}$ quartz, and the inferred basin-averaged erosion rates range from 3.9 to

54 m/My (Table DR-1). The basin averaged erosion rates are highest in the Appalachian

Plateaus (22 ± 12 m/My), followed by the Valley and Ridge (13 ± 6 m/My), and the

Piedmont (9 ± 2 m/My). Relative to the sediment samples, bedrock samples of sandstone

have more $^{10}$Be (1.0 to 1.6 x $10^6$ atoms g$^{-1}$ quartz) and thus lower inferred erosion rates

(2.5 to 4.9 m/My). Samples from a cluster of ridge-top tors (n=3) in the Appalachian

Plateaus yield an erosion rate of 4.3 ± 0.5 m/My. One bedrock sample from a slope of

Wolf Run, a high elevation, low slope Valley and Ridge basin, produced an erosion rate

of 2.5 m/My. These erosion rates for the Susquehanna Basin are broadly consistent with

those measured elsewhere in the Appalachians using cosmogenic nuclides (Bierman,

1993; Matmon et al., 2003b).

A positive correlation exists between $^{10}$Be erosion rate and mean basin slope (Fig.

3). When subdividing the data by physiographic province or lithology, positive

correlations between erosion rate and slope exist for all data groupings except the

Piedmont schist, for which the least variability in the range of basin slopes exists. The relationship between erosion rate and slope also holds within individual basins. Nested, sub-basin samples from the headwaters of three basins (two in the Appalachian Plateaus and one in the Valley and Ridge), for which the upland headwater sample represented a low-slope basin and the downstream sample included a deeply incised part of the basin, also show a positive relationship between erosion rate and mean slope.

Basins of comparable slope but different lithologies appear to be eroding at similar rates. After accounting for slope, no discernible relationship exists between erosion rate and lithology in the sampled basins (Fig. 4). There is more variability in erosion rates between the sandstone basins of the Appalachian Plateaus and the Valley and Ridge than between the sandstone and shale within the Valley and Ridge.

### *Discussion*

Steeply sloped basins in the Appalachian Mountains, considering both the Great Smoky Mountains (Matmon et al., 2003) and the Susquehanna Basin, appear to be eroding more rapidly than gently-sloped basins (Fig. 3). The relationship exists in spite of differences between the Susquehanna and Great Smoky Mountain regions in terms of climate, lithology, and proximity to the Wisconsinan glacial margin. Indeed, correlations between erosion rates and topographic metrics, such as slope and relief, are common globally (Reuter et al., 2004). Such relationships have been described on an inter-regional scale (Ahnert, 1970; Pinet and Souriau, 1988; Summerfield and Hulton, 1994; Vance et al., 2003), within specific geographical regions (Matmon et al., 2003b), and within clusters of small basins that have experienced a drop in base level (Riebe et al., 2000).

Slope may be related to erosion rate because processes such as creep and bioturbation (including tree throw) are more effective at moving material on steep slopes than on gentle slopes (Young, 1960; Heimsath et al., 1997), thus reducing residence time and cosmic-ray dosing on slopes, a testable hypothesis. An additional factor may be that more time is needed to reduce material to a transportable size on gentle slopes than on steep ones. Deeper soils may slow soil production and thus sub-colluvial bedrock erosion (Heimsath et al., 2000); thus, if soils are thicker on less steep slopes, this could feed back into lower basin-scale erosion rates.

The lack of a clear relationship between lithology and erosion rates, after accounting for slope, is seemingly contrary to the topographic expression of lithology for which the Valley and Ridge province is famous (Way, 1999). Lithology is difficult to classify, or to quantify, in terms of resistance, and much variability exists within the classifications used. For example, sandstones in the Susquehanna Basin exhibit a variety of forms that may influence how they erode. Some massive sandstones and quartzites, such as the Tuscarora, form boulders that appear to armor the slopes. Three basins on the Tuscarora are eroding at low rates for their slope (5 to 10 m/My). In contrast, other sandstones, such as the "flagstones" characteristic of the Huntley Mountain Formation (in the Appalachian Plateaus), tend to break apart into small, thin, easily mobile slabs. This formation underlies some of the most rapidly eroding basins. Basins mapped as shale are also diverse in terms of morphology and quartz content. At least one basin (JSQ124) has cemented sandstone interbedded with weak shale on a sub-meter scale. These observations indicate that the distinction between sandstone and shale basins is more of a

continuum than a dichotomy. This variability may help to explain the apparent lack of a lithologic effect.

The lack of a lithologic effect may be consistent with the idea that deep soils slow bedrock erosion (Heimsath et al., 1997). Thus, a thick soil mantle on shale basins could slow erosion, resulting in rates lower than expected based on rock strength alone. Indeed, there is more exposed sandstone than shale, and the $^{10}$Be data show that the exposed sandstone erodes very slowly. However, one would need more information about the soil production function and soil depth in the Susquehanna Basin to understand sub-colluvial erosion from this perspective.

### *Assessing landscape models*

Erosion rates vary spatially across the Susquehanna River Basin, indicating that the landscape is not in a strict topographic steady state. The relationships predicted by Hack for an equilibrium landscape do not hold when considered on the scale of small drainage basins (Fig. 5). The spatial variability of erosion rates implies that the form of the landscape is changing over time, raising the question of whether relief is changing as a consequence, or whether the observed patterns of erosion could be consistent with a "statistical steady state" landscape.

Assessing whether or not relief is changing is pertinent to testing models of landscape behavior. Constraints on the rates of erosion for ridge tops and valley bottoms are particularly useful, since relief is defined as the difference in elevation between the high and low parts of the landscape. The low-slope sandstone basins of both the Valley and Ridge and the Appalachian Plateaus are in the uplands, while the low-slope shale

basins are at low elevations, in the macro-scale valleys of the Valley and Ridge. At the

basin-scale, upland and lowland basins appear to be eroding at similar rates (at least in

the Valley and Ridge province). In contrast, bedrock samples suggest slow ridge erosion

rates of < 5 m/My, lower than almost all of the basin-scale erosion rates. Ridge stability

and the potential for rapid, periodic stream incision, as shown by pulses of very rapid

bedrock incision (Reusser et al., 2004), indicate the potential for increasing relief over

time. Clearly, relief is not diminishing due to rapid ridge erosion, in direct contradiction

to Ahnert's (1970, p. 252) assumption that ridges lower twice as fast as valleys.

Relief can also be reduced by the retreat of slopes, a process reminiscent of the

Davisian perspective in which high-elevation, slowly eroding bits of the landscape are

preserved while valleys erode. If steep slopes retreat headward, then ridge tops will

eventually be reduced from the sides. The [10]Be data are consistent with slope retreat

particularly in the Appalachian Plateaus. Paired samples from nested basins indicate that

the steep-sloped downstream parts of these basins are eroding more quickly than the

lower-slope uplands. Here, higher down-basin erosion rates are likely accommodated by

the retreat of slopes, which would migrate headward into the basin if this relationship is

sustained through time.

Could the spatial pattern of erosion we observe with [10]Be result from a landscape-

scale perturbation? Cosmogenic nuclide measurements in sediment from small Sierra

Nevada drainage basins indicate that slope-dependent erosion is present only in basins

where base level has fallen (Riebe et al., 2000). If Riebe's findings are broadly

applicable, then base-level has changed in the Susquehanna River Basin. Indeed, several

lines of evidence suggest a significant change in the dynamics of the Susquehanna Basin

changed during the Miocene. Fission track data from Pennsylvania suggest a particularly rapid period of exhumation from the Miocene to present (Blackmer et al., 1994) consistent with the sedimentary record, which indicates increased Miocene sediment delivery (Poag and Sevon, 1989; Pazzaglia and Brandon, 1996). Detrital fission track data and detrital chert in Coastal Plain sediments suggest stream capture and drainage reorganization in the Potomac and Susquehanna regions in the Miocene (Naeser et al., 2004).

The spatial distribution of erosion recorded by [10]Be may reflect the continued adjustment of the landscape to base-level fall initiated in the Miocene, adjustments which are still propagating through the basin. The overall erosion rate, as well as the strength of the slope-erosion rate relationship, increases from the Piedmont (9 m/My, $R^2 = 0$) to the Valley and Ridge (13 m/My, $R^2 = 0.37$) and finally to the Appalachian Plateaus (22 m/My, $R^2 = 0.72$); this may be indicative of a system in which the lower reaches are closer to equilibrium and the upper reaches are still adjusting to the effects of a base level fall. Although the Appalachian Plateaus, farthest upstream and last to be impacted by such an event, are eroding most rapidly, the upper, low-slope portions of the Plateaus sub-basins we sampled are eroding slowly, having no knowledge of the base-level fall. To achieve and sustain this gradient of erosion rates in the "statistical steady state" model would require a gradient in rock uplift across the basin, something for which there is no evidence. If the slope-erosion rate relationship we find in the Susquehanna Basin reflects a response to some perturbation, then the similar but weaker relationship in the Great Smoky Mountains suggests they too may have been affected in the past by changing base level.

The spatial distribution of $^{10}$Be-based erosion rates indicates that the Susquehanna Basin landscape is not in steady state, as envisioned by Hack; rather, the basin appears to be responding to a change in boundary conditions, most likely an effective base-level fall. Considered as a function of distance upstream, each physiographic province is behaving differently, perhaps because they are in different phases of response. A critical component for understanding how mountain landscapes age is tracking relief over time. The $^{10}$Be data indicate that headward retreat of slopes is a more effective mechanism of relief reduction than the direct lowering of ridges. Indeed, over the time scale of $10^5$ years, relief appears to be increasing as exposed ridge-top outcrops are more stable than the valleys. Over longer time scales, the retreat of slopes in rapidly eroding, steep basins may serve to reduce relief as ridgelines are devoured from the sides; that is, unless another perturbation starts the cycle of base-level fall and landscape response again.

## *Acknowledgments*

## *References Cited*

Ahnert, F., 1970, Functional relationships between denudation, relief, and uplift in large mid-latitude drainage basins: American Journal of Science, v. 268, p. 243-263.

Baldwin, J.A., Whipple, K.X., and Tucker, G.E., 2003, Implications of the shear stress river incision model for the timescale of postorogenic decay of topography: Journal of Geophysical Research, v. 108, p. 1-17.

Bierman, P.R., 1993, In situ produced cosmogenic isotopes and the evolution of granitic landforms [Ph.D. thesis], University of Washington, Seattle, WA.

Bierman, P.R., and Caffee, M., 2001, Slow rates of rock surface erosion and sediment production across the Namib Desert and escarpment, Southern Africa: American Journal of Science, v. 301, p. 326-358.

Blackmer, G.C., Omar, G.I., and Gold, D.P., 1994, Post-Alleghanian unroofing history of the Appalachian Basin, Pennsylvania, from apatite fission track analysis and thermal models: Tectonics, v. 13, p. 1259-1276.

Bonnet, S., and Crave, A., 2003, Landscape response to climate change: Insights from experimental modeling and implications for tectonic versus climatic uplift of topography: Geology, v. 31, p. 123-126.

Braun, D.D., 2004, The glaciation of Pennsylvania, USA, *in* Ehlers, J., and Gibbard, P.L., eds., Quaternary glaciations--extent and chronology, Part II: Amsterdam, Elsevier, p. 237-242.

Burbank, D.W., 2002, Rates of erosion and their implications for exhumation: Mineralogical Magazine, v. 66, p. 25-52.

Daly, C., and Taylor, G., 1998, Pennsylvania average annual precipitation, 1961-90, http://www.ocs.orst.edu/prism/, accessed: April 2005.

Davis, W.M., 1889, The rivers and valleys of Pennsylvania: National Geographic Magazine, v. 1, p. 183-253.

—, 1899, The geographical cycle: The Geographical Journal, v. 14, p. 481-504.

Gabet, E.J., Pratt-Sitaula, B.A., and Burbank, D.W., 2004, Climatic controls on hillslope angle and relief in the Himalayas: Geology, v. 32, p. 629-632.

Gardner, T.W., 1989, Neotectonism along the Atlantic passive continental margin: A review: Geomorphology, v. 2, p. 71-97.

Gellis, A.C., Banks, W.S.L., Langland, M.J., and Martucci, S.K., 2004, Summary of suspended-sediment data for streams draining the Chesapeake Bay watershed, water years 1952-2002, USGS Scientific Investigations Report 2004-5056, 59 p.

Granger, D.E., Fabel, D., and Palmer, A.N., 2001, Pliocene-Pleistocene incision of the Green River, Kentucky, determined from radioactive decay of cosmogenic [26]Al and [10]Be in Mammoth Cave sediments: Geological Society of America Bulletin, v. 113, p. 825-836.

Hack, J.T., 1960, Interpretation of erosional topography in humid temperate regions: American Journal of Science, v. 258-A, p. 80-97.

Hasbargen, L.E., and Paola, C., 2000, Landscape instability in an experimental drainage basin: Geology, v. 28, p. 1067-1070.

Heimsath, A.M., Chappell, J., Dietrich, W.E., Nishiizumi, K., and Finkel, R.C., 2000, Soil production on a retreating escarpment in southeastern Australia: Geology, v. 28, p. 787-790.

Heimsath, A.M., Dietrich, W.E., Nishiizumi, K., and Finkel, R.C., 1997, The soil production function and landscape equilibrium: Nature, v. 388, p. 358-361.

Hitchcock, E., 1841, Final report on the geology of Massachusetts: Amherst, MA, J. S. and C. Adams, 831 p.

Lal, D., 1991, Cosmic ray labeling of erosion surfaces: in situ nuclide production rates and erosion models: Earth and Planetary Science Letters, v. 104, p. 424-439.

Matmon, A., Bierman, P.R., Larsen, J., Southworth, S., Pavich, M., Finkel, R., and Caffee, M., 2003, Erosion of an ancient mountain range, the Great Smoky Mountains, North Carolina and Tennessee: American Journal of Science, v. 303, p. 817-855.

Miller, D.S., and Duddy, I.R., 1989, Early Cretaceous uplift and erosion of the northern Appalachian Basin, New York, based on apatite fission track analysis: Earth and Planetary Science Letters, v. 93, p. 35-49.

Mills, H.H., Brakenridge, G.R., Jacobson, R.B., Newell, W.L., Pavich, M.J., and Pomeroy, J.S., 1987, Appalachian mountains and plateaus, *in* Graf, W.L., ed., Geomorphic systems of North America, Centennial Special Volume 2: Boulder, Colorado, Geological Society of America, p. 5-50.

Molnar, P., 2003, Nature, nurture and landscape: Nature, v. 426, p. 612-614.

Naeser, C.W., Naeser, N.D., Newell, W.L., Southworth, C.S., Weems, R.E., and Edwards, L.E., 2004, Provenance studies in the Atlantic Coastal Plain: what fission-track ages of detrital zircons can tell us about the source of sediment: Geological Society of America Abstracts with Programs, v. 36, p. 114.

Pazzaglia, F.J., and Brandon, M.T., 1996, Macrogeomorphic evolution of the post-Triassic Appalachian mountains determined by deconvolution of the offshore basin sedimentary record: Basin Research, v. 8, p. 255-278.

Pazzaglia, F.J., and Gardner, T.W., 1993, Fluvial terraces of the lower Susquehanna River: Geomorphology, v. 8, p. 83-113.

Pennsylvania Bureau of Topographic and Geologic Survey, Department of Conservation and Natural Resources, 2001, Digital bedrock geology of Pennsylvania, http://www.dcnr.state.pa.us/topogeo/map1/bedmap.aspx, accessed: March 2005.

Pinet, P., and Souriau, M., 1988, Continental erosion and large-scale relief: Tectonics, v. 7, p. 563-582.

Poag, C.W., and Sevon, W.D., 1989, A record of Appalachian denudation in postrift Mesozoic and Cenozoic sedimentary deposits of the U.S. middle Atlantic continental margin: Geomorphology, v. 2, p. 119-157.

Reusser, L.J., Bierman, P.R., Pavich, M.J., Zen, E., Larsen, J., and Finkel, R., 2004, Rapid late Pleistocene incision of Atlantic passive-margin river gorges: Science, v. 305, p. 499-502.

Reuter, J.M., Bierman, P.R., Pavich, M.J., Larsen, J., and Finkel, R.C., 2004, Linking [10]Be estimates of erosion rates with landscape variables: compilation and consideration of multiple data sets from around the world, 32nd International Geological Conference: Florence.

Riebe, C.S., Kirchner, J.W., Granger, D.E., and Finkel, R.C., 2000, Erosional equilibrium and disequilibrium in the Sierra Nevada, inferred from cosmogenic [26]Al and [10]Be in alluvial sediment: Geology, v. 28, p. 803-806.

Roden, M.K., and Miller, D.S., 1989, Apatite fission-track thermochronology of the Pennsylvania Appalachian Basin: Geomorphology, v. 2, p. 39-51.

Shultz, A.P., editor, 1999, The geology of Pennsylvania: Harrisburg, PA, Pennsylvania Geological Survey, 888 p.

Summerfield, M.A., and Hulton, N.J., 1994, Natural controls of fluvial denudation rates in major world drainage basins: Journal of Geophysical Research, v. 99, p. 13871-13883.

USGS, E.D.C., 1999, National elevation dataset, http://gisdata.usgs.net/ned/, accessed: April 2005.

Vance, D., Bickle, M., Ivy-Ochs, S., and Kubik, P.W., 2003, Erosion and exhumation in the Himalaya from cosmogenic isotope inventories of river sediments: Earth and Planetary Science Letters, v. 206, p. 273-288.

Way, J.H., 1999, Appalachian Mountain section of the Ridge and Valley province, *in* Shultz, C.H., ed., The geology of Pennsylvania: Harrisburg, Pennsylvania Geological Survey, p. 353-361.

Willett, S.D., and Brandon, M.T., 2002, On steady states in mountain belts: Geology, v. 30, p. 175-178.

Young, A., 1960, Soil movement by denudational processes on slopes: Nature, v. 188, p. 120-122.

Figure 1 - Susquehanna River drains 71,250 km$^2$ of New York, Pennsylvania, and Maryland before flowing into Chesapeake Bay. Appalachian Plateaus, Valley and Ridge, and Piedmont are the dominant physiographic provinces south of the Wisconsinan glacial margin (hatched line). Inset map shows the extent of the Appalachian Highlands within the U.S. (gray).

Figure 2 - The outlines of the sampled drainage basins, all at the same scale, are organized according to the sampling strategy, which takes into account physiographic province, lithology, and slope. Nested sub-basins (in black) are shown both independently and within the basins that contain them.

Figure 3 - Erosion rates are positively correlated to mean drainage basin slope within all physiographic provinces and lithologic groupings except the Piedmont schist. A correlation also exists between erosion rate and slope among the pooled Susquehanna samples ($R^2 = 0.57$), as well as among the Susquehanna and Great Smoky Mountain samples (Matmon et al., 2003) when the two data sets are considered together ($R^2 = 0.56$). Parameter estimates for the linear regression lines for each data grouping are shown. Appalachian Plateaus (AP), Valley and Ridge (VR), and Piedmont (PD).

Figure 4 - We calculated residuals for each sample from the linear regression for slope and erosion rate that is based on all Susquehanna samples. Grouped by physiographic province and lithology, the residuals show that after accounting for slope, no clear

distinction exists between lithologies. The box and whisker plots summarize minimum, first quartile, median, third quartile, and maximum values.

Figure 5 - Hack's dynamic equilibrium specifies testable relationships among erosion rate, slope, and lithology (as shown by inset figures). Results are shown for the Valley and Ridge, the one province with two sampled lithologies. We, as others, presume that sandstone is more resistant than shale. A) Hack proposed that erosion would be spatially uniform, with erosion rate and slope unrelated. In contrast, the $^{10}$Be data show a strong relationship. B) Erosion rate and lithology appear not to be related as predicted by Hack. C) While the steepest basins are on sandstone, we find that sandstone and shale basins exist at a range of mean slopes. We do not find the relationship between slope and resistance postulated by Hack.
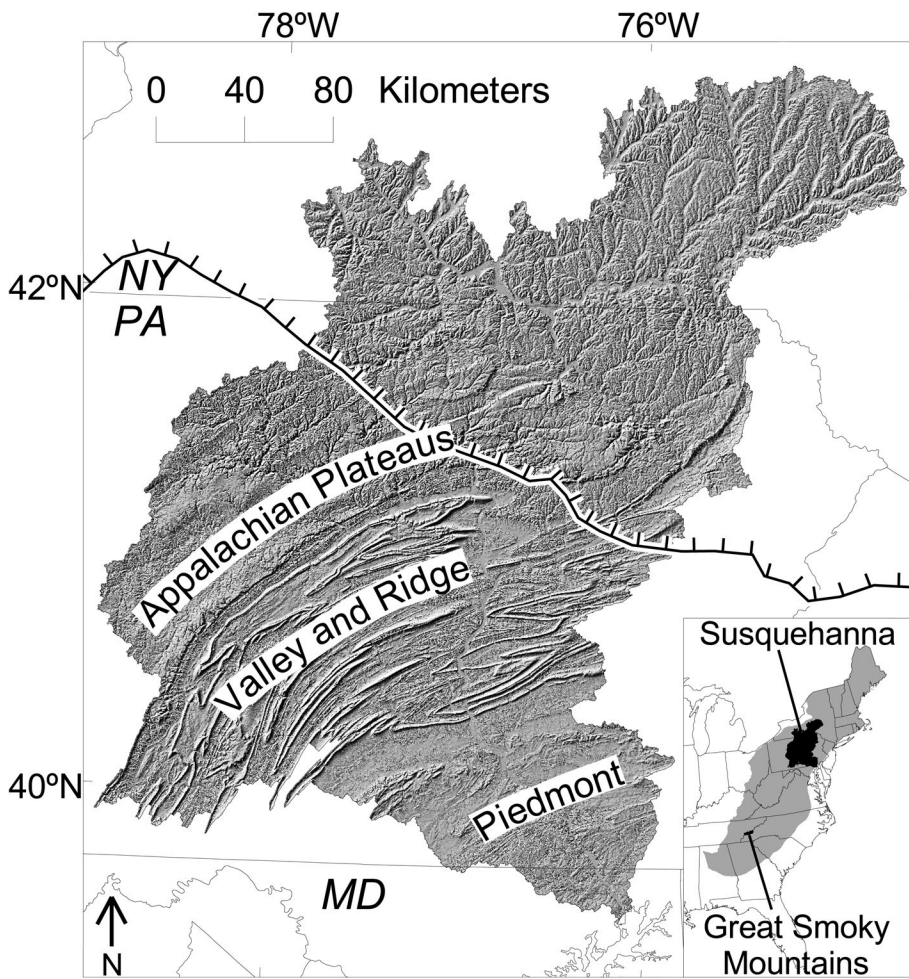
Figure 1. Reuter et al.

*Figure 2. Reuter et al.*

| | slope | intercept | R² |
|---|---|---|---|
| all Susquehanna | 1.43 | 2.9 | 0.57 |
| AP sandstone | 1.62 | 4.9 | 0.72 |
| VR sandstone | 0.76 | 6.8 | 0.35 |
| VR shale | 1.00 | 3.6 | 0.42 |
| PD schist | -0.10 | 9.2 | 0.00 |
| Smokies | 2.16 | 25.2 | 0.40 |
| Susq. & Smokies | 0.90 | 6.4 | 0.55 |
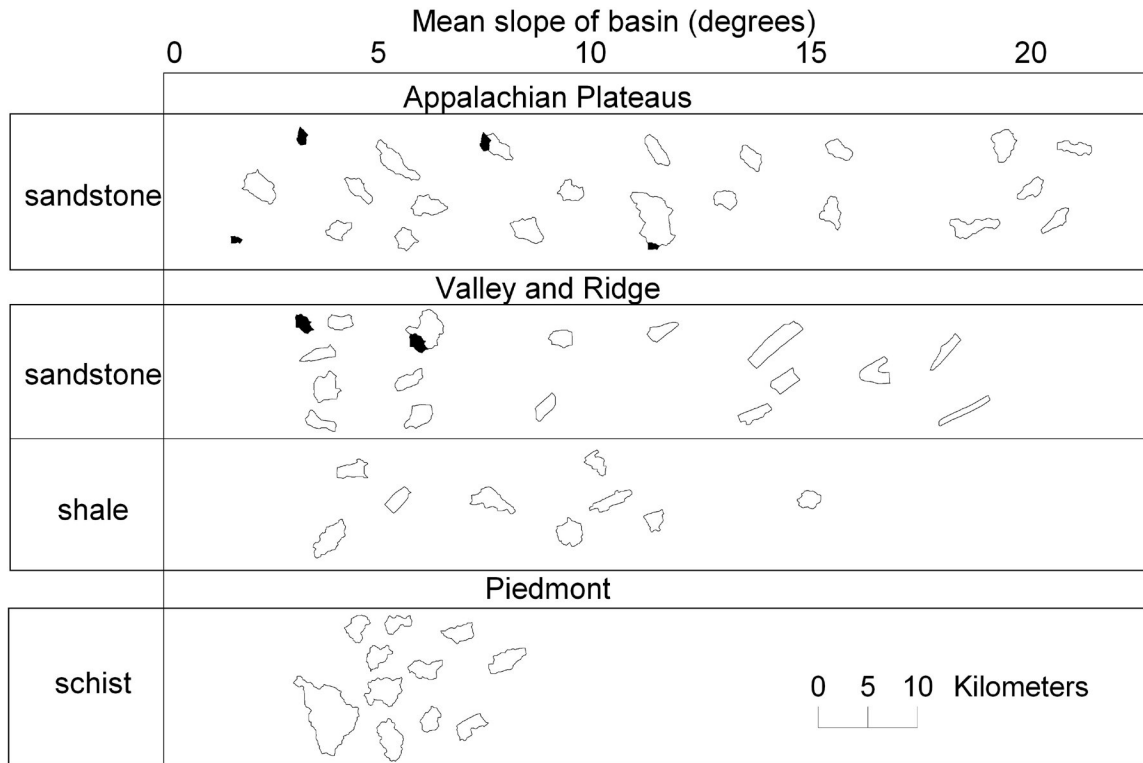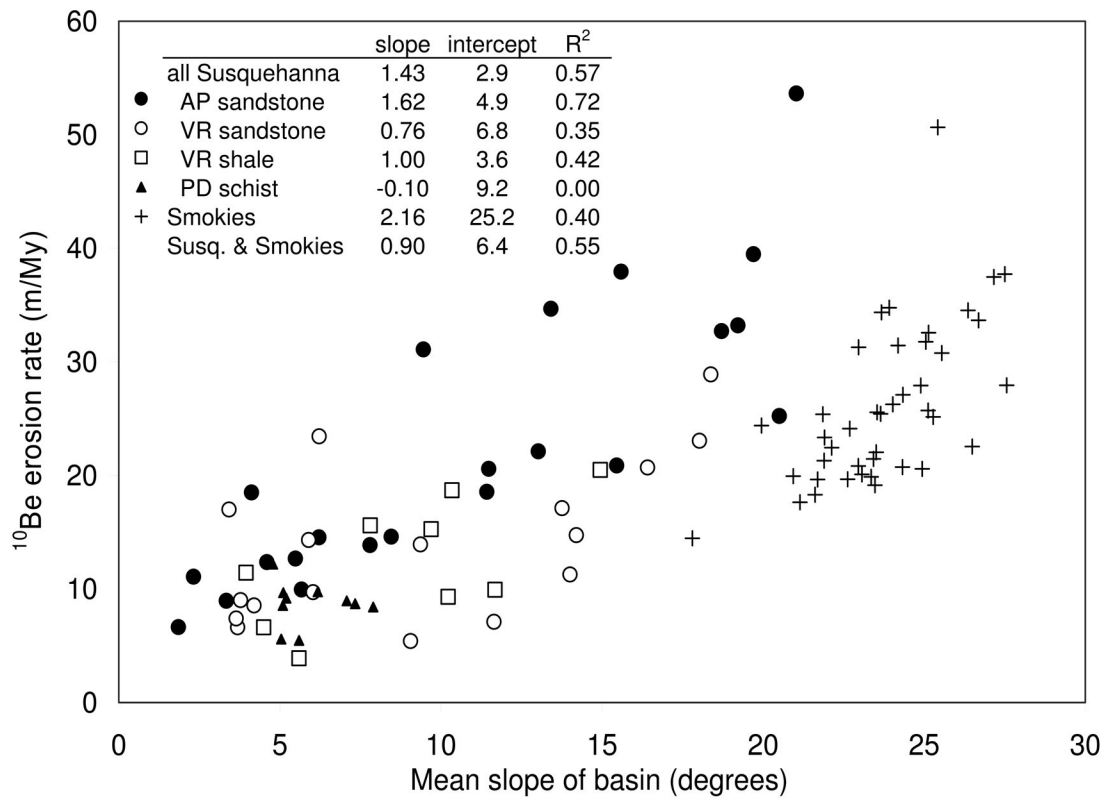
*Figure 3. Reuter et al.*
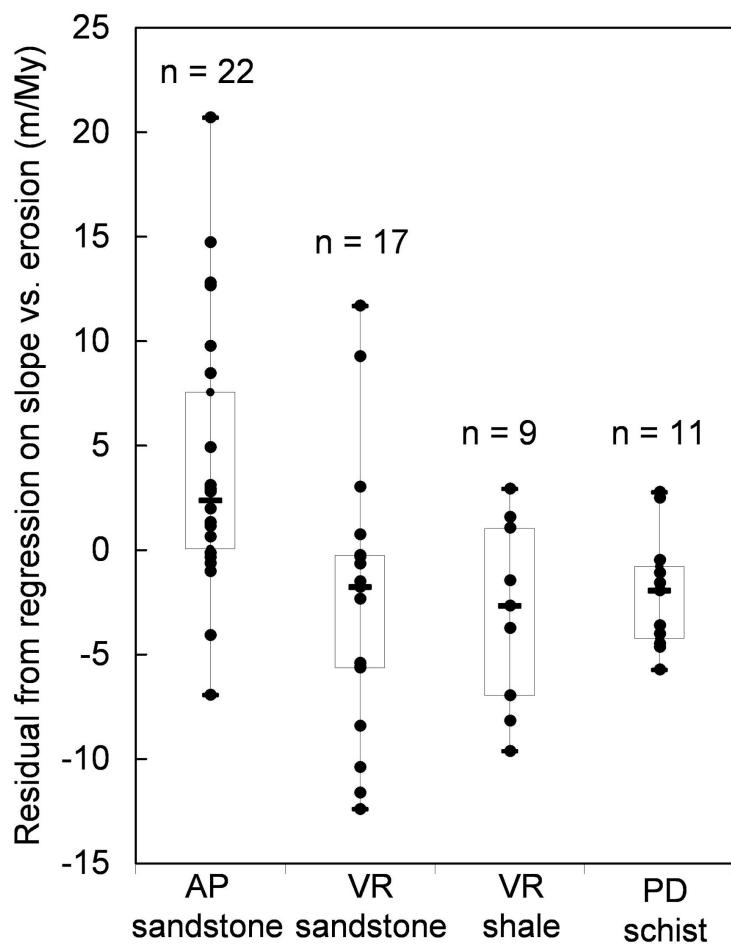
*Figure 4. Reuter et al.*
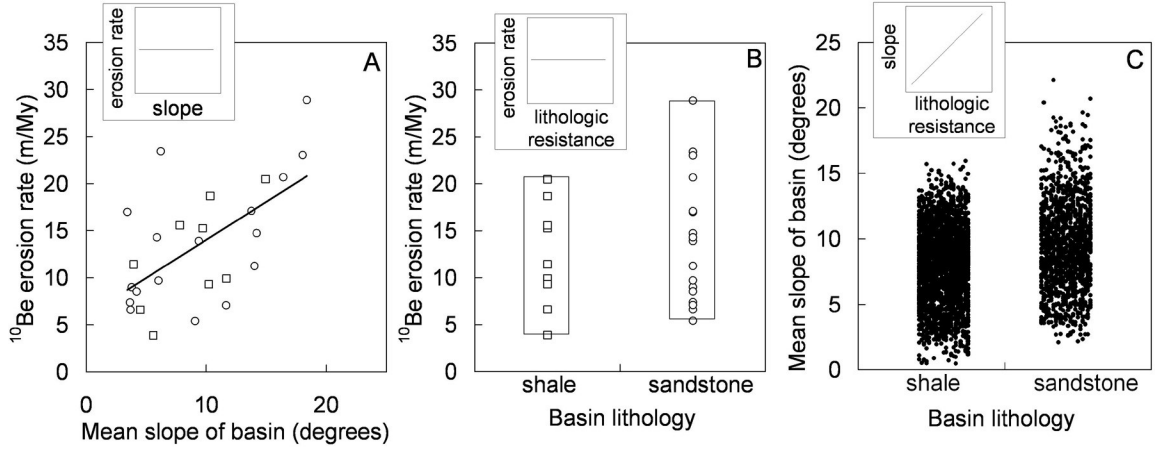
*Figure 5. Reuter et al.*

***Selection of basins for sampling***

In order to examine relationships between slope, lithology, physiographic province, and erosion rate, we used a systematic approach to basin selection, aided by geographic information systems (GIS) analysis. We delineated thousands of candidate sub-basins of the Susquehanna River Basin at a diverse range of scales. Then, we summarized basin characteristics using available GIS data (Table DR-2), analyzed the results, and used this analysis to guide the development of a sampling strategy. The following is an explanation of the analysis and the factors that guided development of the sampling strategy.

Some digital data layers required processing to be suitable for our use. All of the GIS data layers were projected to UTM Zone 18 for analysis. Slope was derived from a DEM with a grid cell size of approximately 30 m. Lithology is based on the digital geologic map of Pennsylvania. Our lithologic analyses are based on the dominant lithology ("Lithology 1" field) of the mapped formations. We classified the lithologies into five broad categories: sandstone, shale, carbonate, igneous/metamorphic, and low-quartz igneous/metamorphic.

Our goals in devising a basin selection strategy were as follows: 1) to select basins large enough to have well developed streams that serve to mix sediment from the basin; 2) to sample only south of the Wisconsinan glacial margin, because glaciation violates assumptions for inferring erosion rates from [10]Be (Bierman and Steig, 1996); 3) to select basins of a single lithology, which allows for more robust interpretation of

47

erosion rates given the assumption that quartz distribution is uniform throughout the basin (Bierman and Steig, 1996); 4) to select basins with a maximum diversity of characteristics (such as mean hillslope) that are expected to be related to erosion, under the assumption that sampling the maximum range of diversity will help to identify an effect, if one exists; and 5) to have enough basins of each sampling category to have statistical power.

These goals led us to select basins that are dominantly in the 3-10 $km^2$ size range. As basin size increases, the range of basin mean slope decreases (Fig. DR-2); thus, a relatively small basin size helps to achieve the goal of maximizing diversity. In addition, single-lithology basins are more common at the scale of small basins. The stream channels in the basins we sampled were well developed; only the carbonate basins did not have an adequate channel at this basin scale, and thus we did not sample those due to a lack of both quartz and a sizable stream channel where visited.

We selected only sandstone basins in the Appalachian Plateaus because of the impact of strip mines in the non-glaciated part of the Appalachian Plateaus where shale is present. We sampled sandstone and shale basins in the Valley and Ridge. Though the Piedmont has a diversity of lithologies, we sampled only schist basins so that we would not spread samples too thinly among numerous rock types.

In selecting basins with a range of slopes, we focused primarily on basins with relatively uniform slope distributions (using the standard deviation of basin slope as an indicator). In addition, we selected a few basins with low slope uplands and deeply incised, steep walled lower valleys. For three such basins (two in the Appalachian Plateaus and one in the Valley and Ridge), we took a pair of samples: one in the low

slope, upland portion of the basin and one in the steep, lowland portion of the basin (Fig. DR-1).

Using GIS, we queried all available basins for desired characteristics, and manually selected basins for sampling. Candidate basins were screened through visual examination of the 1:24,000 digital topographic maps so that undesirable features such as strip mines, dams, and excessive development could be avoided. Access was also a consideration in site selection; in particular, sites were mostly on public land and/or near a road crossing. We selected extra basins in each category (physiographic province, lithology, and slope range) to allow for attrition of sites upon visitation due to access or disturbance issues.

The sample basins span nearly the entire range of existing slopes for the lithologic and physiographic combinations that we decided to sample. However, they do not represent a random sample of basins from the landscape.
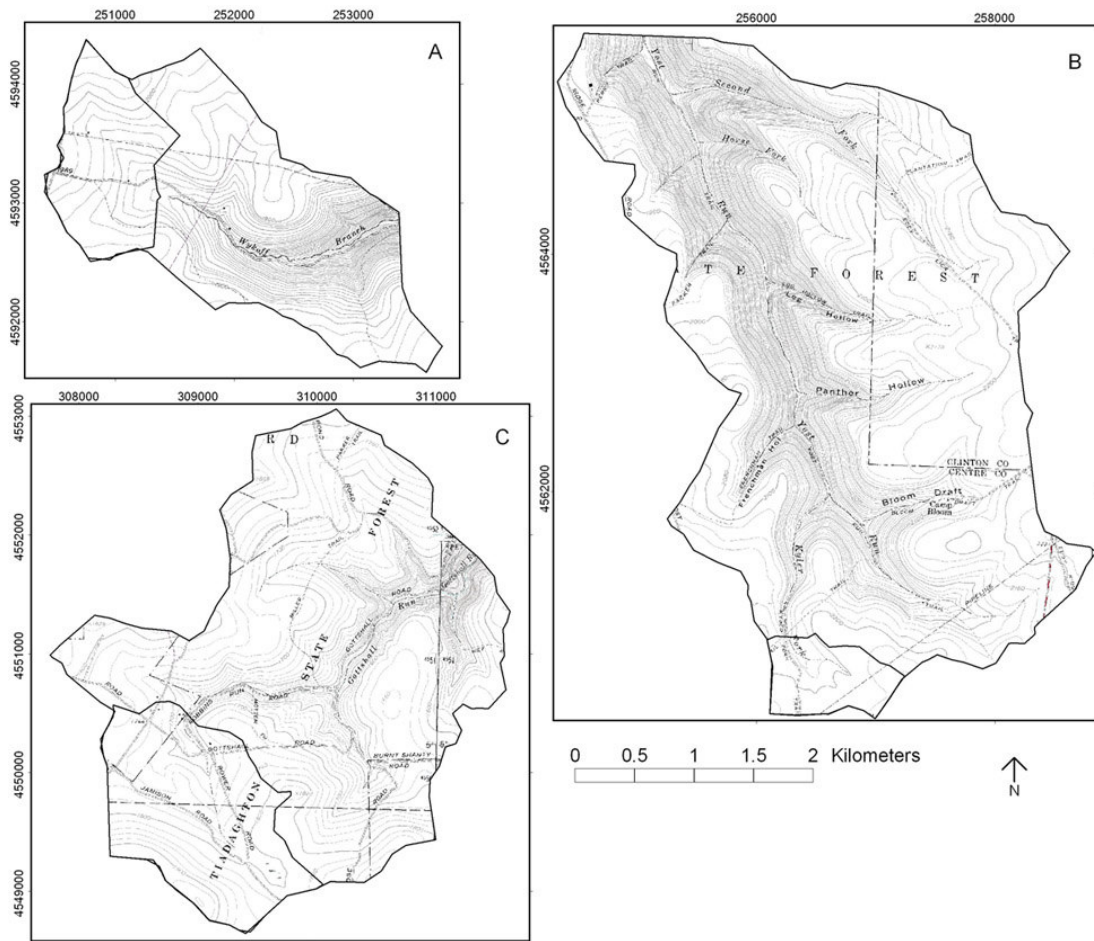
Figure DR-1 - Topographic maps of the basins with a nested sample in the low slope
headwaters. A) Wykoff Branch (JSQ110, headwaters, and JSQ111, downstream), B)
Yost Run (JSQ120, downstream, and JSQ121, headwaters), C) Gottshall Run (JSQ125,
downstream, and JSQ126, headwaters).
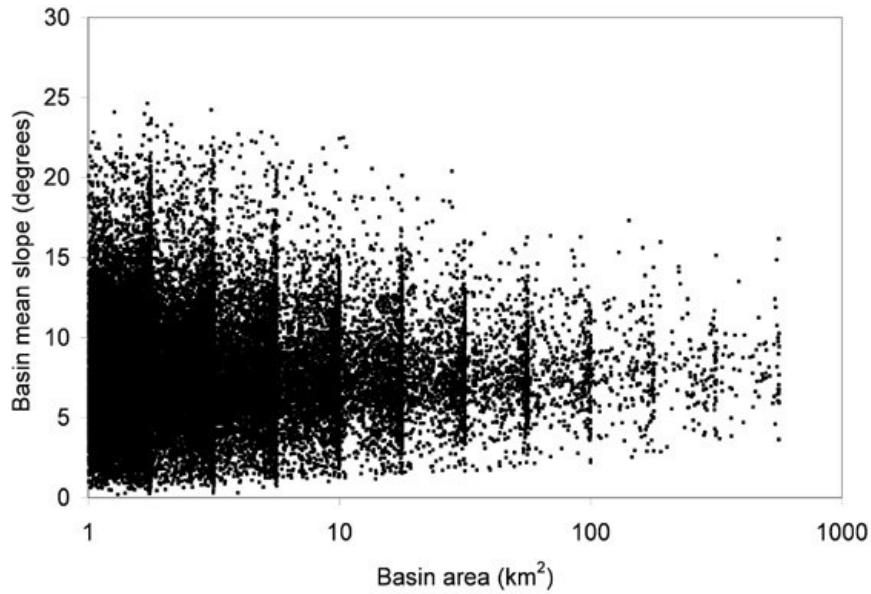
Figure DR-2 - Each point represents a sub-basin of the Susquehanna River. As basin area increases, the range of mean slope decreases. Working with small basins allows for the selection of a broader range of characteristics than working with large basins. The vertical lines are artifacts of the basin size ranges that were specified when delineating basins.

TABLE DR-1. COSMOGENIC NUCLIDE RESULTS AND BASIN CHARACTERISTICS

| Type | Sample ID | Site name | Location* Easting (m) | Location* Northing (m) | Area (km²) | Elevation range (m) | Mean slope (°)† | Bedrock geology§ | Measured 10Be (10⁶ atoms g⁻¹)# | 10Be production factor** | Erosion rate (m/My)†† |
|---|---|---|---|---|---|---|---|---|---|---|---|
| **Appalachian Plateaus sandstone** | | | | | | | | | | | |
| sediment | JSQ100 | Dry Run | 236277 | 4585280 | 3.0 | 280 - 652 | 21 | MDhm, Dck | 0.187 ± 0.014 | 1.50 | 25.2 |
| sediment | JSQ102 | Russell Hollow Run | 236666 | 4594459 | 3.2 | 345 - 707 | 21 | MDhm, Pp | 0.092 ± 0.006 | 1.57 | 53.6 |
| sediment | JSQ103 | Crooked Run | 234402 | 4609402 | 5.6 | 376 - 723 | 19 | MDhm, Dck | 0.150 ± 0.009 | 1.56 | 32.7 |
| sediment | JSQ104 | Heth Run | 247265 | 4621392 | 3.6 | 537 - 738 | 9 | Dck, MDhm | 0.167 ± 0.008 | 1.64 | 31.1 |
| sediment | JSQ105 | Big Run | 213531 | 4595375 | 3.2 | 544 - 635 | 4 | Pp, Pa | 0.273 ± 0.009 | 1.61 | 18.5 |
| sediment | JSQ106 | East Branch | 219380 | 4593970 | 3.2 | 484 - 679 | 13 | MDso, MDhm, Pp | 0.226 ± 0.010 | 1.59 | 22.1 |
| sediment | JSQ107 | another Middle Branch | 219298 | 4591647 | 3.4 | 430 - 702 | 13 | MDso, Dck | 0.141 ± 0.007 | 1.55 | 34.7 |
| sediment | JSQ108 | Bell Draft | 219353 | 4588136 | 5.4 | 497 - 705 | 8 | Pp, MDhm, MDso | 0.347 ± 0.012 | 1.63 | 14.6 |
| sediment | JSQ109 | South Branch Little Portage Creek | 241330 | 4609810 | 3.2 | 461 - 737 | 20 | MDhm, Dck | 0.131 ± 0.009 | 1.64 | 39.5 |
| sediment | JSQ110§§ | Wykoff Branch, high elevation sample | 251417 | 4593267 | 1.3 | 558 - 635 | 3 | Pp | 0.552 ± 0.017 | 1.61 | 9.0 |
| sediment | JSQ111§§ | Wykoff Branch, low elevation sample | 253405 | 4593078 | 4.7 | 363 - 635 | 8 | Pp, MDhm | 0.352 ± 0.013 | 1.57 | 13.9 |
| sediment | JSQ112 | Left Fork Bearfield Run | 253408 | 4585795 | 3.5 | 338 - 684 | 16 | Dck, MDhm | 0.122 ± 0.007 | 1.47 | 37.9 |
| sediment | JSQ113 | Lebo Branch | 251651 | 4582788 | 3.9 | 438 - 680 | 11 | MDhm, Dck | 0.255 ± 0.009 | 1.51 | 18.6 |
| sediment | JSQ114 | Pebble Run | 225309 | 4571094 | 6.5 | 578 - 677 | 2 | Pp | 0.458 ± 0.015 | 1.64 | 11.1 |
| sediment | JSQ115 | Sanders Draft | 229185 | 4574397 | 4.9 | 457 - 648 | 6 | Pp, MDhm | 0.349 ± 0.012 | 1.63 | 14.5 |
| sediment | JSQ116 | Little Birch Island Run | 245209 | 4565813 | 6.5 | 414 - 649 | 5 | Pp, Mb | 0.375 ± 0.012 | 1.53 | 12.7 |
| sediment | JSQ117 | tributary to Little Birch Island Run | 245616 | 4565906 | 3.4 | 405 - 563 | 5 | Mb, Pp, MDhm | 0.370 ± 0.012 | 1.47 | 12.4 |
| sediment | JSQ118 | Drake Hollow | 266408 | 4574231 | 4.0 | 309 - 706 | 15 | MDhm, Mb | 0.237 ± 0.011 | 1.58 | 20.9 |
| sediment | JSQ119 | Laurely Fork | 268183 | 4572905 | 5.3 | 360 - 702 | 19 | MDhm, Dck | 0.148 ± 0.007 | 1.56 | 33.2 |
| sediment | JSQ120§§ | Yost Run, low elevation sample | 255067 | 4566060 | 15.2 | 292 - 690 | 11 | Mb, MDhm | 0.246 ± 0.011 | 1.61 | 20.6 |
| sediment | JSQ121§§ | Yost Run (Kyler Fork), high elev. sample | 256290 | 4560987 | 0.6 | 651 - 683 | 2 | Mb | 0.783 ± 0.031 | 1.71 | 6.6 |
| sediment | JSQ123 | Middle Branch | 265432 | 4565082 | 3.1 | 577 - 698 | 6 | MDhm | 0.516 ± 0.014 | 1.66 | 9.9 |
| bedrock | JSQ122 | Water Rocks, middle tor | 263000 | 4565643 | N.A. | 690 | N.A. | MDhm or Mb## | 1.255 ± 0.037 | 1.73 | 4.0 |
| bedrock | JSQ163 | Water Rocks, northeast tor | 263024 | 4565670 | N.A. | 689 | N.A. | MDhm or Mb## | 1.034 ± 0.031 | 1.73 | 4.9 |
| bedrock | JSQ164 | Water Rocks, southwest tor | 262953 | 4565594 | N.A. | 687 | N.A. | MDhm or Mb## | 1.244 ± 0.038 | 1.73 | 4.0 |
| **Valley and Ridge sandstone** | | | | | | | | | | | |
| sediment | JSQ125§§ | Gottshall Run, low elevation sample | 311375 | 4552031 | 9.7 | 376 - 592 | 6 | Obe | 0.201 ± 0.008 | 1.50 | 23.4 |
| sediment | JSQ126§§ | Gottshall Run, high elevation sample | 308943 | 4550708 | 2.1 | 500 - 592 | 3 | Obe | 0.281 ± 0.008 | 1.53 | 17.0 |
| sediment | JSQ127 | Jamison Run | 306104 | 4549001 | 5.5 | 512 - 606 | 4 | Obe | 0.526 ± 0.015 | 1.54 | 9.0 |
| sediment | JSQ128 | tributary to White Deer Hole Run | 321997 | 4549215 | 3.2 | 410 - 623 | 9 | Oj, Obe | 0.334 ± 0.010 | 1.49 | 13.9 |
| sediment | JSQ129 | Buffalo Creek | 312888 | 4534513 | 3.2 | 561 - 672 | 4 | St | 0.747 ± 0.020 | 1.62 | 6.6 |
| sediment | JSQ133 | Wolf Run | 352071 | 4487189 | 3.0 | 408 - 537 | 4 | Mp | 0.522 ± 0.014 | 1.45 | 8.5 |
| sediment | JSQ137 | Minehart Run | 278951 | 4489887 | 8.7 | 246 - 578 | 14 | Oj, Obe | 0.383 ± 0.011 | 1.39 | 11.3 |
| sediment | JSQ138 | trib to Minehart Run | 279009 | 4489970 | 3.8 | 248 - 551 | 14 | Oj, Obe | 0.290 ± 0.009 | 1.37 | 14.7 |
| sediment | JSQ139 | Wharton Run | 265282 | 4476630 | 3.2 | 323 - 643 | 18 | Oj, St | 0.200 ± 0.007 | 1.47 | 23.0 |
| sediment | JSQ140 | Shores Branch | 241009 | 4468453 | 3.1 | 371 - 543 | 4 | Mp | 0.586 ± 0.020 | 1.42 | 7.4 |
| sediment | JSQ141 | Laurel Run | 235690 | 4469290 | 4.5 | 382 - 599 | 6 | Mp | 0.468 ± 0.016 | 1.47 | 9.7 |

| | Sample | Name | Easting | Northing | Slope | Elevation (min – max) | | Dominant formation | Additional formations | $^{10}$Be concentration | Production factor | Erosion rate |
|---|---|---|---|---|---|---|---|---|---|---|---|---|
| sediment | JSQ143 | Croyle Run | 263179 | 4508820 | 3.0 | 401 | 733 | 9 | St | | 0.870 ± 0.023 | 1.56 | 5.4 |
| sediment | JSQ144 | another Laurel Run | 264404 | 4513401 | 3.2 | 500 | 739 | 12 | St | | 0.712 ± 0.019 | 1.66 | 7.1 |
| sediment | JSQ145 | Swift Run | 296079 | 4521195 | 3.3 | 370 | 625 | 14 | Oj, Obe, St | | 0.272 ± 0.011 | 1.49 | 17.1 |
| sediment | JSQ146 | Pine Swamp Run | 291206 | 4523062 | 3.3 | 516 | 623 | 6 | Obe | | 0.335 ± 0.009 | 1.54 | 14.3 |
| sediment | JSQ147 | Bear Run | 290919 | 4540121 | 3.2 | 309 | 600 | 18 | Oj, Obe | | 0.160 ± 0.007 | 1.47 | 28.9 |
| sediment | JSQ148 | tributary from Kettle Mountain | 290495 | 4539764 | 4.8 | 302 | 704 | 16 | Oj, Obe, St | | 0.228 ± 0.008 | 1.51 | 20.7 |
| bedrock | JSQ162 | Split Rock at Wolf Run | 352098 | 4487104 | N.A. | 412 | | N.A. | Mp | | 1.558 ± 0.046 | 1.36 | 2.5 |
| **Valley and Ridge shale** | | | | | | | | | | | | |
| sediment | JSQ124 | Sulphur Run | 303777 | 4564214 | 2.7 | 206 | 349 | 12 | Dlh | | 0.381 ± 0.021 | 1.23 | 9.9 |
| sediment | JSQ130 | Mud Creek | 364097 | 4548247 | 6.4 | 164 | 265 | 4 | Dh | | 0.308 ± 0.011 | 1.13 | 11.4 |
| sediment | JSQ131 | tributary to Spruce Run Creek | 372135 | 4548244 | 5.2 | 188 | 353 | 10 | Dtr, Dciv | | 0.248 ± 0.013 | 1.21 | 15.3 |
| sediment | JSQ132 | tributary to Plum Creek | 355320 | 4523709 | 3.8 | 166 | 263 | 4 | Dh | | 0.525 ± 0.018 | 1.14 | 6.6 |
| sediment | JSQ134 | Independence Run | 339645 | 4505636 | 5.6 | 132 | 265 | 8 | Dciv, Dtr | | 0.227 ± 0.010 | 1.14 | 15.6 |
| sediment | JSQ135 | Boyers Run | 334526 | 4499965 | 4.0 | 128 | 295 | 10 | Dh | | 0.191 ± 0.006 | 1.14 | 18.7 |
| sediment | JSQ136 | tributary to Lick Run | 274525 | 4472077 | 3.3 | 260 | 371 | 6 | Dciv | | 0.956 ± 0.025 | 1.26 | 3.9 |
| sediment | JSQ142 | trib to Frankstown Branch Juniata River | 219895 | 4482125 | 2.8 | 283 | 397 | 10 | Dbh | | 0.426 ± 0.013 | 1.29 | 9.3 |
| sediment | JSQ149 | Greens Run | 272418 | 4543933 | 3.1 | 243 | 454 | 15 | Dlh | | 0.200 ± 0.011 | 1.31 | 20.5 |
| **Piedmont schist** | | | | | | | | | | | | |
| sediment | JSQ150 | Anderson Run | 386156 | 4407746 | 3.9 | 64 | 213 | 7 | Xo | | 0.373 ± 0.012 | 1.08 | 9.0 |
| sediment | JSQ152 | Mill Creek | 384773 | 4408102 | 3.0 | 123 | 214 | 5 | Xo | | 0.595 ± 0.026 | 1.10 | 5.6 |
| sediment | JSQ153 | tributary to Conowingo Creek | 398306 | 4409431 | 25.3 | 130 | 275 | 4 | Xo | | 0.300 ± 0.010 | 1.11 | 11.5 |
| sediment | JSQ154 | Kellys Run | 385427 | 4410511 | 5.5 | 54 | 259 | 8 | Xo | | 0.413 ± 0.012 | 1.13 | 8.4 |
| sediment | JSQ155 | tributary to Tucquan Creek | 385373 | 4413635 | 4.1 | 98 | 269 | 7 | Xo | | 0.395 ± 0.012 | 1.12 | 8.7 |
| sediment | JSQ156 | tributary to Beaver Creek | 370074 | 4417851 | 4.4 | 178 | 286 | 6 | Xo | | 0.368 ± 0.012 | 1.16 | 9.7 |
| sediment | JSQ157 | tributary to Bald Eagle Creek | 377032 | 4400946 | 3.9 | 143 | 222 | 5 | Xo | | 0.283 ± 0.008 | 1.11 | 12.2 |
| sediment | JSQ158 | Alum Rock Run | 372105 | 4403934 | 7.0 | 137 | 253 | 5 | Xo | | 0.380 ± 0.011 | 1.13 | 9.2 |
| sediment | JSQ159 | another tributary to East Branch | 361305 | 4407459 | 7.5 | 226 | 324 | 5 | Xo | | 0.433 ± 0.014 | 1.20 | 8.6 |
| sediment | JSQ160 | tributary to East Branch | 358792 | 4408665 | 3.8 | 199 | 299 | 5 | Xo | | 0.376 ± 0.012 | 1.18 | 9.7 |
| sediment | JSQ161 | Green Branch | 374105 | 4421671 | 3.4 | 116 | 235 | 6 | Xo | | 0.407 ± 0.014 | 1.12 | 8.4 |

*Coordinates are in UTM Zone 18 North, NAD83.

†Mean slope calculated from DEM with approximately 30 m resolution.

§Geologic formations representing at least 10% of the area of basin, as mapped in Bedrock Geology Map of Pennsylvania, and listed in order of decreasing predominance, by area. Formations names are as follows: Xo (Octoraro Formation), Obe (Bald Eagle Formation), Oj (Juniata Formation), St (Tuscarora Formation), Dciv (Irish Valley Member of Catskill Formation), Dbh (Brallier and Harrell Formations, undivided), Dck (Catskill Formation), Dh (Hamilton Group), Dlh (Lock Haven Formation), Dtr (Trimmers Rock Formation), MDhm (Huntley Mountain Formation), MDso (Shenango Formation through Oswayo Formation, undivided), Mb (Burgoon Sandstone), Mp (Pocono Formation), Pa (Allegheny Formation), Pp

#Concentrations of $^{10}$Be were determined relative to an ICN $^{10}$Be standard ($t_{1/2}$ = 1.5x10$^6$ yr) prepared by K. Nishiizumi.

**Production factor is the ratio between the basin production rate and the sea level, high latitude production rate.

††Erosion rates were calculated using production rates corrected for latitude and altitude considering neutrons only. We used a sea level, high latitude production rate of 5.2 atoms g$^{-1}$ yr$^{-1}$. Density for calculation of erosion rate was 2.7 g cm$^{-3}$. Grain size was 250-500 microns for all sediment samples.

§§Samples from nested basin pairs.

## A geologic contact is mapped through the field of tors, though the three samples were similar lithologically.

53

TABLE DR-2. GIS DATA SOURCES

| GIS dataset | Web link | Scale/Resolution |
|---|---|---|
| National Elevation Dataset (NED) | http://ned.usgs.gov | 1 arc sec (approx. 30 m) |
| Physiographic provinces | http://water.usgs.gov/GIS/metadata/usgswrd/XML/physio.xml | 1:7,000,000 |
| Late Wisconsinan Glacial Border 1:100,000 | http://www.pasda.psu.edu/summary.cgi/dcnr/pags/pags_glacier1k.xml | 1:100,000 |
| Digital bedrock geology of Pennsylvania | http://www.dcnr.state.pa.us/topogeo/map1/bedmap.aspx | 1:250,000 |
| PRISM | http://www.ocs.orst.edu/prism/ | 150 arc sec (approx. 4 km) |
| National Land Cover Data (NLCD) | http://landcover.usgs.gov/natllandcover.asp | 1 arc sec (approx. 30 m) |
| Digital Raster Graphics (DRG) | ftp://www.pasda.psu.edu/pub/pasda/drg24k-cu/ | 1:24,000 |

Sediment dynamics in the Susquehanna River Basin inferred from in situ-produced $^{10}$Be and contemporary sediment yield

Joanna M. Reuter*, Paul R. Bierman**, Milan J. Pavich***, Jennifer Larsen*, Robert C. Finkel****

*Geology Department, University of Vermont, Burlington, Vermont 05405

**Geology Department and School of Natural Resources, University of Vermont, Burlington, Vermont 05405

***U.S. Geological Survey, Reston, Virginia 20192

****Center for Accelerator Mass Spectrometry, Lawrence Livermore National Laboratory, Livermore, California 94550

## *Abstract*

The Susquehanna River drains 71,250 km$^2$ of the Appalachian Highlands and is the largest tributary, as well as the largest contributor of sediment, to Chesapeake Bay. Quantifying rates of sediment transport over time is important not only for understanding the basin itself but also for managing this important estuary. To develop a better understanding of past and present sediment dynamics, we measured $^{10}$Be concentrations from 88 fluvial sediment samples for comparison with sediment-yield data collected at U.S. Geological Survey (USGS) gaging stations.

Twenty eight $^{10}$Be measurements are from samples collected at USGS stream gages that also have sediment yield records. The basins that these samples represent are complex, with multiple lithologies and varying intensities of present-day land use; some were glaciated during the Pleistocene. $^{10}$Be concentrations for these basins range from 0.5 to 4.9 x 10$^5$ atoms g$^{-1}$ quartz overall, and from 1.7 to 4.9 x 10$^5$ atoms g$^{-1}$ quartz for the non-glaciated basins only.

$^{10}$Be concentrations from fluvial sediment of 60 samples from small (4.5 ± 3.5 km$^2$), single lithology basins range from 0.9 to 9.6 x 10$^5$ atoms g$^{-1}$ quartz, from which we infer erosion rates of 4 to 54 m/My. Results from small basins establish relationships between erosion rate and slope that we use to cross-check the results from the complex, USGS basins. The mean erosion rate inferred from small-basin data (16 ± 10 m/My) is similar to the mean erosion rate for the USGS basins (14 ± 4 m/My). We conclude that erosion rates inferred from $^{10}$Be for the non-glaciated basins are relatively robust and not systematically biased. No impact of agriculture, dams, or mining can be detected in this $^{10}$Be data set. Glaciated basins, however, have consistently low nuclide concentrations

(0.5 to 1.2 x $10^5$ atoms g$^{-1}$ quartz) and cannot be directly interpreted in terms of erosion rates because such basins do not conform to the assumptions of steady erosion and constant exposure.

$^{10}$Be-inferred erosion rates for non-glaciated USGS basins range from 8 to 22 m/My; sediment yields, given in the same units, range from 4 to 250 m/My. In contrast to $^{10}$Be results, which do not show evidence of land use impacts, basins with major dams have low sediment yields, and there is a weak positive correlation on the basin scale between sediment yield and percent of agricultural land. The highest sediment yields, as well as the greatest concentration of sediment yields that exceed $^{10}$Be-inferred erosion rates, occur in the Piedmont, a region of present and past intensive agricultural land use.

## *Introduction*

Over the past decade, cosmogenic $^{10}$Be measured in fluvial sediment has become a commonly used tool for inferring erosion rates and tracing sediment movement on a $10^3$ to $10^5$ year time scale (Bierman et al., 2001; Bierman and Nichols, 2004; von Blanckenburg et al., 2004). These erosion-rate estimates are useful for a variety of applications, from assessing whether modern sediment yields are in equilibrium with background sediment generation rates (Kirchner et al., 2001; Schaller et al., 2001; Matmon et al., 2003a) to testing geomorphic theories of landscape change (Matmon et al., 2003b; Reuter et al., in preparation). With its many applications, $^{10}$Be has now been measured from the sediment of more than 450 drainage basins on six continents (Reuter et al., 2004). Though $^{10}$Be was first measured in sediments in relatively small, simple basins (Brown et al., 1995; Granger et al., 1996; Clapp et al., 2000), the technique has

57

since been applied in basins with greater complexity and at larger scales (Schaller et al., 2001; Vance et al., 2003; Bierman et al., in press; Safran et al., in press). However, in more complicated basins, it can be difficult to determine how well assumptions underpinning the interpretation of $^{10}$Be concentrations as erosion rates have been met. Among the factors that could affect the accuracy of erosion rates inferred from $^{10}$Be measured in sediment are a history of glaciation (Vance et al., 2003), uneven quartz distribution (Bierman and Steig, 1996), loess deposition (Schaller et al., 2001), deep-seated land sliding (Niemi et al., 2004), trapping of sediment by dams, and intense land use (von Blanckenburg et al., 2004).

The Susquehanna River Basin (fig. 1) is a region where knowing erosion rates on a multi-millennial time scale is useful to approach a variety of problems related to land management and the history of landscape development (Reuter et al., in preparation). This is a complex basin, with varying lithology and land-use, both of which have the potential to violate assumptions inherent in the accurate interpretation of $^{10}$Be concentrations measured in sediment. However, comparison of existing sediment yield records and $^{10}$Be-based erosion rates is desirable, because it increases understanding of sediment and erosion dynamics over different time scales: multi-millennial in the case of $^{10}$Be and multi-annual to decadal in the case of sediment yield. In the Susquehanna River Basin, sub-basins with established records of sediment yield do not necessarily have characteristics that meet the assumptions for $^{10}$Be erosion rate interpretations (Bierman and Steig, 1996); this is a problem common to many stations with sediment yield records worldwide.

The approach laid out in the paper addresses this issue by sampling not only basins with sediment-yield data, but also a series of relatively small basins that were selected through geographic information systems (GIS) analysis to have characteristics that provide robust $^{10}$Be erosion rate estimates. We use these smaller basins to identify relationships between erosion rates and landscape characteristics; we then use these relationships to cross-check the results from the larger, more complex basins. Together, these data identify long-term, background rates and spatial patterns of erosion in the Susquehanna River Basin, allow us to explore limits of $^{10}$Be as a tool to understand rates of erosion, and suggest how representative $^{10}$Be erosion rate estimates are for complex basins. We compare $^{10}$Be erosion rates with sediment-yield data to determine the degree of similarity between long-term rates of sediment generation and short-term rates of sediment yield.

## *Background*

### *The Susquehanna River Basin*

The history of the Appalachian Mountains includes a series of Phanerozoic mountain building events, followed by rifting in the Triassic/Jurassic which created the passive margin that the Susquehanna River drains today (Shultz, 1999). The Appalachians are a decay-phase orogen that has been studied extensively both geologically and geomorphically (for example, Hitchcock, 1841; Davis, 1889; Hack, 1982; Shultz, 1999).

There are practical reasons to study the Susquehanna River Basin. More than 3.5 million people live within the Basin boundaries (United States Census Bureau, 2004), and

the Susquehanna River is the largest tributary to Chesapeake Bay, draining 71,250 km$^2$ of

New York, Pennsylvania, and Maryland (fig. 1). The river is a major contributor of

sediment to the Chesapeake Bay, the ecosystems of which are threatened by a variety of

human impacts including pollutants and increased sedimentation (Langland and Cronin,

2003). Since the late 1800s, sedimentation in much of Chesapeake Bay has exceeded pre-

land clearance rates (Langland and Cronin, 2003). Controlling sediment delivery to the

Bay is therefore an important management concern, especially because the mainstem

reservoirs of the Susquehanna River are at or near their sediment-storage capacity

(Langland and Hainly, 1997). Developing a better understanding of sediment dynamics in

the Susquehanna River Basin is key to devising effective management strategies.

*Climate and vegetation*

The Susquehanna River Basin climate is humid and temperate, with mean annual

precipitation ranging spatially from about 0.8 to 1.3 meters (Daly and Taylor, 1998).

Mean annual temperatures are 7.7ºC in Binghamton, New York and 12ºC in Harrisburg,

PA (http://www.nrcc.cornell.edu/ccd/nrmavg.html; accessed February 2005). Annual

snowfall averages from approximately 0.9 meters at Harrisburg, Pennsylvania, to 2.1 m at

Binghamton, New York (http://www.nrcc.cornell.edu/ccd/avgsnf98.html; accessed

February 2005). While precipitation varies across the basin (Daly and Taylor, 1998),

temporal climatic variability has exceeded the present-day spatial climate gradient. About

40% of Susquehanna River Basin was covered in glacial ice at the time of the

Wisconsinan glacial maximum (Pennsylvania Bureau of Topographic and Geologic

Survey, 1995a; Braun, 2004), and much of the rest of the Susquehanna River Basin experienced periglacial conditions at that time (Clark and Ciolkosz, 1988).

Vegetation has varied in conjunction with climate. As inferred from pollen data, at the glacial maximum, tundra was present near the glacial margin and boreal forests extended through the southern portion of the Susquehanna River Basin (Delcourt and Delcourt, 1981, 1984). As climate warmed, mixed hardwood and conifer forests returned to the Susquehanna region. Prior to European settlement, the Susquehanna River Basin was largely forested with a mix of hardwoods, pines (including the economically valuable white pine, *Pinus strobus*), and eastern hemlock (*Tsuga canadensis*) (Stranahan, 1993; Abrams and Ruffner, 1995). Currently, forest cover in the basins from which we collected sediment for [10]Be analyses ranges from 9% to 100%.

*Physiography, geology, and land use*

The Susquehanna River Basin is dominated by three physiographic provinces: the Appalachian Plateaus, Valley and Ridge, and Piedmont (fig. 1, fig. 2). The provinces are distinct geologically and topographically, with land use reflecting these factors. Although native Americans long inhabited the Susquehanna River Basin and certainly impacted the landscape, the largest changes have occurred since European settlement began in the late 1600s (Stranahan, 1993). A variety of human impacts can alter sediment dynamics; these include logging, dams, mining, agriculture, roads, and urban and suburban development (fig. 3).

The valleys of the Appalachian Plateaus are incised into relatively undeformed sedimentary bedrock, largely sandstone and shale in Pennsylvania, and also including

carbonate rocks to the north (NYS Museum/NYS Geological Survey, 1999; Pennsylvania

Bureau of Topographic and Geologic Survey, 2001). Some of the steepest topography

within the Susquehanna River Basin occurs in the non-glaciated part of the Plateaus (fig.

2). To the north of the glacial margin, the Plateaus become less rugged with more

farmland. The extensive forests that dominated the Susquehanna River Basin prior to

European settlement provided opportunity for logging across the region; in particular, the

white pine stands of the West Branch of the Susquehanna River, in the Appalachian

Plateaus, were especially valuable, and much of that topographically rugged region was

clear cut in the 1800s (Stranahan, 1993). That region is now largely covered in second

growth forest. Signs of logging are still present in the form of old roads, which are

common in even seemingly remote basins. While logging continues today, the operations

are focused on the less-steep areas.

The Valley and Ridge Province is an ancient fold and thrust belt that has eroded

such that the topography reflects lithology (Way, 1999). Ridges are dominated by

sandstone; valleys are underlain largely by carbonate and shale (USGS, 1999d;

Pennsylvania Bureau of Topographic and Geologic Survey, 2001). Present land use

patterns in the Valley and Ridge are strongly related to topography. Most ridges are

forested, though they have been logged historically. Agriculture dominates in the valleys,

and population centers are also primarily in the lowlands. Coal mining has had a major

impact on parts of the Valley and Ridge, as well as the Appalachian Plateaus (fig. 3).

Both strip mines and underground mines have been used to remove coal (Edmunds,

2003).

The Piedmont is geologically diverse. Carbonate, sandstone, and shale are prevalent in the northern part of the Piedmont, known as the Piedmont Lowlands. Much of the southern part of the Piedmont is underlain by metamorphic rocks (particularly schist); this is the Piedmont Upland Section (Fenneman and Johnson, 1946; Pennsylvania Bureau of Topographic and Geologic Survey, 2001). The Piedmont Upland has a fairly low relief upland surface that is incised by valley and gorges. Of the Susquehanna River Basin's physiographic provinces, the Piedmont has the highest percentage of agricultural land use (USGS, 1999c) and highest population density (United States Census Bureau, 2004).

Dams are common in all physiographic provinces of the Susquehanna River Basin. Small mill dams were built as early as the 1700s, and more than 300 of these were constructed in Lancaster County (in the Piedmont province) alone (Merritts and Walter, 2003). The construction of larger dams for a variety of purposes (including flood control, water supply, hydroelectric power, and recreation) began in the 1800s and peaked in the 1960s and 1970s (USGS, 1999a).

### *Erosion rates from [10]Be in sediment*

[10]Be is produced in quartz near the surface by cosmic-ray bombardment (Lal and Peters, 1967). In an eroding landscape, grains of quartz function as dosimeters, carrying isotopic records that reflect their near-surface exposure histories (Bierman and Steig, 1996). Rivers collect, transport, and mix grains from various parts of the basin. The abundance of cosmogenic isotopes in stream sediments primarily reflects the cosmic ray dosing of rock and soil on slopes and, to varying degrees, dosing during intermittent

storage as material is carried downstream (Bierman and Steig, 1996). The concentration of $^{10}$Be in river sediment reflects the integrated erosional history of the basin over both space and time.

About half of $^{10}$Be production occurs within the upper 50 to 100 centimeters of Earth's surface. In addition to the broad production zone, mixing of sediment near the surface homogenizes the $^{10}$Be profile; as a result, the method has a relatively low sensitivity to erosion caused by human disturbance or natural episodic change (Bierman and Steig, 1996; Phillips et al., 1998; Heimsath et al., 2002), though extreme land use effects (gullying and deep erosion) can impact $^{10}$Be results (von Blanckenburg et al., 2004). The time scale over which cosmogenic analysis is applicable relates to the residence time of material in the near surface where most of the production takes place. The $^{10}$Be-inferred erosion rates are thus averages over time scales long enough to incorporate infrequent geomorphic events; for the Susquehanna River Basin the time period is between 10,000 and 100,000 years

Because $^{10}$Be erosion rates are integrated over many millennia, these rates provide a relatively long-term background value with which to compare contemporary sediment yields, such as those determined by suspended sediment analysis or reservoir filling (Kirchner et al., 2001). Sediment yields have been found to exceed (Clapp et al., 2000; Hewawasam et al., 2003; von Blanckenburg et al., 2004), match (Matmon et al., 2003a), and fall below (Kirchner et al., 2001) the rates of sediment generation inferred from $^{10}$Be. In some cases, authors have suggested the discrepancy results from human impact; in other cases, natural variability, including extreme hydrologic events, has been cited as

driving the disequilibrium between long-term rates of sediment generation and short term rates of sediment delivery.

## *Methods*

### *Sampling Design*

Our approach included sampling two groups of basins: 1) the "USGS basins," a group of 28 samples from U.S. Geological Survey stream gaging stations, 26 of which have suspended sediment yield records (Gellis et al., 2004a) and 2) the "GIS-selected basins," a group of 60 small, relatively simple basins which were selected using GIS such that they would yield straight-forward erosion-rate interpretations from $^{10}$Be and such that they could be used to test for relationships between erosion rate, physiography, slope, and lithology. The motivation for sampling the USGS basins was to be able to determine if and where the modern sediment fluxes are in equilibrium with long-term sediment generation rates; the GIS-selected basins provide a cross-check for the complex USGS basins.

### *USGS basins*

Samples from USGS stream gage sites (n = 28) represent basins with a broad range of characteristics (tables 1 and 2). These basins range in scale from about 15 km$^2$ to 62,400 km$^2$; many are nested within each other. Most of the USGS basins are underlain by more than one lithology, and several span more than one physiographic province (table 2). Although most of these basins were not directly impacted by glaciation, seven are located entirely north of the Wisconsinan glacial margin, and three drain a

combination of glaciated and non-glaciated parts of the Susquehanna River Basin. These basins also have varying degrees of human impact from agriculture, dams, mining, and development (fig. 3, table 2).

*GIS-selected basins*

We sampled 60 non-glaciated basins, 0.6 to 25 km$^2$ in area ($4.5 \pm 3.5$ km$^2$, mean $\pm$ $1\sigma$), that span a range of mean slopes (2º to 21º) in three physiographic provinces; all of these basins are mapped as a single lithology: sandstone in the Appalachian Plateaus, sandstone and shale in the Valley and Ridge, and schist in the Piedmont (tables 3 and 4). Because of their size, uniform lithology, and location south of the glacial margin, these basins meet assumptions for accurately inferring erosion rates from $^{10}$Be concentrations.

We selected the sampled basins from thousands of candidate sub-basins with the goal of identifying relationships between landscape characteristics and $^{10}$Be erosion rates. After delineating boundaries of thousands of sub-basins at a range of scales using ESRI software, we summarized landscape characteristics within the basin boundaries, using a variety of digital spatial data sets: topography (USGS, 1999d), bedrock geology (Pennsylvania Bureau of Topographic and Geologic Survey, 2001), glacial extent (Pennsylvania Bureau of Topographic and Geologic Survey, 1995a), precipitation (Daly and Taylor, 1998), land cover (USGS, 1997, 1999c, 1999b), and physiographic province (Fenneman and Johnson, 1946; Pennsylvania Bureau of Topographic and Geologic Survey, 1995b).

Decisions regarding which basins to sample and at what scale were guided by an analysis of the characteristics of the available candidate basins. For example, we found

that if we selected small basins, we could sample basins over a wider range of mean basin slope than if we selected large basins (fig. 4). We were also able to ascertain limits on the maximum size of basins that we could sample if we wanted to restrict selected basins to those mapped as a single lithology.

The basins we chose based on this approach span nearly the entire range of existing slopes for the lithologic and physiographic combinations we decided to sample. However, we did not sample all lithologic and physiographic combinations. For example, even though carbonate is a common lithology in the Susquehanna River Basin, we did not sample such basins because they lack the quartz needed for [10]Be analysis. Because we selected basins on the basis of specific characteristics, sampled basins are not randomly distributed on the landscape.

Most of the GIS-selected basins are not nested, but we did sample four nested pairs. Two of these are in the Appalachian Plateaus, one is in the Valley and Ridge, and one is in the Piedmont. The Appalachian Plateaus and Valley and Ridge basins were sampled as nested pairs to capture low-slope, low-relief uplands in the small nested basin, and to capture steep slopes of a deeply incised valley in the lower part of the basin, such that the overall mean slope of the larger basin is substantially greater than for the smaller, inset basin. Although we did not find a Piedmont basin with analogous characteristics, we sampled a nested pair of basins on Mill Creek, a direct tributary to Holtwood Gorge on the Susquehanna River. (This basin is hereafter referred to as "Holtwood Mill Creek" to distinguish it from the USGS stream gage site, Mill Creek at Eshelman Mill Road near Lyndon, PA.) The stream gradient near the outlet of Holtwood Mill Creek is quite steep, with extensive exposed bedrock and several waterfalls. We took one sample in this reach

67

of the stream and a second sample upstream, where the channel gradient is less steep, and the morphology is more similar to the stream channels observed elsewhere in the Susquehanna River Basin: a meandering channel within alluvial fill. Although the channel gradient and appearance change substantially between the two sample sites, the mean basin slope for the two nested basins represented by the samples differs by < 1°.

*Sample collection and processing*

At each site, we acquired a sample of sediment from the active channel or flood plain. When water was available (as it was in most streams during the wet summer of 2003), we sieved the samples in the field to include the 250-850 micron size fraction. We used the 250-500 micron size fraction of quartz for all analyses of sediment. This size fraction was chosen due to its abundance, and because the sand-sized fraction tends to provide the most representative erosion rates (Matmon et al., 2003b). We used standard procedures to purify 40 grams of quartz (Kohl and Nishiizumi, 1992) and to isolate beryllium (Bierman and Caffee, 2001). We measured [10]Be with the Accelerator Mass Spectrometer at Lawrence Livermore National Laboratory. A process blank was included with every batch of seven samples and used to correct measured isotopic ratios for that batch.

*Calculation of [10]Be erosion rates*

We used an accepted interpretative model for calculating erosion rates (Bierman and Steig, 1996) with a sea level, high latitude production rate of 5.2 atoms $g^{-1}$ quartz $yr^{-1}$, an attenuation depth of 165 $g/cm^2$, and a rock density of 2.7 g $cm^{-3}$. We did not make

minor model corrections for muons, topographic shielding, quartz enrichment (Riebe et al., 2001a), magnetic field variations, or snow cover (Schildgen et al., 2005).

We calculated latitude- and elevation-corrected, basin-wide production rates based on the polynomials from Lal (1991). We applied the polynomials on a pixel-by-pixel basis to calculate the production factor for each pixel according to its elevation and latitude. The basin-wide production factor is a mean of the production factors calculated for each pixel within the basin boundaries. The results are the same as for a hypsometric approach, as commonly applied previously (for example, Matmon et al., 2003b).

We took this pixel-by-pixel approach a step further to account for non-uniform quartz distribution within basins. Pixels are weighted according to their estimated quartz content, and we calculated a production rate that weights quartz-rich regions of a basin more heavily than quartz-poor regions. This is a somewhat crude approach, as it does not account for dosing during transport, and it assumes that erosion rates do not vary by lithology. However, the calculation of quartz-weighted production rates can be used to begin to assess one bias associated with the common problem of non-uniform quartz source distribution. To apply this approach for the Susquehanna River Basin, we weighted quartz distribution based on mapped lithology and constrained the percent quartz based on quartz recovery during sample processing. It turns out that weighting the rate for quartz distribution changes the inferred erosion rates by less than 10% (table 5); because of this, and because of uncertainties in quartz contents, we chose to present results based on the traditional use of production rates unweighted by lithology.

69

***Cross-checking[10]Be erosion rates for USGS basins using relationships established by
GIS-selected basins***

We use relationships established between erosion rates and landscape
characteristics for the GIS-selected basins to predict erosion rates for the USGS basins.
Erosion rate and slope are positively correlated for the GIS-selected basins (fig. 5, Reuter
and others, in preparation), and the erosion-slope regression varies by physiographic
province. After accounting for slope, we did not detect any relationship between erosion
rate and lithology (Reuter et al., in preparation).

Based upon these relationships, we made three sets of predictions for erosion rates
of the non-glaciated USGS basins. All predictions incorporate relationships between
erosion rate and slope. Because slope is dependent on the size of the area within which it
is averaged (fig. 4), we resampled the slope map to a grid cell size of approximately 5
$km^2$, which is similar to the mean area of the GIS-selected basins from which the
relationships were established.

The three approaches for predicting erosion rates for the USGS basin are as
follows:

1) We used the single best regression between erosion rate and slope based upon the data
for all GIS-selected basins collectively. For each cell:

predicted erosion rate (m/My) = 1.44 * mean slope of cell (º) + 2.66

We took the mean value of the cells within each basin to obtain a predicted erosion rate
based on this method.

2) We made separate predictions for each physiographic province, based on regressions
between erosion rate and slope for the GIS-selected basins within each province. Because

there was no correlation between erosion rate and slope within the Piedmont, we used the mean erosion rate from the GIS-selected basins for that region.

App. Plateaus predicted erosion rate (m/My) = 1.62 * mean slope of cell (º) + 4.87

Valley & Ridge predicted erosion rate (m/My) = 0.81 * mean slope of cell (º) + 5.96

Piedmont predicted erosion rate (m/My) = 8.9

We used physiographic classifications based on Fenneman and Johnson (1946). A small part of the Susquehanna River Basin is mapped as Blue Ridge (primarily affects Yellow Breeches Creek), and because we do not have separate GIS-selected basins for this physiographic province, we treated it with the Valley and Ridge.

3) We used the approach in (2) with modifications to account for non-uniform quartz distribution. Even if different lithologies erode at similar rates, as our data suggest, the lithologies with higher quartz contents will contribute more quartz to the sample. To account for this, we calculated a weighted average based on estimated relative quartz contents of the mapped lithologies assuming the following quartz contents: sandstone, 90%; shale, 20%; metamorphic/igneous rocks, 20%; carbonate rocks, 5%.

*Sediment yield*

We compare the [10]Be results to sediment yield data from Gellis and others (2004a), Williams and Reed (1972), and unpublished data from A. Gellis. The sediment yield results are based only on suspended sediment yield. Records for individual gages range from 2 to 29 years and span the period from 1953 to 2001. We do not attempt corrections to incorporate dissolved load or bedload, so the sediment yield data provide minimum values of sediment export from the basins during the period of record. Bedload

71

is commonly assumed to represent about 10% of the total load (Knighton, 1998), while dissolved load varies considerably depending upon basin lithology and climate (Judson and Ritter, 1964). To compare the sediment yield with $^{10}$Be erosion rates, we compute the basin-average erosion rates that the sediment yield would represent assuming that the sediment transport out of the basin is in equilibrium with upland erosion; we use a density of 2.7 g cm$^{-3}$.

### *Data and interpretations*

### $^{10}$Be concentrations

River and stream sediment from the Susquehanna River Basin contains significant and varied concentrations of $^{10}$Be. For the small, GIS-selected basins, the measured $^{10}$Be concentrations range from 0.92 to 9.6 x 10$^5$ atoms g$^{-1}$ quartz (table 6). In comparison, the larger USGS non-glaciated basins have a narrower range of $^{10}$Be concentrations (1.7 to 4.9 x 10$^5$ atoms g$^{-1}$ quartz; table 5). The concentration of $^{10}$Be in large, partly-glaciated USGS basins overlaps the low end of the range for the USGS non-glaciated basin (1.3 to 2.5 x 10$^5$ atoms g$^{-1}$ quartz). The lowest $^{10}$Be concentrations were measured from fully glaciated basins (0.5 to 1.2 x 10$^5$ atoms g$^{-1}$ quartz). Because the basins affected by glaciation are a distinct population (fig. 6), violating the assumptions underlying the interpretation of $^{10}$Be concentrations as erosion rates, we do not make erosion rate calculations directly for these samples.

Normalized for latitude and altitude, the average $^{10}$Be concentration in river-transported quartz for the smaller GIS-selected basins, (2.7 ± 1.4 x 10$^5$ atoms g$^{-1}$ quartz, mean and standard deviation, n= 60), is similar to the average for the larger non-glaciated

USGS basins ($2.4 \pm 0.8$ x $10^5$ atoms g$^{-1}$ quartz, n=18). Although the averages are similar across basin scale, the range in $^{10}$Be concentrations decreases with increasing basin area (fig. 7A).

### *$^{10}$Be erosion rates*

The inferred erosion rates for the smaller GIS-selected basins range from 4 to 54 m/My (fig. 8), while the larger USGS non-glaciated basin erosion rates range from 8 to 22 m/My (fig. 9). When grouped by physiographic province, the results for the USGS non-glaciated basins are broadly consistent with the results from the GIS-selected basins for the corresponding region (fig.10). For the Appalachian Plateaus and the Valley and Ridge, the range of erosion rates for the small, GIS-selected basins exceeds and includes the range of erosion rates from $^{10}$Be for the larger USGS basins (fig. 10); this corresponds to the pattern observed for the Susquehanna River Basin as a whole (fig. 7). The pattern in the Piedmont province is different; there, the USGS basins have higher $^{10}$Be-inferred erosion rates on average than the GIS-selected basins.

When small, GIS-selected basins are subdivided by physiographic province and lithology (fig 5), a positive correlation exists between erosion rate and slope for each physiographic and lithologic grouping except the Piedmont schist (Reuter et al., in preparation). The sandstone and shale results for the Valley and Ridge span a similar range of slopes; the lower maximum slope for shale reflects a lack of steep shale basins. After accounting for slope, no discernible relationship exists between erosion rate and lithology (Reuter and others, in preparation, fig. 10). Although slope is a useful predictor

of erosion rates for the small, GIS-selected basins, the larger but less-steep, non-glaciated USGS basins show no relationship between erosion rate and slope.

The results for the nested GIS-selected basins show that when the mean basin slopes differ substantially in the nested pairs, the erosion rates are slower for the less steep basins and faster for the steeper basins (table 6). However, in the Holtwood Mill Creek Basin, which has a steeper channel gradient in the lower portion of the basin but not steeper mean basin slopes, the results are indistinguishable, with 5.6 m/My for the upstream sample (JSQ152) and 5.5 m/My for the downstream sample (JSQ151).

### Cross-checking [10]Be erosion rates for USGS basins with relationships established from GIS-selected basins

For the non-glaciated USGS basins, erosion rates inferred from measured [10]Be are consistent with the erosion rates predicted from GIS-selected basin relationships (table 7). The average difference between the inferred and predicted values is about 5 m/My or 39%. The largest discrepancy between predicted and inferred values for a basin is a little more than a factor of two. For method 2, approximately 75% of the predicted erosion rates are within 50% of the values inferred directly from [10]Be. The average of the predicted values for all USGS non-glaciated basins is 13 ± 5 m/My, closely corresponding to the average of the measured value for the same basins (14 ± 4 m/My).

The broad agreement indicates that the inferred [10]Be erosion rates for the non-glaciated USGS basins are not systematically biased. In spite of the complexity of these basins in terms of lithology and land use, the [10]Be measurements yield individual inferred erosion rates that are likely to be accurate within a factor of two at worst. When

74

considered as an average, the $^{10}$Be inferred erosion rates for these large, complex basins are likely more accurate (10-20%). The inability to make better predictions of USGS-basin erosion rates from the GIS-selected basin data probably reflects the substantial scatter that is present in the data set upon which the relationships for the predictions are based. The relationships for the predictions are, after all, based only upon slope and physiographic province, and the predictions are applied across lithologies that were not represented in the population of GIS-selected basins.

## *Discussion*

Data from small basins demonstrate that $^{10}$Be-inferred erosion rates for the large, non-glaciated USGS basins do indeed reflect long-terms rates of erosion. This finding, that the inferred $^{10}$Be erosion rates for the non-glaciated USGS basins are robust, presents the opportunity to compare isotopic results with the sediment yield data for the same basins. We use this comparison to assess human impact within the Susquehanna River Basin and to consider spatial and temporal scaling relationships for sediment generation and yield.

### *Robust long-term erosion rates from $^{10}$Be data for non-glaciated regions*

The observed patterns in the isotopic data suggest that $^{10}$Be-inferred erosion rates for the non-glaciated USGS basins do indeed reflect long-term rates of erosion. Specifically, the ability to predict erosion rates for the large, complex USGS basins based on results from the small GIS-selected basins indicates that the results for the USGS basins are not systematically biased (table 7). This conclusion is also supported by the observed collapse in the range of erosion rates as basin scale increases (fig. 7), a pattern

75

that is commonly observed in [10]Be data generated from sediments collected along drainage networks (Bierman et al., 2001; Matmon et al., 2003a; Bierman et al., in press). Furthermore, no relationship exists between [10]Be erosion rate and land use (fig. 11A), indicating once again that this isotopic method of erosion rate determination is insensitive to recent land-use impacts.

[10]Be-inferred erosion rates are insensitive to many land-use impacts because eroding soil profiles tend to be vertically well mixed with respect to [10]Be (Phillips et al., 1998; Heimsath et al., 2002), thus buffering the system against shallow erosion (dm to m scale). Although it is possible for the impacts of land use to be detectable in [10]Be results in extreme cases of deep and sustained erosion (von Blanckenburg et al., 2004), our data do not indicate that land use impacts affect [10]Be results in the Susquehanna River Basin (fig. 11B). Even basins that have intense farming, high sediment yields, and a large amount of historical sediment in storage (Merritts and Walter, 2003) have [10]Be concentrations that fall well within the range of values from less-impacted basins (table 5).

Dams have the potential to affect both sediment yield and [10]Be results by changing the proportion of sediment that reaches the sampling site from various parts of the basin. The impact is likely to be subtle and difficult to detect for [10]Be data, and, indeed, the two non-glaciated USGS basins with large dams that impact >10% of their basin area (Juniata and Codorus) show no detectable signs of dam impact in their [10]Be data. The impact of dams on suspended sediment yield is far more easily detected; rates for the basins impacted by major dams (9 ± 3 m/My, n = 5; dammed area >10% during period of record) are notably lower than for the other basins (39 ± 61 m/My, n = 21; table

76

2, table 5). The pattern of consistently low suspended sediment yield from basins with dam impact is also apparent in figure 7B; this figure includes additional dam-impacted stations (ones that were not sampled for $^{10}$Be) on the mainstem of the lower Susquehanna River (Gellis et al., 2004a).

Mining has the potential to introduce rock, excavated from depth and containing little or no $^{10}$Be, directly into surface streams and rivers. Of the non-glaciated basins sampled, only one basin, West Branch Susquehanna at Bower, PA, has notable strip mine impact. Based on the land cover data (USGS, 1999c), about 3% of the basin is classified as barren, a classification that tends to be a good proxy for strip mines in this region, based on spot checks with USGS quadrangle maps. In this basin, the strip mines do not appear to substantially impact $^{10}$Be data. The erosion rate from the measured $^{10}$Be is 19 m/My, a value that reasonably matches the erosion rates predicted from the GIS-selected basin relationships (16 m/My, average of the three methods). Though the sediment yield record is short for this station, the inferred erosion rate of 15 m/My is consistent with the $^{10}$Be data.

Although we find that $^{10}$Be data are robust to a variety of human impacts, samples from glaciated regions do not yield results that can be directly interpreted as erosion rates. Glaciers affect $^{10}$Be production because the ice shields the ground surface, absorbing neutrons that would otherwise produce $^{10}$Be in surficial material; in addition, ice erodes material irradiated during interglacial periods. Consistently low $^{10}$Be concentrations in samples collected from the glaciated regions suggests that these areas have not yet regained isotopic steady state, that is, a condition in which the production of $^{10}$Be is matched by its export from the basin in sediment. Although $^{10}$Be measured in

77

sediment from glaciated basins cannot be used to infer erosion rates directly and thus cannot be compared to sediment yield data, the consistently low $^{10}$Be concentrations from the glaciated Susquehanna sub-basins are consistent with their geologic history.

### *Comparison of $^{10}$Be and sediment yield data*

Although $^{10}$Be and sediment yield are fundamentally different measurements, both apply on the scale of drainage basins, and a comparison of the two types of data can provide insight about sediment dynamics on different time scales. $^{10}$Be data provide long-term, background rates of erosion and thus maximum rates of sediment generation on a $10^4$ to $10^5$ year time scale for the Susquehanna River Basin. In contrast, the time scale associated with sediment yield data corresponds to the period of collection, which ranges from years to decades for the Susquehanna River Basin. Sediment yield represents the amount of sediment leaving the basin, but it does not necessarily fully reflect the movement of sediment within a basin (Trimble, 1977; Phillips, 2003). Furthermore, a variety of human impacts, including farming, logging, and development, have been shown repeatedly to change rates of sediment movement from, as well as within, drainage basins (Wolman, 1967; Trimble, 1997).

Many Susquehanna River Basin gaging stations have broadly similar sediment yields and $^{10}$Be-inferred erosion rates (fig. 9, table 5). However, when expressed in comparable units, the range of sediment yields exceeds the range of $^{10}$Be erosion rates by an order of magnitude. For stations with 3 or more years of record, sediment yields range from 12 to 480 metric tons km$^{-2}$ year$^{-1}$, corresponding to basin average erosion rates of 4 to 180 m/My with a mean of 28 m/My and a median of 14 m/My (table 5), in contrast to

a range of 8 to 22 m/My (mean and median, 14 m/My) from [10]Be for the non-glaciated

USGS basins. The [10]Be data show no relationship with land use (fig. 11A). In contrast, a

weak but positive relationship exists between sediment yield data and the percent of land

classified as "herbaceous planted/cultivated," a proxy for present-day agricultural impact

(fig. 11B).

A comparison of the [10]Be-inferred erosion rates and sediment yield results by

physiographic province shows that Piedmont stations consistently have the highest ratios

of sediment yield to [10]Be-inferred erosion rate; few stations in the Appalachian Plateaus

and Valley and Ridge show large discrepancies (fig. 9, fig. 10). In addition to having high

sediment yields, the Piedmont is also the physiographic province with the highest

percentage of agricultural land (fig. 3, fig. 11).

Sediment yield data show not only that the Piedmont sediment yields are currently

high; comparison with [10]Be-inferred erosion rates indicates that present-day sediment

yields are unsustainable, as they are greatly elevated relative to the long-term background

rates of sediment generation. Furthermore, the high sediment yields tend to be in areas

with high percentages of agricultural land, suggesting that past and present agricultural

practices contribute to high Piedmont sediment yields. Correlation need not imply

causation, however, and other factors may matter as well. Indeed, the connection between

upland land use and sediment delivery is not always direct and immediate. For example,

the Piedmont has a long agricultural legacy, and present sediment yields likely reflect

ongoing impacts of past land use. Of particular importance is the legacy of mill dams and

the large volume of previously mobilized sediment stored behind them (Merritts and

Walter, 2003). This sediment, mobilized as the result of past land use, went into

79

temporary storage as colluvium and alluvium, and now is likely contributing to high, present-day sediment yields (Trimble, 1977).

### *Spatial and temporal scaling*

Considering the differences between $^{10}$Be and sediment yield data provides insight into rates and patterns of erosion across differing spatial and temporal scales. The range of $^{10}$Be-inferred erosion rates in the Susquehanna River Basin decreases with increasing spatial scale (fig. 7), an observation common to many river network studies done with this isotope (Bierman et al., 2001; Matmon et al., 2003a; Bierman et al., in press). Clearly, this collapse in variability testifies to the efficiency with which rivers mix sediments from different sub-basins. Furthermore, the lack of downstream changes in $^{10}$Be concentration suggests that most irradiation occurs on hillslopes rather than in channels or during near-channel storage. Indeed, the isotopic data suggest that over geologic time scales, sediment residence times are much longer on hillslopes than they are in and near channels.

Sediment yield data have a very different spatial pattern and tell a very different story. Sediment yields are high relative to background sediment generation rates in areas of intense agriculture and low where existing dams trap sediment. The collapse in variability so evident in the $^{10}$Be data (fig. 7A) is nowhere to be found in the sediment yield plots (fig. 7B); rather, there is an apparent decline in sediment yields at larger basin areas that likely reflects trapping by dams on the mainstem Susquehanna River. Together, the $^{10}$Be and sediment yield data suggest that present-day sediment discharge from a

number of Susquehanna sub-basins is out of equilibrium with background rates of sediment generation.

Although the patterns of [10]Be and sediment yield with area are different (fig. 7), it is notable that the magnitude of the sediment yield results are consistent with rates of sediment generation inferred from [10]Be with only a few exceptions. Perhaps such similarity is also the result of human impact, with much recently eroded sediment still trapped on the landscape in temporary storage. Whether held in colluvial or alluvial deposits, or retained behind thousands of mill dams (Merritts and Walter, 2003), much human-induced erosion of the uplands is not detected by contemporary sediment loads (Costa, 1975; Trimble, 1977). Such temporary storage likely buffers the sediment delivery system, tending to keep short-term sediment yields reasonably similar to long-term sediment generation rates (Phillips, 2003) until and unless stored sediment is released by breaching of dams or the erosion of recent fill terraces (Wolman, 1967; Trimble, 1997).

## *References cited*

Abrams, M.D., and Ruffner, C.M., 1995, Physiographic analysis of witness-tree distribution (1765-1798) and present forest cover through north central Pennsylvania: Canadian Journal of Forest Research, v. 25, p. 659-668.

Bierman, P., Clapp, E., Nichols, K., Gillespie, A., and Caffee, M.W., 2001, Using cosmogenic nuclide measurements in sediments to understand background rates of erosion and sediment transport, *in* Harmon, R.S., and Doe III, W.W., eds., Landscape Erosion and Evolution Modeling: New York, Kluwer, p. 89-115.

Bierman, P., and Nichols, K.K., 2004, Rock to sediment--Slope to sea with 10-Be--Rates of landscape change: Annual review of Earth and Planetary Sciences, v. 32, p. 215-255.

Bierman, P., and Steig, E.J., 1996, Estimating rates of denudation using cosmogenic isotope abundances in sediment: Earth Surface Processes and Landforms, v. 21, p. 125-139.

Bierman, P.R., and Caffee, M., 2001, Slow rates of rock surface erosion and sediment production across the Namib Desert and escarpment, Southern Africa: American Journal of Science, v. 301, p. 326-358.

Bierman, P.R., Reuter, J.M., Pavich, M., Gellis, A., Caffee, M.W., and Larsen, J., in press, Using cosmogenic nuclides to contrast rates of erosion and sediment yield in a semi-arid, arroyo-dominated landscape, Rio Puerco Basin, New Mexico: Earth Surface Processes and Landforms.

Braun, D.D., 2004, The glaciation of Pennsylvania, USA, *in* Ehlers, J., and Gibbard, P.L., eds., Quaternary glaciations--extent and chronology, Part II: Amsterdam, Elsevier, p. 237-242.

Brown, E.T., Stallard, R.F., Larsen, M.C., Raisbeck, G.M., and Yiou, F., 1995, Denudation rates determined from the accumulation of in situ-produced [10]Be in the Luquillo Experimental Forest, Puerto Rico: Earth and Planetary Science Letters, v. 129, p. 193-202.

Clapp, E.M., Bierman, P.R., Schick, A.P., Lekach, J., Enzel, Y., and Caffee, M., 2000, Sediment yield exceeds sediment production in arid region drainage basins: Geology, v. 28, p. 995-998.

Clark, G.M., and Ciolkosz, E.J., 1988, Periglacial geomorphology of the Appalachian Highlands and Interior Highlands south of the glacial border--a review: Geomorphology, v. 1, p. 191-220.

Costa, J.E., 1975, Effects of agriculture on erosion and sedimentation in the Piedmont province, Maryland: Geological Society of America Bulletin, v. 86, p. 1281-1286.

Daly, C., and Taylor, G., 1998, Pennsylvania average annual precipitation, 1961-90, http://www.ocs.orst.edu/prism/, accessed: April 2005.

Davis, W.M., 1889, The rivers and valleys of Pennsylvania: National Geographic Magazine, v. 1, p. 183-253.

Delcourt, P.A., and Delcourt, H.R., 1981, Vegetation maps for eastern North America: 40,000 yr B.P. to the present, *in* Romans, R.C., ed., Geobotany II: New York, Plenum Press, p. 123-165.

—, 1984, Late Quaternary paleoclimates and biotic responses in eastern North America and the western North Atlantic Ocean: Palaeogeography, Palaeoclimatology, Palaeoecology, v. 48, p. 263-284.

Edmunds, W.M., 2003, Coal in Pennsylvania (2nd ed.): Harrisburg, Pennsylvania Geological Survey, 28 p.

Fenneman, N.M., and Johnson, D.W., 1946, Physiographic divisions of the coterminous U.S., http://water.usgs.gov/GIS/metadata/usgswrd/XML/physio.xml, accessed: March 2005.

Gellis, A.C., Banks, W.S.L., Langland, M.J., and Martucci, S.K., 2004, Summary of suspended-sediment data for streams draining the Chesapeake Bay watershed, water years 1952-2002, USGS Scientific Investigations Report 2004-5056, 59 p.

Granger, D.E., Kirchner, J.W., and Finkel, R., 1996, Spatially averaged long-term erosion rates measured from in situ-produced cosmogenic nuclides in alluvial sediments: Journal of Geology, v. 104, p. 249-257.

Hack, J.T., 1982, Physiographic divisions and differential uplift in the Piedmont and Blue-Ridge, USGS Professional Paper 1265, 49 p.

Heimsath, A.M., Chappell, J., Spooner, N.A., and Questiaux, D.G., 2002, Creeping soil: Geology, v. 30, p. 111-114.

Hewawasam, T., von Blanckenburg, F., Schaller, M., and Kubik, P., 2003, Increase of human over natural erosion rates in tropical highlands constrained by cosmogenic nuclides: Geology, v. 31, p. 597-600.

Hitchcock, E., 1841, Final report on the geology of Massachusetts: Amherst, MA, J. S. and C. Adams, 831 p.

Judson, S., and Ritter, D.F., 1964, Rates of regional denudation in the United States: Journal of Geophysical Research, v. 69, p. 3395-3401.

Kirchner, J.W., Finkel, R.C., Riebe, C.S., Granger, D.E., Clayton, J.L., King, J.G., and Megahan, W.F., 2001, Mountain erosion over 10 yr, 10 k.y., and 10 m.y. time scales: Geology, v. 29, p. 591-594.

Knighton, D., 1998, Fluvial forms and processes: a new perspective: New York, Oxford University Press Inc., 383 p.

Kohl, C.P., and Nishiizumi, K., 1992, Chemical isolation of quartz for measurement of in-situ -produced cosmogenic nuclides: Geochimica et Cosmochimica Acta, v. 56, p. 3583-3587.

Lal, D., 1991, Cosmic ray labeling of erosion surfaces: in situ nuclide production rates and erosion models: Earth and Planetary Science Letters, v. 104, p. 424-439.

Lal, D., and Peters, B., 1967, Cosmic ray produced radioactivity on the earth, *in* Sitte, K., ed., Handbuch der Physik: New York, Springer-Verlag, p. 551-612.

Langland, M., and Cronin, T., 2003, A summary report of sediment processes in Chesapeake Bay and watershed: New Cumberland, Pennsylvania, USGS Water-Resources Investigations Report 03-4123, 109 p.

Langland, M.J., and Hainly, R.A., 1997, Changes in bottom surface-elevations in three reservoirs on the lower Susquehanna River, Pennsylvania and Maryland, following the January 1996 flood--Implications for nutrient and sediment loads to Chesapeake Bay, USGS Water-Resources Investigations Report 97-4138, 34 p.

Matmon, A., Bierman, P.R., Larsen, J., Southworth, S., Pavich, M., and Caffee, M., 2003a, Temporally and spatially uniform rates of erosion in the southern Appalachian Great Smoky Mountains: Geology, v. 31, p. 155–158.

Matmon, A., Bierman, P.R., Larsen, J., Southworth, S., Pavich, M., Finkel, R., and Caffee, M., 2003b, Erosion of an ancient mountain range, the Great Smoky Mountains, North Carolina and Tennessee: American Journal of Science, v. 303, p. 817-855.

Merritts, D., and Walter, R., 2003, Colonial mill ponds of Lancaster County Pennsylvania as a major source of sediment pollution to the Susquehanna River and Chesapeake Bay, *in* Merritts, D., Walter, R., and de Wet, A., eds., Channeling through time: landscape evolution, land use change, and stream restoration in the lower Susquehanna River Basin: Southeast Friends of the Pleistocene Fall 2003 Fieldtrip Guidebook, p. 56-65.

Niemi, N., Oskin, M., and Burbank, D., 2004, A numerical simulation of the effects of mass-wasting on cosmogenically determined erosion rates: Eos Transactions American Geophysical Union, Fall Meeting Supplement, Abstract H51C-1157, v. 85.

NYS Museum/NYS Geological Survey, 1999, Statewide bedrock geology, http://www.nysm.nysed.gov/gis.html, accessed: March 2005.

Pennsylvania Bureau of Topographic and Geologic Survey, Department of Conservation and Natural Resources., 1995a, Late Wisconsinan glacial border 1:100,000, http://www.pasda.psu.edu/documents.cgi/dcnr/pags/pags_glacier1k.xml, accessed: March 2005.

—, 1995b, Physiographic provinces 1:100,000, http://www.pasda.psu.edu/documents.cgi/dcnr/pags/pags_physprov1k.xml, accessed: March 2005.

—, 2001, Digital bedrock geology of Pennsylvania, http://www.dcnr.state.pa.us/topogeo/map1/bedmap.aspx, accessed: March 2005.

Phillips, J., 2003, Alluvial storage and the long-term stability of sediment yields: Basin Research, v. 15, p. 153-163.

Phillips, W.M., McDonald, E.V., Reneau, S.L., and Poths, J., 1998, Dating soils and alluvium with cosmogenic 21Ne depth profiles: case studies from the Pajarito Plateau, New Mexico, USA: Earth and Planetary Science Letters, v. 160, p. 209-223.

Reuter, J.M., Bierman, P.R., Pavich, M.J., Larsen, J., and Finkel, R.C., 2004, Linking [10]Be estimates of erosion rates with landscape variables: compilation and consideration of multiple data sets from around the world, 32nd International Geological Conference: Florence.

—, in preparation, Testing models of Appalachian Mountain geomorphology with erosion rates inferred from cosmogenic [10]Be.

Riebe, C.S., Kirchner, J.W., and Granger, D.E., 2001, Quantifying quartz enrichment and its consequences for cosmogenic measurements of erosion rates from alluvial sediment and regolith: Geomorphology, v. 40, p. 15-19.

Safran, E.B., Bierman, P.R., Aalto, R., Dunne, T., Whipple, K.X., and Caffee, M., in press, Erosion rates driven by channel network incision in the Bolivian Andes: Earth Surface Processes and Landforms.

Schaller, M., von Blanckenburg, F., Hovius, N., and Kubik, P.W., 2001, Large-scale erosion rates from in situ-produced cosmogenic nuclides in European river sediments: Earth and Planetary Science Letters, v. 188, p. 441-458.

Schildgen, T.F., Phillips, W.M., and Purves, R.S., 2005, Simulation of snow shielding corrections for cosmogenic nuclide surface exposure studies: Geomorphology, v. 64, p. 67-85.

Shultz, A.P., editor, 1999, The geology of Pennsylvania: Harrisburg, PA, Pennsylvania Geological Survey, 888 p.

Stranahan, S.Q., 1993, Susquehanna, river of dreams: Baltimore, The Johns Hopkins University Press, 322 p.

Trimble, S.W., 1977, The fallacy of stream equilibrium in contemporary denudation studies: American Journal of Science, v. 277, p. 876-887.

—, 1997, Contribution of stream channel erosion to sediment yield from an urbanizing watershed: Science, v. 278, p. 1442-1444.

Tully, J., 2001, Coal fields of the United States, http://www.nationalatlas.gov/metadata/coalfdp050.html, accessed: March 2005.

United States Census Bureau, 2004, U.S. Census Database, 2000, http://nationalatlas.gov/atlasftp.html, accessed: March 2005.

USGS, 1997, New York land cover data set, http://landcover.usgs.gov/nlcd/show_data.asp?code=NY&state=New_York, accessed: April 2005.

—, 1999a, Major dams of the United States, http://nationalatlas.gov/atlasftp.html, accessed: June 2003.

—, 1999b, Maryland land cover data set, http://landcover.usgs.gov/nlcd/show_data.asp?code=MD&state=Maryland, accessed: April 2005.

—, 1999c, Pennsylvania land cover data set, http://landcover.usgs.gov/nlcd/show_data.asp?code=PA&state=Pennsylvania, accessed: April 2005.

—, 2002, Cities and towns of the United States, http://nationalatlas.gov/atlasftp.html, accessed: April 2005.

USGS, E.D.C., 1999d, National elevation dataset, http://gisdata.usgs.net/ned/, accessed: April 2005.

Vance, D., Bickle, M., Ivy-Ochs, S., and Kubik, P.W., 2003, Erosion and exhumation in the Himalaya from cosmogenic isotope inventories of river sediments: Earth and Planetary Science Letters, v. 206, p. 273-288.

von Blanckenburg, F., Hewawasam, T., and Kubik, P.W., 2004, Cosmogenic nuclide evidence for low weathering and denudation in the wet, tropical highlands of Sri Lanka: Journal of Geophysical Research, v. 109, p. 1-22.

Way, J.H., 1999, Appalachian Mountain section of the Ridge and Valley province, *in* Shultz, C.H., ed., The geology of Pennsylvania: Harrisburg, Pennsylvania Geological Survey, p. 353-361.

Williams, D.F., and Reed, L.A., 1972, Appraisal of stream sedimentation in the Susquehanna River Basin, USGS Water-Supply Paper 1532-F, 24 p.

Wolman, G.M., 1967, A cycle of sedimentation and erosion in urban river channels: Geografiska Annaler, v. 49A, p. 385-395.

## Figure Captions

Fig. 1. The Susquehanna River drains 71,250 km$^2$ of New York, Pennsylvania, and Maryland before flowing into Chesapeake Bay. Dominant physiographic provinces, shown on map, are the Appalachian Plateaus, Valley and Ridge, and Piedmont. Extent of Wisconsinan glaciation shown by hatched line. Inset map shows location of the Susquehanna Basin (black) and the extent of the Appalachian Highlands (gray) within the United States. Shaded relief was derived from the National Elevation Dataset (USGS, 1999d).

Fig. 2. Photos of typical topography and land use in each physiographic province. (A) In the Appalachian Plateaus, valleys are deeply incised into relatively undeformed bedrock. Forests dominate the landscape south of the glacial margin. (View from Hyner View State Park, N 41º 19'35", W 77º 37'30".) (B) Ridges of the Valley and Ridge are typically underlain by sandstone; shale and carbonate underlie the valley in the foreground. Agriculture and development tend to be concentrated in the valleys, while many ridges are forested. (View is to the northwest across the Juniata River from approximately N 40º 27'50", W 77º 42' 15".) (C) Photo of the Piedmont shows the gently rolling topography typical of the Piedmont Upland. Agriculture, shown here, and development are typical land uses in the Piedmont. (Photo is from N 39º 47' 40", W 76º 37'10"). Coordinates in NAD 83.

Fig. 3. Maps of the Susquehanna Basin showing aspects of human impact. (A) Regions of cleared or agricultural land (as of 1992) shown in gray. Regions of most intense

agriculture are in the Piedmont, in the valleys of the Valley and Ridge, and in the lower

relief, northern part of the Appalachian Plateaus. (B) Map shows other aspects of human

impact. Major dams are those > 15 meters high with drainage areas >50 km$^2$ (USGS,

1999a). Coal fields show broad regions underlain by coal bearing rock; extent and type of

mining (strip mining or underground) varies locally (Tully, 2001). City populations are

based on the 1990 census (USGS, 2002).

Fig. 4. Relationship between mean basin slope and basin area for both sampled and

unsampled basins. Each gray point represents a sub-basin of the Susquehanna River; the

vertical lines are artifacts of the basin size ranges that were specified when delineating

basins. Black points represent basins for which we made $^{10}$Be measurements. As basin

area increases, the range of mean basin slopes decreases. By selecting small basins for

sampling, we were able to select a broader range of mean basin slopes than represented

by large basins.

Fig. 5. Erosion rates are positively correlated to mean basin slope for the GIS-selected

basins. However, no discernable relationship exist for the USGS basins, which span a

smaller range of basin slopes.

Fig. 6. Data for the USGS basins based on glacial impact. For the indicated groups of

data, box and whisker plots show the maximum, 3$^{rd}$ quartile, median, first quartile, and

minimum values. $^{10}$Be axis is scaled such that the $^{10}$Be concentration (which has been

normalized for elevation and latitude) increases from top to bottom, so that it is possible

to read maximum limiting erosion rates from the axis on the right; however, $^{10}$Be-inferred

erosion rates for basins impacted by glaciation are not robust. The glaciated basins have

the lowest $^{10}$Be concentrations, the non-glaciated basins have the highest $^{10}$Be

concentrations, and the partly glaciated basins fall in between. Median erosion rates inferred from sediment yield data are similar regardless of glacial impact; these are also broadly similar to the median erosion rate inferred from [10]Be for the non-glaciated basins. The same basins are represented in both the [10]Be and sediment yield portions of the figure, with the exception of two basins for which sediment yield data are not available: Driftwood Branch Sinnemahoning Creek and Little Conestoga at Millersville. Inferred erosion rates for sediment yield are based on suspended sediment data only (Williams and Reed, 1972; Gellis et al., 2004a, Gellis, unpublished data); they do not include bed load or dissolved load. Figure includes stations with poor-quality sediment yield data, but the inclusion or exclusion of these stations has little effect on the general appearance of the plots.

Fig. 7. (A) As basin area increases, the range of [10]Be erosion rates decreases. Only [10]Be erosion rates from non-glaciated basins are included in this plot. (B) No clear relationship exists between basin area and erosion rate inferred from sediment yield (Williams and Reed, 1972; Gellis et al., 2004a, Gellis, unpublished data). Plot includes data for glaciated and non-glaciated basins, not all of which have [10]Be data. Those that do have [10]Be data, and that are shown in (A) (and thus are non-glaciated), are indicated by large circles around the points. Those that were glaciated are indicated by squares (whether or not they have [10]Be data). Basins without a large circle or square were not glaciated but do not have [10]Be data.

Fig. 8. Maps showing erosion rates inferred from [10]Be (m/My) for the GIS-selected basins for the (A) Appalachian Plateaus, (B) Valley and Ridge, and (C) Piedmont. The outline of the Susquehanna River Basin is shown in the upper left corner of each map

along with a rectangle that shows the extent and location of the map. Note that scales differ for each map.

Fig. 9. Maps of the Susquehanna Basin show results for the USGS basins. (A) Station names and $^{10}$Be concentrations ($10^5$ atoms g$^{-1}$). (B) Erosion rates inferred from $^{10}$Be shown in the larger font; erosion rates inferred from sediment yield are shown in smaller font and in parentheses. $^{10}$Be erosion rates shown only for basins that have not been glaciated.

Fig. 10. Box and whisker plots show the maximum, 3$^{rd}$ quartile, median, first quartile, and minimum values. Axis for erosion rates on the right applies across the plot; normalized $^{10}$Be applies to the first four columns, which contain $^{10}$Be data. Results shown here are only for non-glaciated basins. Within each physiographic province, median values are broadly consistent when comparing between $^{10}$Be results for GIS-selected basins, $^{10}$Be results for USGS basins, and sediment yield results. Most notable deviation is in the Piedmont, where median erosion rate based on the sediment yield is substantially higher than median erosion rate determined from $^{10}$Be data. Sandstone and shale results for the Valley and Ridge span a similar range; the lower maximum for shale reflects a lack of steep-sloped shale basins; no discernible relationship exists for lithology after accounting for slope (Reuter et al., in preparation). For the Appalachian Plateaus and the Valley and Ridge (though not for the Piedmont), the range of erosion rates for the small, GIS-selected basins exceeds the range of erosion rates from $^{10}$Be for the USGS basins. The USGS basins represented in the $^{10}$Be part of the figure are the same basins that have sediment yield, with the exception of two basins that do not have sediment yield data available: Driftwood Branch Sinnemahoning Creek in the Appalachian Plateaus and

Little Conestoga at Millersville in the Piedmont. Inferred erosion rates for sediment yield are based on suspended sediment data only (Williams and Reed, 1972; Gellis et al., 2004a, Gellis, unpublished data). Figure includes stations with poor-quality sediment yield data, but the inclusion or exclusion of these station has little effect on the general appearance of the plots.

Fig. 11. (A) No relationship exists between the [10]Be erosion rate and the amount of cleared land (USGS, 1997, 1999b, 1999c). Only [10]Be erosion rates from non-glaciated basins are included in this plot (B) A weak positive exponential correlation exists between erosion rate from sediment yield data (Williams and Reed, 1972; Gellis et al., 2004a, Gellis, unpublished data) and percent of cleared land. Plot includes basins for which [10]Be data exist, both glaciated and non-glaciated.

## TABLE 1

*Location and identification information for samples from USGS stream gages in the Susquehanna River Basin*

| Sample ID | USGS station name | USGS station ID | Sample location[1] N Latitude | W Longitude | Basin area (km²) | Dominant physiographic province | Glaciated? |
|---|---|---|---|---|---|---|---|
| JSQ101 | Driftwood Br Sinnemahoning Cr at Sterling Run, PA | 1543000 | 41° 24' 48" | 78° 11' 50" | 705 | Appalachian Plateaus | no |
| JSQ11 | West Branch Susquehanna River at Bower, PA | 1541000 | 40° 53' 49" | 78° 40' 38" | 816 | Appalachian Plateaus | no |
| JSQ7 | Juniata River at Newport, PA | 1567000 | 40° 28' 42" | 77° 07' 46" | 8689 | Valley and Ridge | no |
| JSQ5 | Sherman Creek at Shermans Dale, PA | 1568000 | 40° 19' 24" | 77° 10' 09" | 518 | Valley and Ridge | no |
| JSQ12 | Raystown Branch Juniata River at Saxton, PA | 1562000 | 40° 12' 57" | 78° 15' 56" | 1958 | Valley and Ridge | no |
| JSQ13 | Dunning Creek at Belden, PA | 1560000 | 40° 04' 18" | 78° 29' 34" | 445 | Valley and Ridge | no |
| JSQ10 | Bald Eagle Creek bl Spring Creek at Milesburg, PA | 1547200 | 40° 56' 35" | 77° 47' 12" | 686 | Valley and Ridge | no |
| JSQ6 | Bixler Run near Loysville, PA | 1567500 | 40° 22' 15" | 77° 24' 09" | 39 | Valley and Ridge | no |
| JSQ9 | Spring Creek near Axemann, PA | 1546500 | 40° 53' 23" | 77° 47' 40" | 226 | Valley and Ridge | no |
| JSQ3 | Yellow Breeches Creek near Camp Hill, PA | 1571500 | 40° 13' 29" | 76° 53' 54" | 559 | Valley and Ridge | no |
| JS39 | Swatara Creek at Harper Tavern, PA | 1573000 | 40° 24' 09" | 76° 34' 39" | 873 | Valley and Ridge | no |
| JSQ2 | West Conewago Creek near Manchester, PA | 1574000 | 40° 04' 56" | 76° 43' 13" | 1321 | Piedmont | no |
| JS44 | Little Conestoga Creek near Churchtown, PA | 1576085 | 40° 08' 41" | 75° 59' 20" | 15 | Piedmont | no |
| JSQ1 | Codorus Creek near York, PA | 1575500 | 39° 56' 46" | 76° 45' 20" | 575 | Piedmont | no |
| JS45 | Pequea Creek at Martic Forge, PA | 1576787 | 39° 54' 21" | 76° 19' 43" | 383 | Piedmont | no |
| JS42 | Conestoga River at Conestoga, PA | 1576754 | 39° 56' 47" | 76° 22' 05" | 1217 | Piedmont | no |
| JS43 | Mill Creek at Eshelman Mill Road near Lyndon, PA | 1576540 | 40° 00' 36" | 76° 16' 39" | 140 | Piedmont | no |
| JSQ165 | Little Conestoga Creek near Millersville, PA | 1576712 | 40° 01' 15" | 76° 21' 33" | 110 | Piedmont | no |
| JSQ35 | Tunkhannock Creek near Tunkhannock, PA | 1534000 | 41° 33' 30" | 75° 53' 42" | 992 | Appalachian Plateaus | yes |
| JSQ34 | Susquehanna River at Towanda, PA | 1531500 | 41° 45' 55" | 76° 26' 28" | 20194 | Appalachian Plateaus | yes |
| JSQ29 | Chemung River at Chemung, NY | 1531000 | 42° 00' 08" | 76° 38' 06" | 6491 | Appalachian Plateaus | yes |
| JSQ31 | Tioga River at Tioga, PA | 1518000 | 41° 54' 30" | 77° 07' 47" | 730 | Appalachian Plateaus | yes |
| JSQ30 | Tioga River at Lindley, NY | 1520500 | 42° 01' 43" | 77° 07' 57" | 1997 | Appalachian Plateaus | yes |
| JSQ33 | Elk Run near Mainesburg, PA | 1517000 | 41° 48' 54" | 76° 57' 55" | 26 | Appalachian Plateaus | yes |
| JSQ32 | Corey Creek near Mainesburg, PA | 1516500 | 41° 47' 27" | 77° 00' 54" | 32 | Appalachian Plateaus | yes |
| JS27 | West Branch Susquehanna River at Lewisburg, PA | 1553500 | 40° 58' 03" | 76° 52' 36" | 17734 | mixed | part |
| JSQ4 | Susquehanna River at Harrisburg, PA | 1570500 | 40° 15' 17" | 76° 53' 11" | 62419 | mixed | part |
| JS19 | Susquehanna River at Danville, PA | 1540500 | 40° 57' 29" | 76° 37' 10" | 29060 | mixed | part |

[1] Latitude and longitude are in the NAD 27 datum.

TABLE 2
*Basin characteristics for samples from USGS stream gages in the Susquehanna River Basin*

| Sample ID | Abbreviated station name | Mean basin slope (degrees)[1] | Glaciated region (% of basin area) | Dam impact (%)[2] | Lithology[3] Sandstone (%) | Shale (%) | Carbonate (%) | Metamorphic or igneous (%) | Land cover[4] Forested upland (%) | Herbaceous planted/ cultivated (%) | Water & wetlands (%) | Developed (%) | Barren (%) |
|---|---|---|---|---|---|---|---|---|---|---|---|---|---|
| JSQ101 | Driftwood | 14 | 0 | | 97 | 3 | 0 | 0 | 96.6 | 2.5 | 0.0 | 0.4 | 0.4 |
| JSQ11 | W Branch SQ Bower | 8 | 0 | | 37 | 63 | 0 | 0 | 77.4 | 18.6 | 0.1 | 1.0 | 2.9 |
| JSQ7 | Juniata | 9 | 0 | 54 | 32 | 51 | 16 | 0 | 69.1 | 27.5 | 1.2 | 1.6 | 0.6 |
| JSQ5 | Sherman | 9 | 0 | | 15 | 73 | 12 | 0 | 68.6 | 29.7 | 1.3 | 0.2 | 0.2 |
| JSQ12 | Raystown | 9 | 0 | | 41 | 45 | 14 | 0 | 64.9 | 32.6 | 0.6 | 1.4 | 0.5 |
| JSQ13 | Dunning | 9 | 0 | | 40 | 55 | 4 | 0 | 63.6 | 35.1 | 0.3 | 0.9 | 0.1 |
| JSQ10 | Bald Eagle | 8 | 0 | | 35 | 24 | 41 | 0 | 60.6 | 34.4 | 0.5 | 4.1 | 0.3 |
| JSQ6 | Bixler | 8 | 0 | | 8 | 69 | 22 | 0 | 48.3 | 50.6 | 1.0 | 0.1 | 0.0 |
| JSQ9 | Spring | 5 | 0 | | 24 | 5 | 71 | 0 | 37.1 | 53.8 | 0.4 | 8.6 | 0.1 |
| JSQ3 | Yellow Breeches | 6 | 0 | | 32 | 29 | 25 | 14 | 54.8 | 37.4 | 1.6 | 5.7 | 0.6 |
| JS39 | Swatara | 6 | 0 | | 24 | 70 | 1 | 5 | 53.2 | 41.4 | 1.7 | 2.3 | 1.4 |
| JSQ2 | W Conewago | 4 | 0 | | 36 | 34 | 5 | 24 | 31.3 | 63.6 | 2.1 | 2.6 | 0.3 |
| JS44 | L Conestoga Churchtown | 4 | 0 | | 51 | 0 | 49 | 0 | 29.0 | 69.6 | 0.1 | 1.3 | 0.0 |
| JSQ1 | Codorus | 6 | 0 | 63 | 29 | 4 | 8 | 58 | 27.2 | 67.2 | 2.2 | 3.2 | 0.3 |
| JS45 | Pequea | 4 | 0 | | 22 | 4 | 55 | 19 | 24.7 | 72.4 | 0.5 | 2.4 | 0.0 |
| JS42 | Conestoga | 4 | 0 | | 31 | 7 | 58 | 4 | 24.4 | 64.0 | 1.3 | 9.8 | 0.4 |
| JS43 | Mill near Lyndon | 2 | 0 | | 9 | 2 | 88 | 2 | 10.9 | 81.6 | 0.3 | 7.2 | 0.0 |
| JSQ165 | L Conestoga Millersville | 2 | 0 | | 5 | 13 | 79 | 2 | 8.8 | 62.4 | 0.6 | 27.3 | 0.9 |
| JSQ35 | Tunkhannock | 7 | 100 | | 100 | 0 | 0 | 0 | 66.8 | 27.9 | 3.5 | 1.7 | 0.0 |
| JSQ34 | SQ Towanda | 7 | 100 | 14 | 10 | 10 | 0 | 0 | 68.3 | 28.6 | 1.3 | 1.7 | 0.1 |
| JSQ29 | Chemung | 8 | 100 | 31* | 16 | 17 | 0 | 0 | 66.2 | 31.4 | 0.7 | 1.6 | 0.1 |
| JSQ31 | Tioga Tioga | 8 | 100 | 99* | 73 | 27 | 0 | 0 | 65.7 | 32.1 | 0.6 | 0.8 | 0.9 |
| JSQ30 | Tioga Lindley | 8 | 100 | 91* | 51 | 37 | 0 | 0 | 63.3 | 35.1 | 0.7 | 0.6 | 0.4 |
| JSQ33 | Elk | 8 | 100 | | 80 | 20 | 0 | 0 | 50.2 | 49.6 | 0.1 | 0.0 | 0.1 |
| JSQ32 | Corey | 8 | 100 | | 68 | 32 | 0 | 0 | 47.2 | 52.2 | 0.5 | 0.1 | 0.1 |
| JS27 | W Branch SQ Lewisburg | 10 | 17 | 20 | 74 | 22 | 4 | 0 | 82.8 | 13.8 | 0.6 | 1.1 | 1.7 |
| JSQ4 | SQ Harrisburg | 8 | 49 | 18 | 41 | 28 | 5 | 0 | 70.8 | 25.0 | 1.4 | 1.9 | 0.9 |
| JS19 | SQ Danville | 7 | 94 | 11* | 28 | 16 | 0 | 0 | 68.2 | 27.4 | 1.7 | 2.4 | 0.4 |

[1]Slope was calculated from a digital elevation model with grid cell size of approximately 30 m. [2]Percent of the basin area impacted by major dams is shown for basins which have at least 10% impact; major dams are those higher than 15 meters, that have a drainage area >50 km² at the dam, and that are included in the USGS (1999a) dataset. An * indicates that the impact of dams during the period of sediment yield record was substantially less than in 1999. [3]Lithology is based on the digital geologic map of Pennsylvania (Pennsylvania Bureau of Topographic and Geologic Survey, 2001), and the dominant lithology ("Lithology 1" field) was used to generalize to the categories shown here. Because lithology is for Pennsylvania only, basins that extend into New York or Maryland do not sum to 100%. [4]Land cover comes from the National Land Cover Database and is based on Landsat imagery from 1992 (USGS, 1997; USGS, 1999b; USGS, 1999c).

93

TABLE 3
*Location and identification information for samples from GIS-selected sites in the Susquehanna River Basin*

| Sample ID | | Sample location[1] | | Basin area (km$^2$) | Physiographic province |
| --- | --- | --- | --- | --- | --- |
| | | North Latitude | West Longitude | | |
| JSQ100 | Dry Run | 41° 22' 33" | 78° 09' 14" | 3.0 | Appalachian Plateaus |
| JSQ102 | Russell Hollow Run | 41° 27' 30" | 78° 09' 11" | 3.2 | Appalachian Plateaus |
| JSQ103 | Crooked Run | 41° 35' 32" | 78° 11' 13" | 5.6 | Appalachian Plateaus |
| JSQ104 | Heth Run | 41° 42' 15" | 78° 02' 16" | 3.5 | Appalachian Plateaus |
| JSQ105 | Big Run | 41° 27' 32" | 78° 25' 48" | 3.2 | Appalachian Plateaus |
| JSQ106 | East Branch | 41° 26' 54" | 78° 21' 34" | 3.2 | Appalachian Plateaus |
| JSQ107 | another Middle Branch | 41° 25' 38" | 78° 21' 34" | 3.4 | Appalachian Plateaus |
| JSQ108 | Bell Draft | 41° 23' 45" | 78° 21' 26" | 5.4 | Appalachian Plateaus |
| JSQ109 | South Branch Little Portage Creek | 41° 35' 53" | 78° 06' 14" | 3.2 | Appalachian Plateaus |
| JSQ110 | Wykoff Branch, high elevation sample | 41° 27' 09" | 77° 58' 35" | 1.2 | Appalachian Plateaus |
| JSQ111 | Wykoff Branch, low elevation sample | 41° 27' 05" | 77° 57' 09" | 4.7 | Appalachian Plateaus |
| JSQ112 | Left Fork Bearfield Run | 41° 23' 09" | 77° 56' 58" | 3.4 | Appalachian Plateaus |
| JSQ113 | Lebo Branch | 41° 21' 30" | 77° 58' 09" | 3.9 | Appalachian Plateaus |
| JSQ114 | Pebble Run | 41° 14' 40" | 78° 16' 42" | 6.4 | Appalachian Plateaus |
| JSQ115 | Sanders Draft | 41° 16' 32" | 78° 14' 01" | 4.8 | Appalachian Plateaus |
| JSQ116 | Little Birch Island Run | 41° 12' 13" | 78° 02' 20" | 6.5 | Appalachian Plateaus |
| JSQ117 | tributary to Little Birch Island Run | 41° 12' 16" | 78° 02' 03" | 3.4 | Appalachian Plateaus |
| JSQ118 | Drake Hollow | 41° 17' 08" | 77° 47' 23" | 4.0 | Appalachian Plateaus |
| JSQ119 | Laurely Fork | 41° 16' 27" | 77° 46' 05" | 5.3 | Appalachian Plateaus |
| JSQ120 | Yost Run, low elevation sample | 41° 12' 32" | 77° 55' 18" | 15 | Appalachian Plateaus |
| JSQ121 | Kyler Fork of Yost Run | 41° 09' 49" | 77° 54' 18" | 0.6 | Appalachian Plateaus |
| JSQ123 | Middle Branch | 41° 12' 11" | 77° 47' 52" | 3.1 | Appalachian Plateaus |
| JSQ125 | Gottshall Run, low elevation sample | 41° 05' 51" | 77° 14' 47" | 9.7 | Valley and Ridge |
| JSQ126 | Gottshall Run, high elevation sample | 41° 05' 06" | 77° 16' 30" | 2.1 | Valley and Ridge |
| JSQ127 | Jamison Run | 41° 04' 09" | 77° 18' 29" | 5.5 | Valley and Ridge |
| JSQ128 | tributary to White Deer Hole Run | 41° 04' 29" | 77° 07' 09" | 3.2 | Valley and Ridge |
| JSQ129 | Buffalo Creek | 40° 56' 25" | 77° 13' 23" | 3.1 | Valley and Ridge |
| JSQ133 | Wolf Run | 40° 31' 20" | 76° 44' 48" | 3.0 | Valley and Ridge |
| JSQ137 | Minehart Run | 40° 31' 49" | 77° 36' 36" | 8.6 | Valley and Ridge |
| JSQ138 | tributary to Minehart Run | 40° 31' 51" | 77° 36' 34" | 3.8 | Valley and Ridge |
| JSQ139 | Wharton Run | 40° 24' 26" | 77° 45' 59" | 3.2 | Valley and Ridge |
| JSQ140 | Shores Branch | 40° 19' 35" | 78° 02' 55" | 3.1 | Valley and Ridge |
| JSQ141 | Laurel Run | 40° 19' 56" | 78° 06' 42" | 4.5 | Valley and Ridge |
| JSQ143 | Croyle Run | 40° 41' 46" | 77° 48' 11" | 3.0 | Valley and Ridge |
| JSQ144 | another Laurel Run | 40° 44' 16" | 77° 47' 26" | 3.2 | Valley and Ridge |
| JSQ145 | Swift Run | 40° 48' 59" | 77° 25' 05" | 3.3 | Valley and Ridge |
| JSQ146 | Pine Swamp Run | 40° 49' 55" | 77° 28' 36" | 3.3 | Valley and Ridge |
| JSQ147 | Bear Run | 40° 59' 08" | 77° 29' 08" | 3.2 | Valley and Ridge |
| JSQ148 | tributary from Kettle Mountain | 40° 58' 56" | 77° 29' 26" | 4.8 | Valley and Ridge |
| JSQ124 | Sulphur Run | 41° 12' 20" | 77° 20' 26" | 2.7 | Valley and Ridge |
| JSQ130 | Mud Creek | 41° 04' 27" | 76° 37' 05" | 6.4 | Valley and Ridge |
| JSQ131 | tributary to Spruce Run Creek | 41° 04' 31" | 76° 31' 21" | 5.2 | Valley and Ridge |
| JSQ132 | tributary to Plum Creek | 40° 51' 06" | 76° 43' 00" | 3.8 | Valley and Ridge |
| JSQ134 | Independence Run | 40° 41' 09" | 76° 53' 53" | 5.6 | Valley and Ridge |
| JSQ135 | Boyers Run | 40° 37' 30" | 76° 57' 24" | 4.0 | Valley and Ridge |
| JSQ136 | tributary to Lick Run | 40° 22' 07" | 77° 39' 21" | 3.3 | Valley and Ridge |
| JSQ142 | tributary to Frankstown Branch Juniata River | 40° 26' 33" | 78° 18' 10" | 2.8 | Valley and Ridge |
| JSQ149 | Greens Run | 41° 00' 53" | 77° 42' 24" | 3.0 | Valley and Ridge |
| JSQ150 | Anderson Run | 39° 48' 43" | 76° 19' 49" | 3.9 | Piedmont |
| JSQ151 | Mill Creek, low elevation sample | 39° 49' 01" | 76° 20' 20" | 3.5 | Piedmont |
| JSQ152 | Mill Creek, high elevation sample | 39° 48' 54" | 76° 20' 48" | 3.0 | Piedmont |
| JSQ153 | trib to Conowingo Creek | 39° 49' 43" | 76° 11' 19" | 25 | Piedmont |
| JSQ154 | Kellys Run | 39° 50' 12" | 76° 20' 22" | 5.4 | Piedmont |
| JSQ155 | tributary to Tucquan Creek | 39° 51' 54" | 76° 20' 26" | 4.1 | Piedmont |
| JSQ156 | tributary to Beaver Creek | 39° 54' 02" | 76° 31' 13" | 4.4 | Piedmont |
| JSQ157 | tributary to Bald Eagle Creek | 39° 44' 58" | 76° 26' 08" | 3.9 | Piedmont |
| JSQ158 | Alum Rock Run | 39° 46' 32" | 76° 29' 37" | 7.0 | Piedmont |
| JSQ159 | another trib to East Branch | 39° 48' 21" | 76° 37' 14" | 7.5 | Piedmont |
| JSQ160 | tributary to East Branch | 39° 48' 58" | 76° 39' 00" | 3.8 | Piedmont |
| JSQ161 | Green Branch | 39° 56' 09" | 76° 28' 26" | 3.4 | Piedmont |

[1]Latitude and longitude are in the NAD 27 datum.

TABLE 4
*Basin characteristics for samples from GIS-selected sites in the Susquehanna River Basin*

| Sample ID | Mean basin slope (degrees)[1] | Lithology[2] | Land cover[3] | | | | |
|---|---|---|---|---|---|---|---|
| | | | Forested upland (%) | Herbaceous planted/ cultivated (%) | Water & wetlands (%) | Developed (%) | Barren (%) |
| JSQ100 | 21 | sandstone | 97.3 | 0.0 | 0.0 | 0.0 | 2.7 |
| JSQ102 | 21 | sandstone | 99.2 | 0.8 | 0.0 | 0.0 | 0.0 |
| JSQ103 | 19 | sandstone | 99.9 | 0.1 | 0.0 | 0.0 | 0.0 |
| JSQ104 | 9 | sandstone | 89.6 | 10.4 | 0.0 | 0.0 | 0.0 |
| JSQ105 | 4 | sandstone | 97.3 | 2.7 | 0.0 | 0.0 | 0.0 |
| JSQ106 | 13 | sandstone | 99.8 | 0.2 | 0.0 | 0.0 | 0.0 |
| JSQ107 | 13 | sandstone | 100.0 | 0.0 | 0.0 | 0.0 | 0.0 |
| JSQ108 | 8 | sandstone | 99.9 | 0.1 | 0.0 | 0.0 | 0.0 |
| JSQ109 | 20 | sandstone | 100.0 | 0.0 | 0.0 | 0.0 | 0.0 |
| JSQ110 | 3 | sandstone | 100.0 | 0.0 | 0.0 | 0.0 | 0.0 |
| JSQ111 | 8 | sandstone | 99.9 | 0.1 | 0.0 | 0.0 | 0.0 |
| JSQ112 | 16 | sandstone | 99.9 | 0.1 | 0.0 | 0.0 | 0.0 |
| JSQ113 | 11 | sandstone | 99.8 | 0.1 | 0.1 | 0.0 | 0.0 |
| JSQ114 | 2 | sandstone | 99.7 | 0.1 | 0.0 | 0.2 | 0.0 |
| JSQ115 | 6 | sandstone | 99.9 | 0.1 | 0.0 | 0.0 | 0.1 |
| JSQ116 | 5 | sandstone | 100.0 | 0.0 | 0.0 | 0.0 | 0.0 |
| JSQ117 | 5 | sandstone | 99.9 | 0.0 | 0.0 | 0.0 | 0.1 |
| JSQ118 | 15 | sandstone | 99.5 | 0.5 | 0.0 | 0.0 | 0.0 |
| JSQ119 | 19 | sandstone | 99.9 | 0.1 | 0.0 | 0.0 | 0.0 |
| JSQ120 | 11 | sandstone | 99.8 | 0.1 | 0.0 | 0.0 | 0.0 |
| JSQ121 | 2 | sandstone | 98.9 | 0.6 | 0.0 | 0.0 | 0.5 |
| JSQ123 | 6 | sandstone | 98.0 | 1.2 | 0.0 | 0.0 | 0.8 |
| JSQ125 | 6 | sandstone | 98.5 | 1.5 | 0.0 | 0.0 | 0.0 |
| JSQ126 | 3 | sandstone | 96.0 | 3.9 | 0.1 | 0.0 | 0.0 |
| JSQ127 | 4 | sandstone | 85.3 | 13.9 | 0.7 | 0.1 | 0.0 |
| JSQ128 | 9 | sandstone | 98.5 | 1.5 | 0.0 | 0.0 | 0.0 |
| JSQ129 | 4 | sandstone | 99.9 | 0.1 | 0.0 | 0.0 | 0.0 |
| JSQ133 | 4 | sandstone | 99.9 | 0.0 | 0.1 | 0.0 | 0.0 |
| JSQ137 | 14 | sandstone | 99.9 | 0.1 | 0.0 | 0.0 | 0.0 |
| JSQ138 | 14 | sandstone | 99.8 | 0.1 | 0.0 | 0.0 | 0.1 |
| JSQ139 | 18 | sandstone | 99.3 | 0.6 | 0.0 | 0.0 | 0.1 |
| JSQ140 | 4 | sandstone | 92.4 | 7.4 | 0.2 | 0.0 | 0.0 |
| JSQ141 | 6 | sandstone | 99.3 | 0.3 | 0.0 | 0.0 | 0.4 |
| JSQ143 | 9 | sandstone | 99.9 | 0.1 | 0.0 | 0.0 | 0.0 |
| JSQ144 | 12 | sandstone | 100.0 | 0.0 | 0.0 | 0.0 | 0.0 |
| JSQ145 | 14 | sandstone | 99.2 | 0.8 | 0.0 | 0.0 | 0.0 |
| JSQ146 | 6 | sandstone | 96.7 | 0.0 | 3.3 | 0.0 | 0.0 |
| JSQ147 | 18 | sandstone | 98.3 | 1.7 | 0.0 | 0.0 | 0.0 |
| JSQ148 | 16 | sandstone | 100.0 | 0.0 | 0.0 | 0.0 | 0.0 |
| JSQ124 | 12 | shale | 82.7 | 17.1 | 0.2 | 0.0 | 0.0 |
| JSQ130 | 4 | shale | 15.7 | 84.2 | 0.1 | 0.0 | 0.0 |
| JSQ131 | 10 | shale | 63.5 | 36.5 | 0.0 | 0.0 | 0.0 |
| JSQ132 | 4 | shale | 22.8 | 77.0 | 0.2 | 0.0 | 0.0 |
| JSQ134 | 8 | shale | 30.4 | 69.5 | 0.1 | 0.1 | 0.0 |
| JSQ135 | 10 | shale | 88.2 | 11.8 | 0.0 | 0.0 | 0.0 |
| JSQ136 | 6 | shale | 99.9 | 0.1 | 0.0 | 0.0 | 0.0 |
| JSQ142 | 10 | shale | 93.4 | 6.4 | 0.2 | 0.1 | 0.0 |
| JSQ149 | 15 | shale | 82.2 | 17.8 | 0.0 | 0.0 | 0.0 |
| JSQ150 | 7 | schist | 39.5 | 59.9 | 0.0 | 0.6 | 0.0 |
| JSQ151 | 6 | schist | 30.5 | 69.3 | 0.2 | 0.0 | 0.0 |
| JSQ152 | 5 | schist | 24.2 | 75.5 | 0.2 | 0.0 | 0.0 |
| JSQ153 | 4 | schist | 15.5 | 83.0 | 0.8 | 0.7 | 0.0 |
| JSQ154 | 8 | schist | 48.3 | 50.6 | 1.1 | 0.0 | 0.0 |
| JSQ155 | 7 | schist | 40.0 | 59.1 | 0.3 | 0.7 | 0.0 |
| JSQ156 | 6 | schist | 35.9 | 62.3 | 0.7 | 1.1 | 0.0 |
| JSQ157 | 5 | schist | 33.5 | 65.7 | 0.7 | 0.1 | 0.0 |
| JSQ158 | 5 | schist | 16.5 | 82.8 | 0.6 | 0.1 | 0.0 |
| JSQ159 | 5 | schist | 20.9 | 77.6 | 0.9 | 0.5 | 0.0 |
| JSQ160 | 5 | schist | 27.1 | 72.2 | 0.6 | 0.1 | 0.0 |
| JSQ161 | 6 | schist | 40.0 | 59.7 | 0.1 | 0.1 | 0.0 |

[1]Slope was calculated from a digital elevation model with grid cell size of approximately 30 m. [2]Lithology is based on the digital geologic map of Pennsylvania (Pennsylvania Bureau of Topographic and Geologic Survey, 2001), and the dominant lithology ("Lithology 1" field) was used to generalize to the categories shown here. [3]Land cover comes from the National Land Cover Database and is based on Landsat imagery from 1992 (USGS, 1997; USGS, 1999b; USGS, 1999c).

95

TABLE 5

*Results for samples from USGS stream gages in the Susquehanna River Basin*

| Sample ID | Name | Measured $^{10}$Be ($10^5$ atoms g$^{-1}$) | $^{10}$Be production factor[1] | Quartz-weighted $^{10}$Be production factor[2] | $^{10}$Be erosion rate (m/My)[3] | Erosion rate from sediment yield (m/My)[4] | | Period of sediment yield record |
|---|---|---|---|---|---|---|---|---|
| JSQ101 | Driftwood | 2.22 ± 0.10 | 1.53 | 1.53 | 21.6 | N.D. | | N.D. |
| JSQ11 | W Branch SQ Bower | 2.43 ± 0.08 | 1.50 | 1.49 | 19.4 | 15.2 | (1) | 1964-1967 |
| JSQ7 | Juniata | 2.20 ± 0.10 | 1.33 | 1.41 | 18.9 | 4.3 | (2) | 1985-2001 |
| JSQ5 | Sherman | 3.47 ± 0.11 | 1.24 | 1.34 | 11.1 | 6.1 | (2) | 1984-1991 |
| JSQ12 | Raystown | 4.68 ± 0.15 | 1.41 | 1.46 | 9.3 | 33.6 | (2) | 1988-1992 |
| JSQ13 | Dunning | 4.91 ± 0.15 | 1.45 | 1.54 | 9.1 | 7.5 | (3) | N.A. |
| JSQ10 | Bald Eagle | 2.58 ± 0.08 | 1.36 | 1.44 | 16.4 | 13.0 | (1) | 1956-1958 |
| JSQ6 | Bixler | 4.81 ± 0.26 | 1.21 | 1.26 | 7.7 | 8.6 | (2) | 1954-1971 |
| JSQ9 | Spring | 3.14 ± 0.10 | 1.34 | 1.42 | 13.3 | 14.3 | (3) | N.A. |
| JSQ3 | Yellow Breeches | 1.92 ± 0.06 | 1.18 | 1.26 | 19.1 | 16.8 | (3) | N.A. |
| JS39 | Swatara | 2.64 ± 0.09 | 1.16 | 1.22 | 13.7 | 40.0 | (2) | 1959-1960, 1976-1979 |
| JSQ2 | W Conewago | 2.46 ± 0.08 | 1.11 | 1.11 | 14.1 | 28.0 | (3) | N.A. |
| JS44 | L Conestoga Churchtown | 3.56 ± 0.12 | 1.12 | 1.14 | 9.7 | 180 | (2) | 1983-1992 |
| JSQ1 | Codorus | 2.61 ± 0.08 | 1.14 | 1.13 | 13.5 | 8.4 | (2) | 1985-1989 |
| JS45 | Pequea | 1.74 ± 0.06 | 1.08 | 1.10 | 19.4 | 250 | (1) | 1977-1979 |
| JS42 | Conestoga | 1.84 ± 0.06 | 1.07 | 1.10 | 18.2 | 22.6 | (2) | 1985-1998, 2001 |
| JS43 | Mill near Lyndon | 2.99 ± 0.09 | 1.06 | 1.11 | 11.0 | 41.7 | (2) | 1993-1995 |
| JSQ165 | L Conestoga Millersville | 3.34 ± 0.10 | 1.04 | 1.06 | 9.6 | N.A. | | N.A. |
| JSQ35 | Tunkhannock | 0.59 ± 0.03 | 1.37 | 1.37 | - | 2.4 | (1) | 1965-1966 |
| JSQ34 | SQ Towanda | 0.52 ± 0.06 | 1.45 | 1.50 | - | 13.4 | (2) | 1985-2001 |
| JSQ29 | Chemung | 0.71 ± 0.05 | 1.49 | 1.55 | - | 42.9 | (2) | 1975-1977 |
| JSQ31 | Tioga Tioga | 1.23 ± 0.10 | 1.54 | 1.57 | - | 5.2 | (2) | 1973-1978 |
| JSQ30 | Tioga Lindley | 0.84 ± 0.11 | 1.53 | 1.56 | - | 52.2 | (2) | 1975-1981 |
| JSQ33 | Elk | 0.72 ± 0.10 | 1.56 | 1.58 | - | 21.0 | (2) | 1955-1967 |
| JSQ32 | Corey | 0.69 ± 0.14 | 1.54 | 1.57 | - | 14.4 | (2) | 1953-1967 |
| JS27 | W Branch SQ Lewisburg | 1.61 ± 0.06 | 1.46 | 1.49 | - | 7.3 | (2) | 1975-2001 |
| JSQ4 | SQ Harrisburg | 1.29 ± 0.06 | 1.39 | 1.44 | - | 10.1 | (2) | 1964-1992 |
| JS19 | SQ Danville | 2.53 ± 0.09 | 1.42 | 1.41 | - | 11.8 | (2) | 1974-2001 |

[1]Production factor is the ratio between the basin production rate and the sea level, high latitude production rate. [2]The quartz-weighted production factor accounts for distribution of quartz within the basin by convolving lithology with elevation and latitude on a pixel-by-pixel basis. [3]We do not report $^{10}$Be erosion rates for basins impacted by glaciation due to violations of interpretive model assumptions. [4]The number in parentheses indicates the data source for the sediment yield data: (1) Gellis, unpublished data; (2) Gellis and others, 2004; (3) Williams and Reed, 1972. The data from source (2) have longer records and/or are better quality than those from sources (1) and (3). N.D.–no data exist. N.A.–data not available.

96

TABLE 6
*Results for samples from GIS-selected sites in the*
*Susquehanna River Basin*

| Sample ID | Measured $^{10}$Be ($10^5$ atoms g$^{-1}$) | $^{10}$Be production factor[1] | $^{10}$Be erosion rate (m/My) |
|---|---|---|---|
| JSQ100 | 1.87 ± 0.14 | 1.50 | 25.2 |
| JSQ102 | 0.92 ± 0.06 | 1.57 | 53.6 |
| JSQ103 | 1.50 ± 0.09 | 1.56 | 32.7 |
| JSQ104 | 1.67 ± 0.08 | 1.64 | 31.1 |
| JSQ105 | 2.73 ± 0.09 | 1.61 | 18.5 |
| JSQ106 | 2.26 ± 0.10 | 1.59 | 22.1 |
| JSQ107 | 1.41 ± 0.07 | 1.55 | 34.7 |
| JSQ108 | 3.47 ± 0.12 | 1.63 | 14.6 |
| JSQ109 | 1.31 ± 0.09 | 1.64 | 39.5 |
| JSQ110 | 5.52 ± 0.17 | 1.61 | 9.0 |
| JSQ111 | 3.52 ± 0.13 | 1.57 | 13.9 |
| JSQ112 | 1.22 ± 0.07 | 1.47 | 37.9 |
| JSQ113 | 2.55 ± 0.09 | 1.51 | 18.6 |
| JSQ114 | 4.58 ± 0.15 | 1.64 | 11.1 |
| JSQ115 | 3.49 ± 0.12 | 1.63 | 14.5 |
| JSQ116 | 3.75 ± 0.12 | 1.53 | 12.7 |
| JSQ117 | 3.70 ± 0.12 | 1.47 | 12.4 |
| JSQ118 | 2.37 ± 0.11 | 1.58 | 20.9 |
| JSQ119 | 1.48 ± 0.07 | 1.56 | 33.2 |
| JSQ120 | 2.46 ± 0.11 | 1.61 | 20.6 |
| JSQ121 | 7.83 ± 0.31 | 1.71 | 6.6 |
| JSQ123 | 5.16 ± 0.14 | 1.66 | 9.9 |
| JSQ125 | 2.01 ± 0.08 | 1.50 | 23.4 |
| JSQ126 | 2.81 ± 0.08 | 1.53 | 17.0 |
| JSQ127 | 5.26 ± 0.15 | 1.54 | 9.0 |
| JSQ128 | 3.34 ± 0.10 | 1.49 | 13.9 |
| JSQ129 | 7.47 ± 0.20 | 1.62 | 6.6 |
| JSQ133 | 5.22 ± 0.14 | 1.45 | 8.5 |
| JSQ137 | 3.83 ± 0.11 | 1.39 | 11.3 |
| JSQ138 | 2.90 ± 0.09 | 1.37 | 14.7 |
| JSQ139 | 2.00 ± 0.07 | 1.47 | 23.0 |
| JSQ140 | 5.86 ± 0.20 | 1.42 | 7.4 |
| JSQ141 | 4.68 ± 0.16 | 1.47 | 9.7 |
| JSQ143 | 8.70 ± 0.23 | 1.56 | 5.4 |
| JSQ144 | 7.12 ± 0.19 | 1.66 | 7.1 |
| JSQ145 | 2.72 ± 0.11 | 1.49 | 17.1 |
| JSQ146 | 3.35 ± 0.09 | 1.54 | 14.3 |
| JSQ147 | 1.60 ± 0.07 | 1.47 | 28.9 |
| JSQ148 | 2.28 ± 0.08 | 1.51 | 20.7 |
| JSQ124 | 3.81 ± 0.21 | 1.23 | 9.9 |
| JSQ130 | 3.08 ± 0.11 | 1.13 | 11.4 |
| JSQ131 | 2.48 ± 0.13 | 1.21 | 15.3 |
| JSQ132 | 5.25 ± 0.18 | 1.14 | 6.6 |
| JSQ134 | 2.27 ± 0.10 | 1.14 | 15.6 |
| JSQ135 | 1.91 ± 0.06 | 1.14 | 18.7 |
| JSQ136 | 9.56 ± 0.25 | 1.26 | 3.9 |
| JSQ142 | 4.26 ± 0.13 | 1.29 | 9.3 |
| JSQ149 | 2.00 ± 0.11 | 1.31 | 20.5 |
| JSQ150 | 3.73 ± 0.12 | 1.08 | 9.0 |
| JSQ151 | 6.05 ± 0.20 | 1.09 | 5.5 |
| JSQ152 | 5.95 ± 0.26 | 1.10 | 5.6 |
| JSQ153 | 3.00 ± 0.10 | 1.11 | 11.5 |
| JSQ154 | 4.13 ± 0.12 | 1.13 | 8.4 |
| JSQ155 | 3.95 ± 0.12 | 1.12 | 8.7 |
| JSQ156 | 3.68 ± 0.12 | 1.16 | 9.7 |
| JSQ157 | 2.83 ± 0.08 | 1.11 | 12.2 |
| JSQ158 | 3.80 ± 0.11 | 1.13 | 9.2 |
| JSQ159 | 4.33 ± 0.14 | 1.20 | 8.6 |
| JSQ160 | 3.76 ± 0.12 | 1.18 | 9.7 |
| JSQ161 | 4.07 ± 0.14 | 1.12 | 8.4 |

[1]The production factor is the ratio between the basin production rate and the sea level, high latitude production rate. We do not present a separate quartz-weighted production rate for these basins because each basin is mapped as a single lithology.

TABLE 7
*Inferred and predicted erosion rates for the non-glaciated USGS basins in the Susquehanna River Basin*

| Sample ID | USGS station name | Erosion rates inferred from measured [10]Be (m/My) | Predicted erosion rates | | |
|---|---|---|---|---|---|
| | | | Method 1 (m/My)[1] | Method 2 (m/My)[2] | Method 3 (m/My)[3] |
| JSQ101 | Driftwood Br Sinnemahoning Cr at Sterling Run, PA | 21.6 | 22.2 | 26.8 | 26.8 |
| JSQ11 | West Branch Susquehanna River at Bower, PA | 19.4 | 13.3 | 16.9 | 17.2 |
| JSQ7 | Juniata River at Newport, PA | 18.9 | 16.0 | 14.1 | 15.6 |
| JSQ12 | Raystown Branch Juniata River at Saxton, PA | 9.3 | 15.3 | 14.5 | 16.3 |
| JSQ13 | Dunning Creek at Belden, PA | 9.1 | 14.9 | 16.5 | 21.2 |
| JSQ10 | Bald Eagle Creek bl Spring Creek at Milesburg, PA | 16.4 | 14.5 | 12.6 | 13.9 |
| JSQ6 | Bixler Run near Loysville, PA | 7.7 | 14.3 | 13.5 | 20.6 |
| JSQ9 | Spring Creek near Axemann, PA | 13.3 | 10.4 | 10.1 | 10.9 |
| JSQ5 | Sherman Creek at Shermans Dale, PA | 11.1 | 15.9 | 13.5 | 14.5 |
| JSQ3 | Yellow Breeches Creek near Camp Hill, PA | 19.1 | 11.0 | 10.4 | 12.4 |
| JS39 | Swatara Creek at Harper Tavern, PA | 13.7 | 11.4 | 11.0 | 13.4 |
| JSQ2 | West Conewago Creek near Manchester, PA | 14.1 | 8.1 | 9.2 | 9.3 |
| JS44 | Little Conestoga Creek near Churchtown, PA | 9.7 | 8.3 | 8.9 | 13.0 |
| JSQ1 | Codorus Creek near York, PA | 13.5 | 11.4 | 8.9 | 9.0 |
| JS45 | Pequea Creek at Martic Forge, PA | 19.5 | 8.6 | 8.9 | 9.2 |
| JS42 | Conestoga River at Conestoga, PA | 18.2 | 7.9 | 8.9 | 9.5 |
| JS43 | Mill Creek at Eshelman Mill Road near Lyndon, PA | 11.0 | 6.0 | 8.9 | 18.7 |
| JSQ165 | Little Conestoga Creek near Millersville, PA | 9.6 | 5.6 | 8.9 | 6.6 |

[1]Erosion rates predicted using single best regression between slope and erosion rate based upon the data for all GIS-selected basins. [2]Erosion rates predicted separately for each physiographic province, based upon regression between slope and erosion rate for the GIS-selected basins within each province. [3]Erosion rates based on Method 2 with modifications to account for non-uniform quartz distribution.
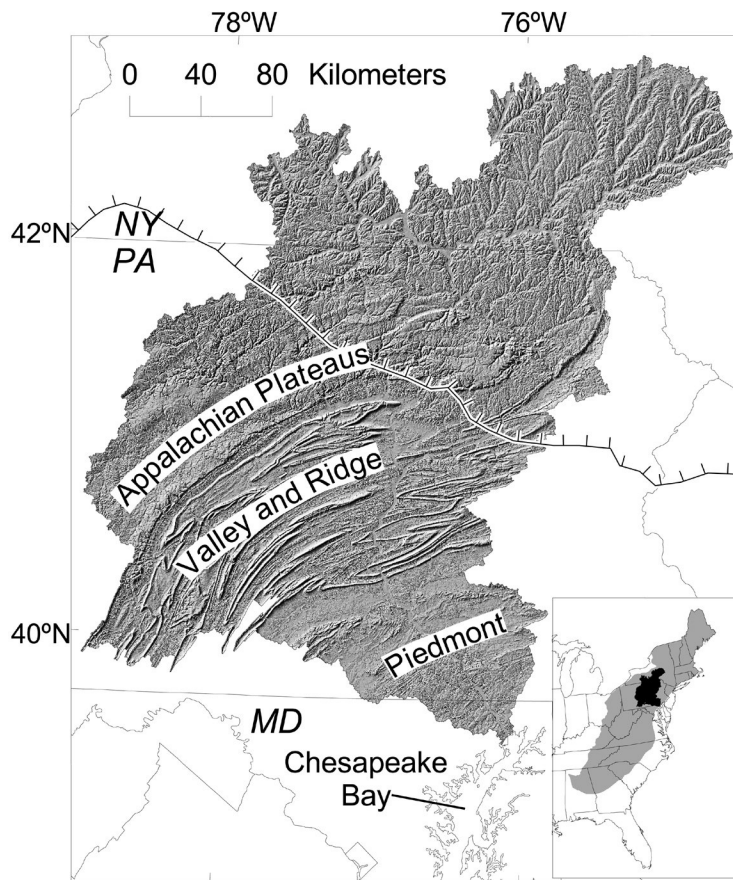
*Fig. 1. Reuter and others*

A



B



C

*Fig. 2. Reuter and others*
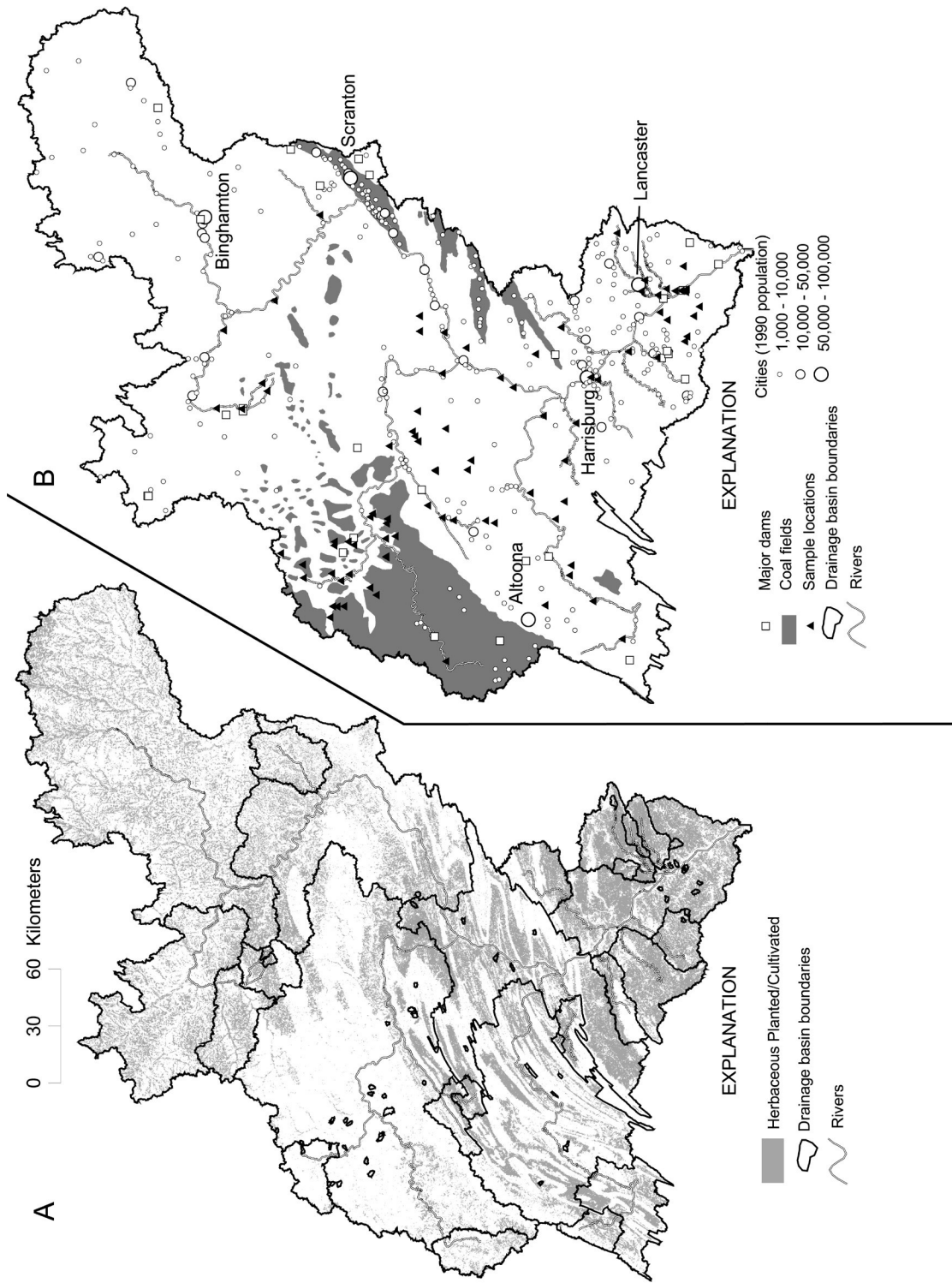
*Fig. 3. Reuter and others*
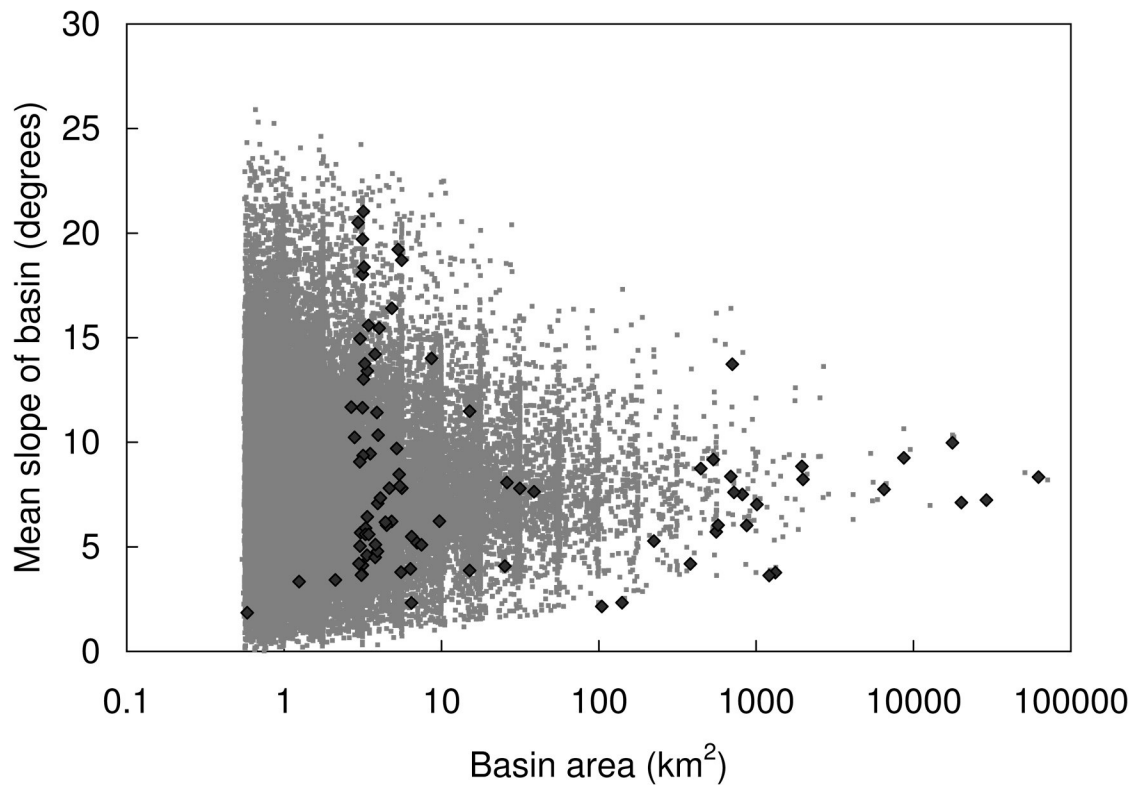
*Fig. 4. Reuter and others*

*Fig. 5. Reuter and others*

103
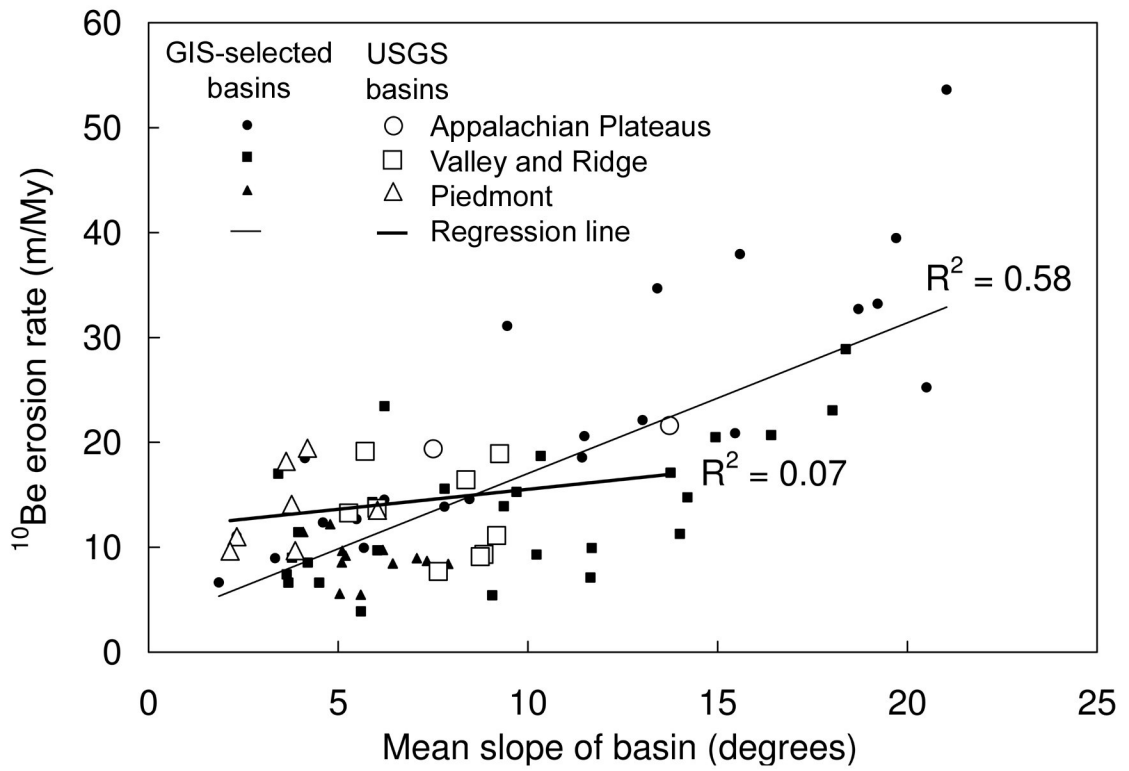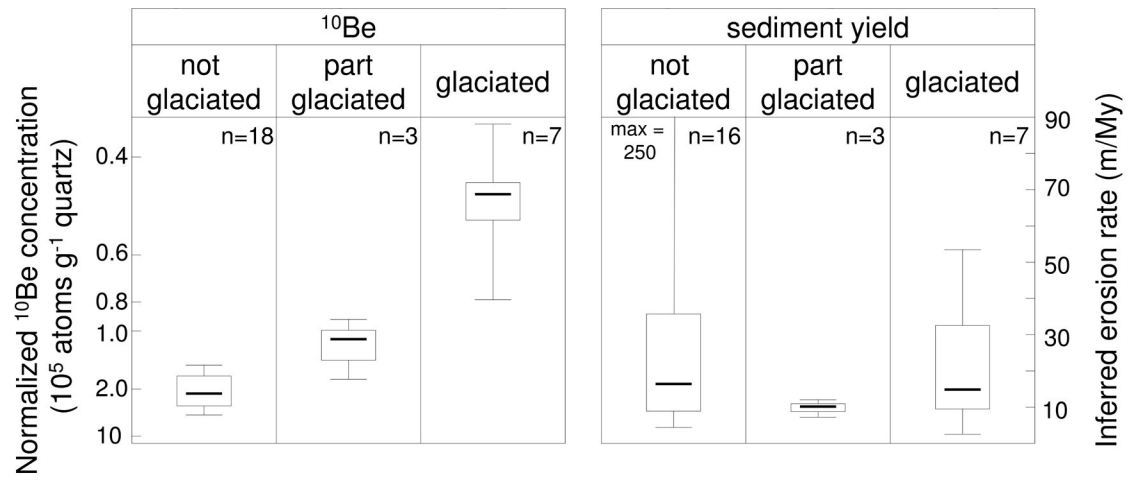
*Fig. 6. Reuter and others*

A

B
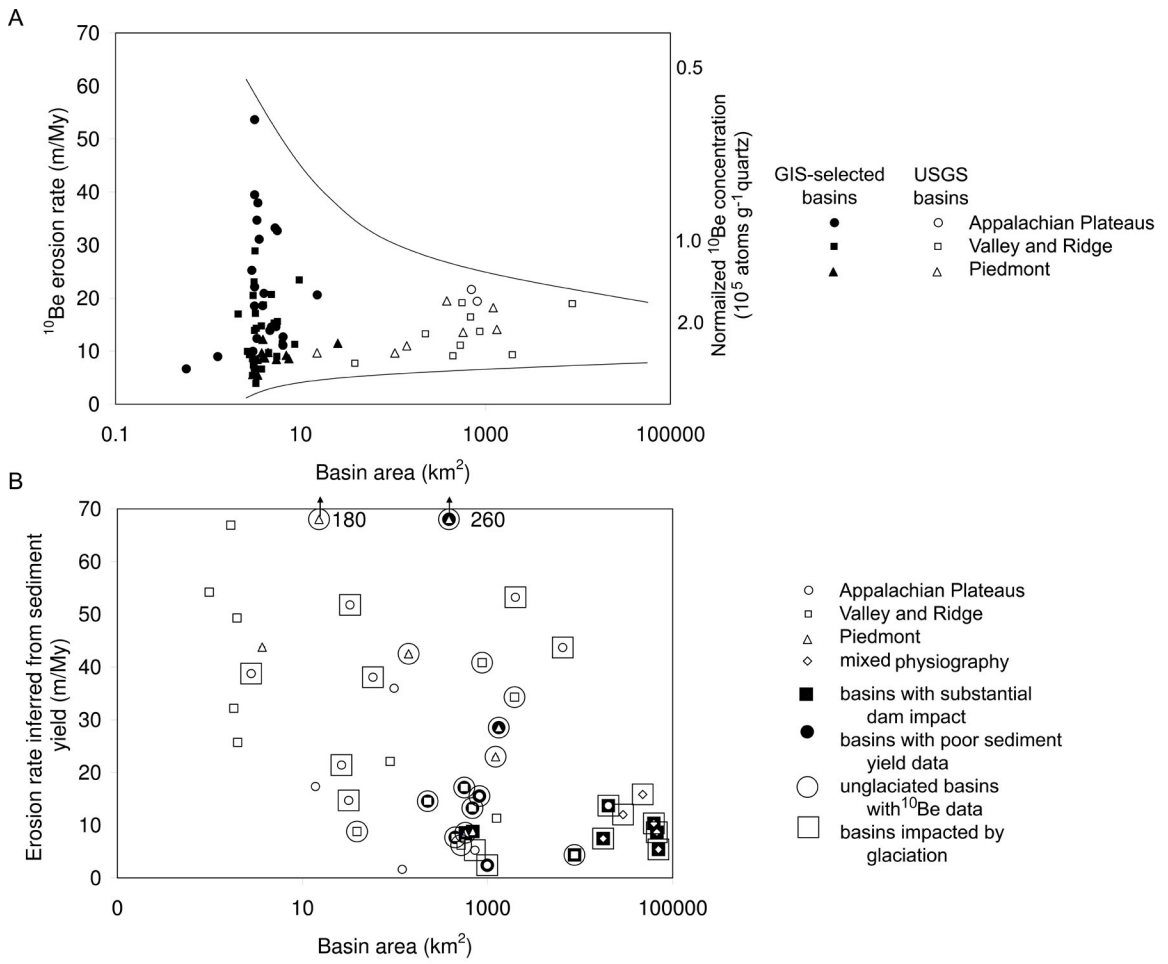
*Fig. 7. Reuter and others*

A
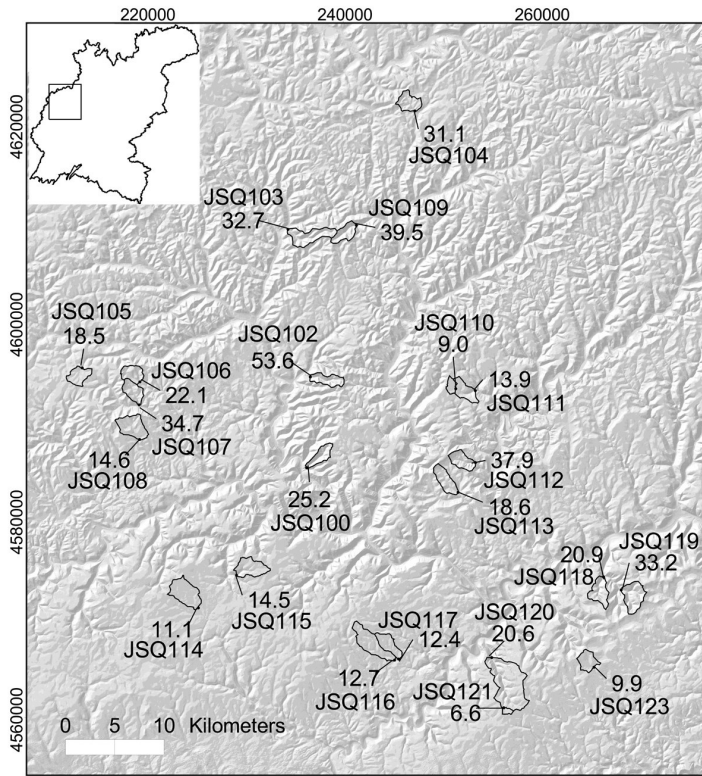
B
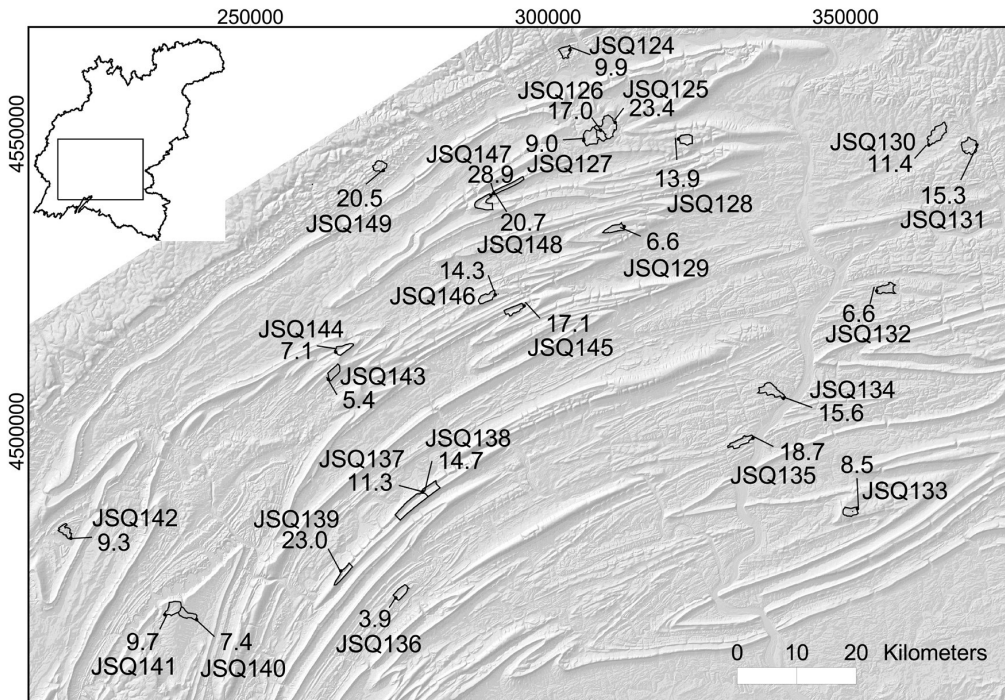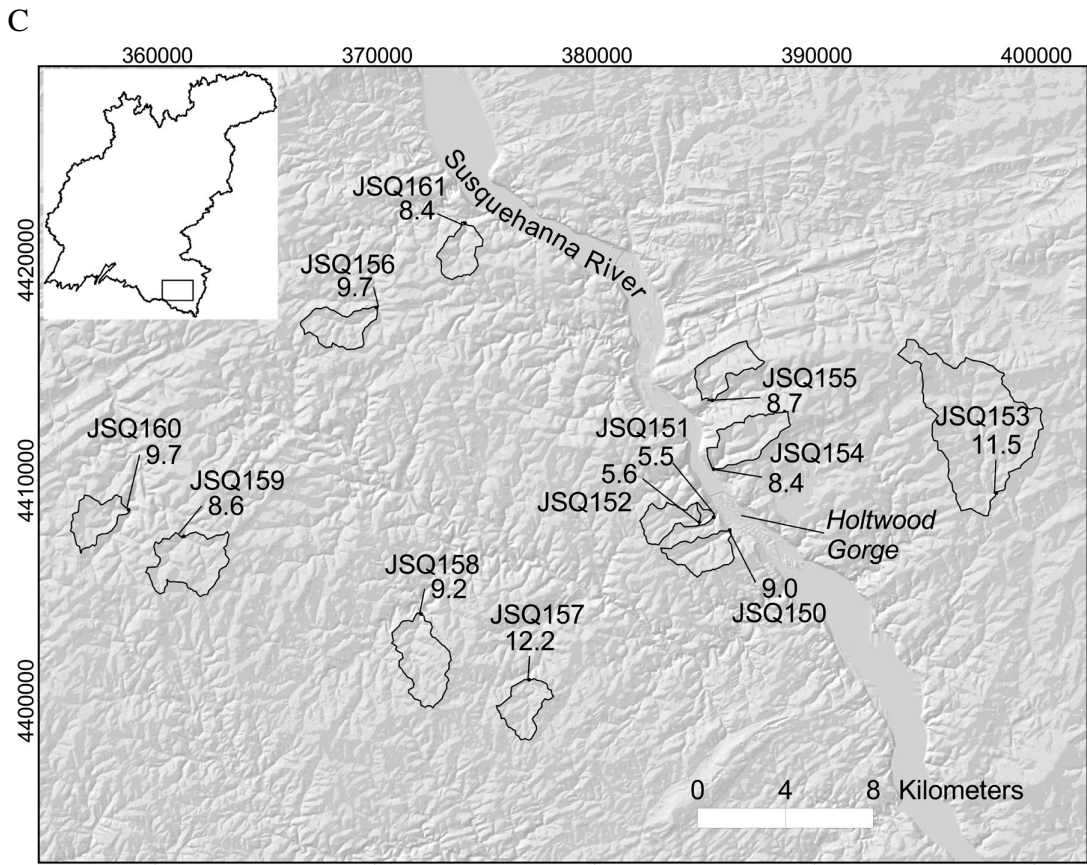
*Fig. 8. Reuter and others*
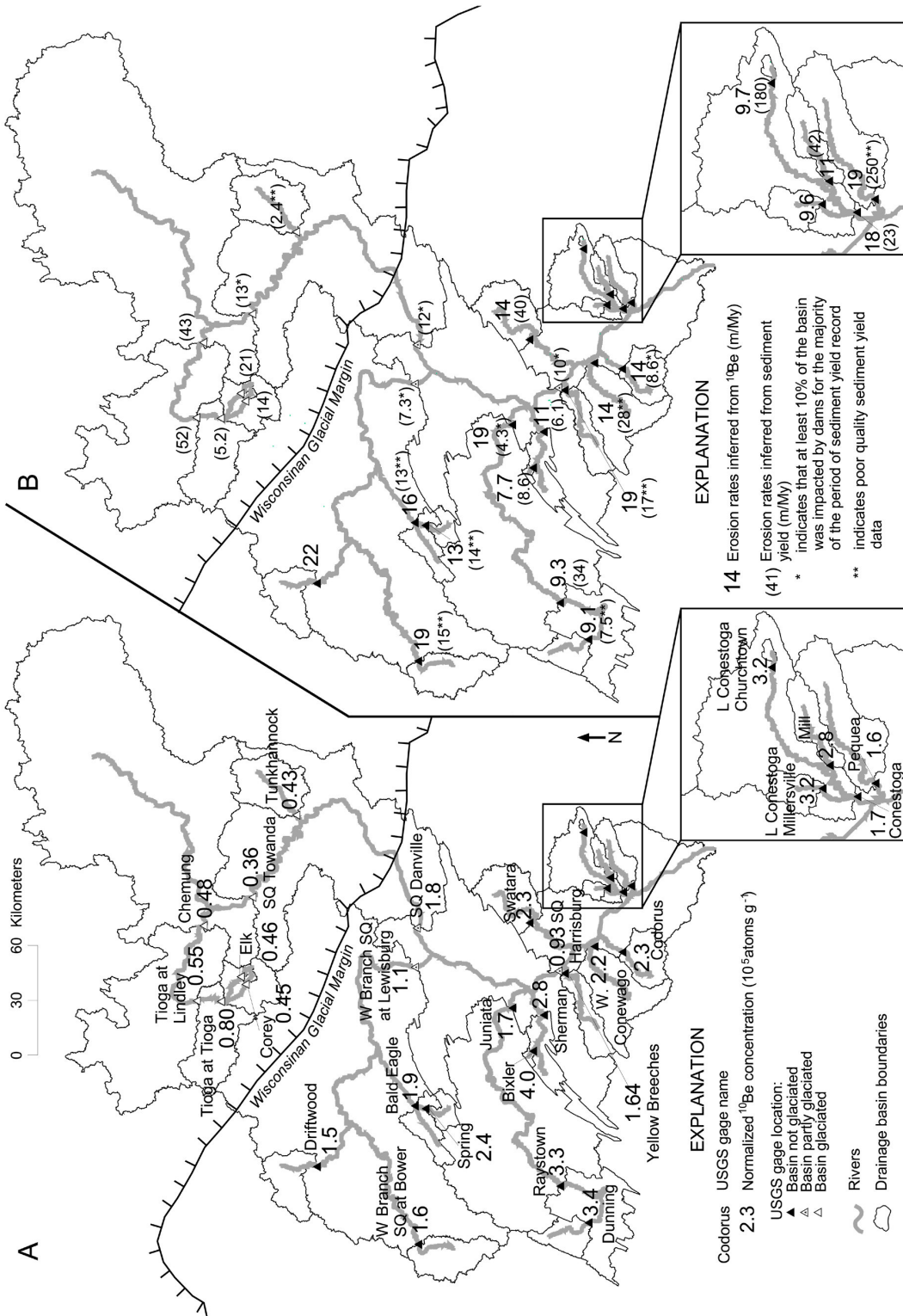
*Fig. 9. Reuter and others*

108
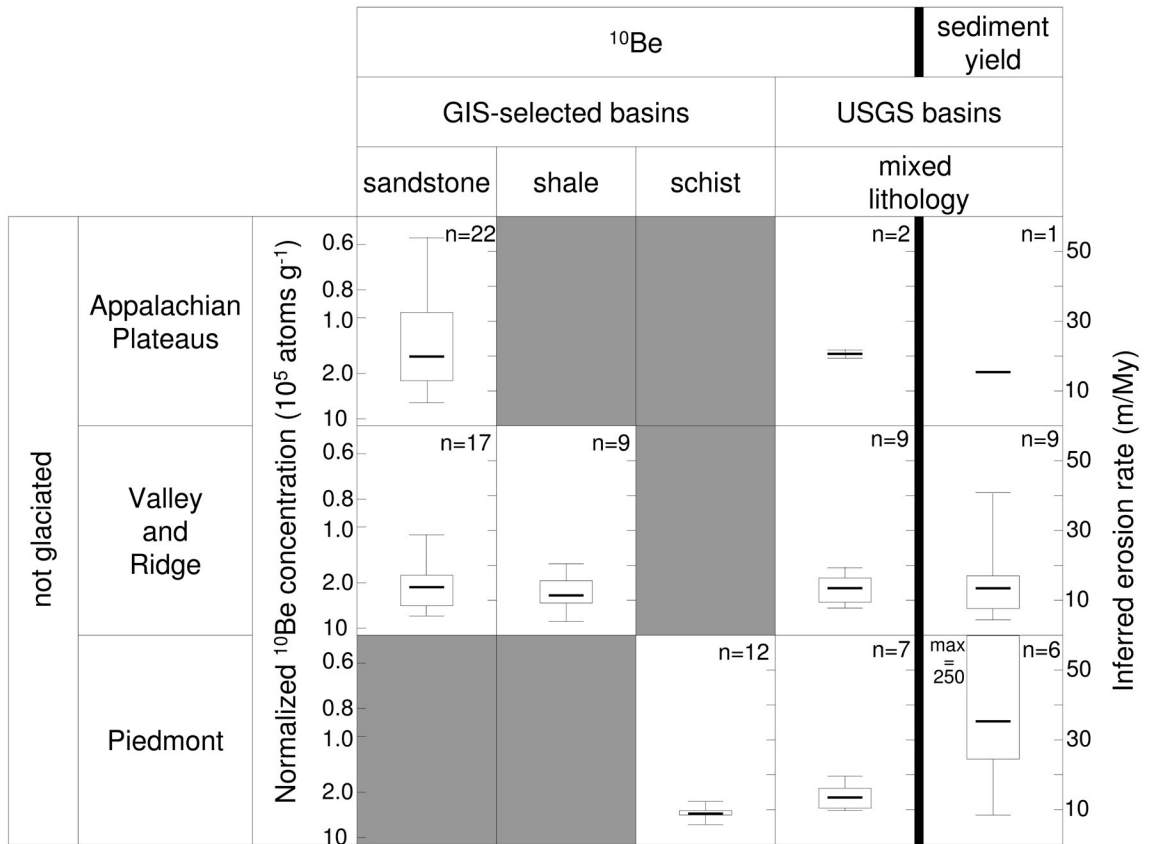
*Fig. 10. Reuter and others*

A



B
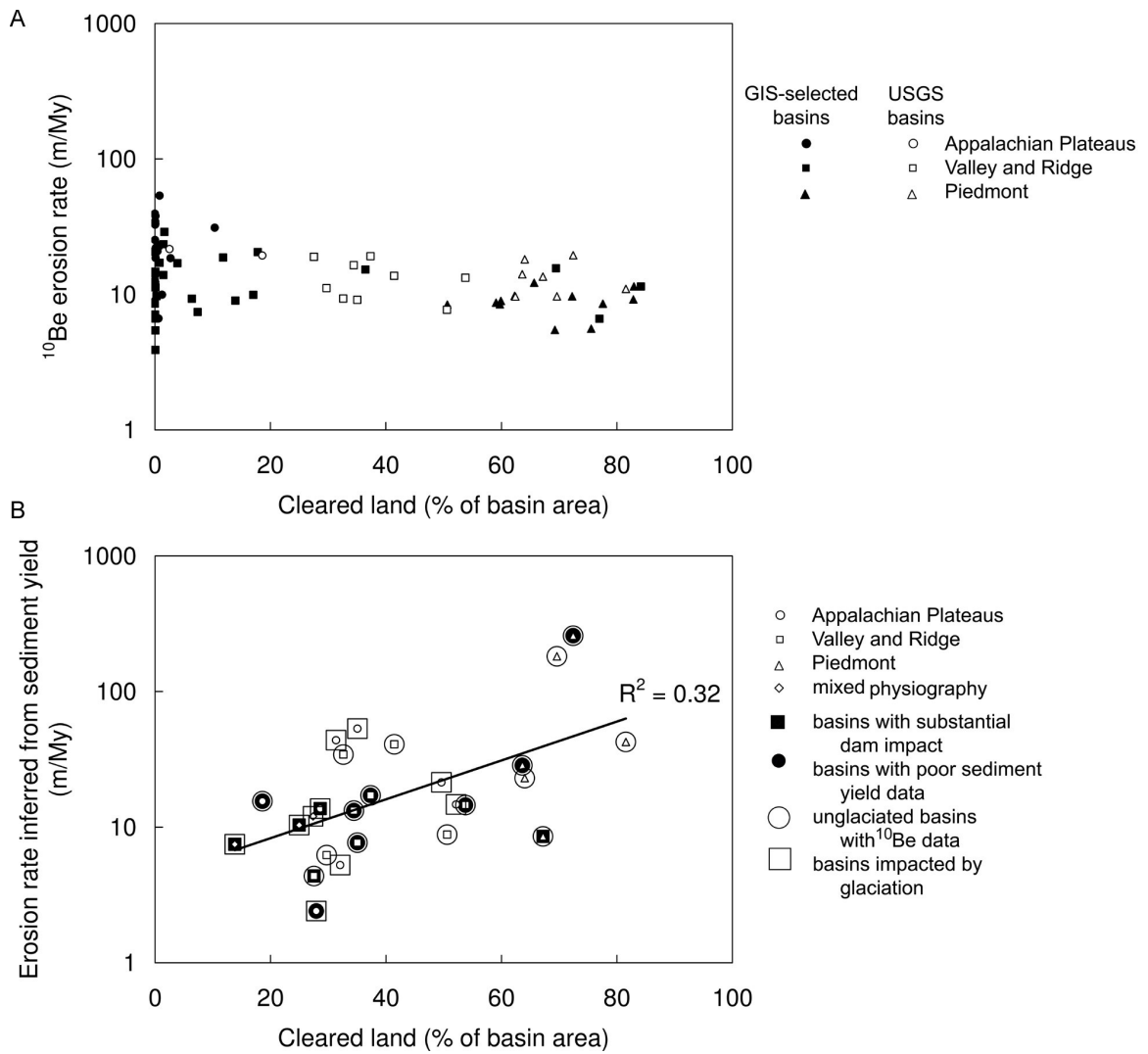
*Fig. 11. Reuter and others*

***Tectonics, topography, lithology, climate, vegetation, and history:***

***Setting erosion rates and patterns of the Susquehanna River Basin in a global context***

Erosion rates inferred from $^{10}$Be measured in fluvial sediment collected from the Susquehanna River Basin range from 4 to 54 m/My, a wide range that overlaps the erosion rates from a variety of regions globally. The lowest erosion rates from the Susquehanna River Basin are comparable to those from western Namibia (Bierman and Caffee, 2001) and Wilpena Pound (Bierman et al., 1998) in south central Australia. The highest measured erosion rate from the Susquehanna River Basin overlaps the lowest recorded rate for the tectonically active Bolivian Andes (Safran et al., in press). Overall, however, the rates for the Susquehanna River Basin are similar to those from other tectonically quiescent regions.

The spatial variability of erosion rates within the Susquehanna River Basin is best explained by topography. Mean basin slope, in particular, is a topographic metric that is positively correlated with $^{10}$Be erosion rate. Slope explains about 72% of the variance in $^{10}$Be erosion rates among the non-glaciated Appalachian Plateaus basins, and about 57% of the variance among the small, GIS-selected basins collectively. Although both mean basin slope and mean basin elevation explain variability of $^{10}$Be erosion rates on a global scale, mean basin elevation is not a useful predictor variable within the Susquehanna River Basin. Indeed, some of the most slowly eroding basins are at high elevations in the Valley and Ridge; the low slope of these basins, rather than the high elevation, is the most useful predictor of their erosion rates. It is worth noting, however, that slope

emerges as an important predictor variable only among groups of basins representing a wide range of average slopes. For the larger USGS basins, which exhibit a relatively small range of mean basin slopes, no relationship between erosion rate and slope was detected.

Lithology is another factor for which I specifically sought out relationships with $^{10}$Be erosion rates. However, no influence of lithology on erosion rate is detectable from this suite of samples, even though the Valley and Ridge is a classic location for demonstrating the relation between rock type and topography. One possible explanation for this is that erosion rates vary with soil thicknesses (Heimsath et al., 1997) in a way that compensates for differing erosional susceptibility of underlying lithologies. Whether or not this is the case, in the attempt to understand how bedrock affects erosion, a confounding factor is that lithology does not have a one to one relationship with characteristics that are commonly considered to influence susceptibility to erosion. For example, not all sandstones are equal, as demonstrated by the resistant Tuscarora and the easily dismantled Huntley Mountain Formation. Geologic maps rarely quantify the assortment of factors that are associated with susceptibility to erosion. These include, for example, joint or fracture densities, degree of cementation, orientation of planes of weakness, and thickness of bedding. The lack of critical information for determining bedrock strength is compounded on a global scale, as the Susquehanna River Basin's geology is well mapped by global standards.

Topography and lithology vary significantly across the Susquehanna River Basin; climatic factors do not. Precipitation in the Susquehanna River Basin is not highly seasonal, a characteristic that appears to be associated with low erosion rates in a global

112

context. Climatic conditions in the Susquehanna River Basin are conducive to forests, which are generally considered to have dominated the region prior to European settlement (Merritts and Walter, 2003). Although the Susquehanna River Basin is not a good place to try to tease apart the influence of either precipitation or vegetation on long term erosion rates, the long term temporal variability of climate is directly related to another factor of importance to $^{10}$Be methodology: glaciation. Glaciers, and both the erosion and neutron shielding they induce, violate assumptions necessary for the interpretation of $^{10}$Be concentrations as erosion rates. Samples from regions of the Susquehanna River Basin that experienced Wisconsinan glaciation yield low $^{10}$Be concentrations, an observation that is consistent with the interpretation that isotopic steady state has not yet been regained.

History is not a characteristic of landscapes that can be mapped, unlike the major factors considered thus far: tectonics, topography, rock type, climate, and vegetation. However, a knowledge of the geologic and geomorphic history of a region may be necessary for a more complete understanding of a region's erosion patterns, and, conversely, erosion patterns may themselves be useful in testing hypotheses regarding the geologic history of a region. With respect to this, my results are consistent with the interpretation that drainage capture in the Miocene started a wave of incision through the upper Susquehanna River Basin, an idea that had been proposed for the central Appalachian region (Naeser et al., 2004). This interpretation of the Susquehanna River Basin as a dynamic landscape contrasts with the steady-state form advocated by Hack (1960), and it also has implications for renewal of relief in passive margin settings. If this interpretation is correct for the Susquehanna River Basin, in a relatively stable tectonic

113

setting, then it raises the question of whether it is common for regions to experience

prolonged periods of adjustment, with relief changing and landscapes evolving from one

form to another. If so, this might have implications for the global data. If the strength and

nature of relationships between erosion rates and landscape characteristics are influenced

by historical factors, such as whether or not there was a recent base level fall (Riebe et

al., 2000), then high-resolution predictability of erosion rates may be unachievable based

solely on mappable landscape characteristics.

### *$^{10}$Be and sediment yield comparisons: $^{10}$Be as an applied tool*

This work demonstrates that $^{10}$Be data can be useful for developing a better

understanding of sediment dynamics as needed to address problems such as high

sediment loads to Chesapeake Bay. The results of this work show that inferred $^{10}$Be

erosion rates for the Susquehanna River Basin are relatively robust to complicating

factors such as human impact and lithology, though glaciation is an exception. Therefore,

the $^{10}$Be erosion rates for the non-glaciated regions can be compared to sediment yield. In

the Piedmont province of the Susquehanna River Basin, this comparison demonstrates

that the sediment yields are substantially higher than background sediment generation

rates. Furthermore, the Piedmont is a region with intense past and present agricultural

land use, something that certainly contributes to the high sediment yields. The results

presented in this thesis attest to the usefulness of $^{10}$Be as an applied tool for

understanding the landscape behavior.

# COMPREHENSIVE BIBLIOGRAPHY

Abrams, M.D., and Ruffner, C.M., 1995, Physiographic analysis of witness-tree distribution (1765-1798) and present forest cover through north central Pennsylvania: Canadian Journal of Forest Research, v. 25, p. 659-668.

Ahnert, F., 1970, Functional relationships between denudation, relief, and uplift in large mid-latitude drainage basins: American Journal of Science, v. 268, p. 243-263.

Baldwin, J.A., Whipple, K.X., and Tucker, G.E., 2003, Implications of the shear stress river incision model for the timescale of postorogenic decay of topography: Journal of Geophysical Research, v. 108, p. 1-17.

Bierman, P., Clapp, E., Nichols, K., Gillespie, A., and Caffee, M.W., 2001, Using cosmogenic nuclide measurements in sediments to understand background rates of erosion and sediment transport, *in* Harmon, R.S., and Doe III, W.W., eds., Landscape Erosion and Evolution Modeling: New York, Kluwer, p. 89-115.

Bierman, P., and Nichols, K.K., 2004, Rock to sediment--Slope to sea with 10-Be--Rates of landscape change: Annual review of Earth and Planetary Sciences, v. 32, p. 215-255.

Bierman, P., and Steig, E.J., 1996, Estimating rates of denudation using cosmogenic isotope abundances in sediment: Earth Surface Processes and Landforms, v. 21, p. 125-139.

Bierman, P.R., 1993, In situ produced cosmogenic isotopes and the evolution of granitic landforms [Ph.D. thesis], University of Washington, Seattle, WA.

Bierman, P.R., Albrecht, A., Bothner, M.H., Brown, E.T., Bullen, T.D., Gray, L.B., and Turpin, L., 1998, Weathering, erosion and sedimentation, *in* Kendall, C., and McDonnell, J.J., eds., Isotope Tracers in Catchment Hydrology, Elsevier, p. 647-678.

Bierman, P.R., and Caffee, M., 2001, Slow rates of rock surface erosion and sediment production across the Namib Desert and escarpment, Southern Africa: American Journal of Science, v. 301, p. 326-358.

Bierman, P.R., Reuter, J.M., Pavich, M., Gellis, A., Caffee, M.W., and Larsen, J., in press, Using cosmogenic nuclides to contrast rates of erosion and sediment yield in a semi-arid, arroyo-dominated landscape, Rio Puerco Basin, New Mexico: Earth Surface Processes and Landforms.

Blackmer, G.C., Omar, G.I., and Gold, D.P., 1994, Post-Alleghanian unroofing history of the Appalachian Basin, Pennsylvania, from apatite fission track analysis and thermal models: Tectonics, v. 13, p. 1259-1276.

Bonnet, S., and Crave, A., 2003, Landscape response to climate change: Insights from experimental modeling and implications for tectonic versus climatic uplift of topography: Geology, v. 31, p. 123-126.

Braun, D.D., 2004, The glaciation of Pennsylvania, USA, *in* Ehlers, J., and Gibbard, P.L., eds., Quaternary glaciations--extent and chronology, Part II: Amsterdam, Elsevier, p. 237-242.

Brown, E.T., Stallard, R.F., Larsen, M.C., Bourlès, D.L., Raisbeck, G.M., and Yiou, F., 1998, Determination of predevelopment denudation rates of an agricultural watershed (Cayaguás River, Puerto Rico) using in-situ-produced [10]Be in river-borne quartz: Earth and Planetary Science Letters, v. 160, p. 723-728.

Brown, E.T., Stallard, R.F., Larsen, M.C., Raisbeck, G.M., and Yiou, F., 1995, Denudation rates determined from the accumulation of in situ-produced [10]Be in the Luquillo Experimental Forest, Puerto Rico: Earth and Planetary Science Letters, v. 129, p. 193-202.

Burbank, D.W., 2002, Rates of erosion and their implications for exhumation: Mineralogical Magazine, v. 66, p. 25-52.

Clapp, E.M., Bierman, P.R., and Caffee, M., 2002, Using [10]Be and [26]Al to determine sediment generation rates and identify sediment source areas in an arid region drainage basin: Geomorphology, v. 45, p. 89-104.

Clapp, E.M., Bierman, P.R., Schick, A.P., Lekach, J., Enzel, Y., and Caffee, M., 2000, Sediment yield exceeds sediment production in arid region drainage basins: Geology, v. 28, p. 995-998.

Clark, G.M., and Ciolkosz, E.J., 1988, Periglacial geomorphology of the Appalachian Highlands and Interior Highlands south of the glacial border--a review: Geomorphology, v. 1, p. 191-220.

Costa, J.E., 1975, Effects of agriculture on erosion and sedimentation in the Piedmont province, Maryland: Geological Society of America Bulletin, v. 86, p. 1281-1286.

Daly, C., and Taylor, G., 1998, Pennsylvania average annual precipitation, 1961-90, http://www.ocs.orst.edu/prism/, accessed: April 2005.

Davis, W.M., 1889, The rivers and valleys of Pennsylvania: National Geographic Magazine, v. 1, p. 183-253.

—, 1899, The geographical cycle: The Geographical Journal, v. 14, p. 481-504.

DeFries, R.S., Hansen, M.C., Townshend, J.R.G., Janetos, A.C., and Loveland, T.R., 2000, A new global 1-km dataset of percentage tree cover derived from remote sensing: Global Change Biology, v. 6, p. 247-254.

Delcourt, P.A., and Delcourt, H.R., 1981, Vegetation maps for eastern North America: 40,000 yr B.P. to the present, *in* Romans, R.C., ed., Geobotany II: New York, Plenum Press, p. 123-165.

—, 1984, Late Quaternary paleoclimates and biotic responses in eastern North America and the western North Atlantic Ocean: Palaeogeography, Palaeoclimatology, Palaeoecology, v. 48, p. 263-284.

Dole, R.B., and Stabler, H., 1909, Denudation: USGS Water-Supply Paper 234, p. 78-93.

Edmunds, W.M., 2003, Coal in Pennsylvania (2nd ed.): Harrisburg, Pennsylvania Geological Survey, 28 p.

Ehlers, J., and Gibbard, P.L., editors, 2004a, Quaternary glaciations--extent and chronology, part I: Europe: Amsterdam, Elsevier, 475 p.

—, 2004b, Quaternary glaciations--extent and chronology, part II: North America: Amsterdam, Elsevier, 440 p.

—, 2004c, Quaternary glaciations--extent and chronology, part III: South America, Asia, Africa, Australia, Antarctica: Amsterdam, Elsevier, 380 p.

Fenneman, N.M., and Johnson, D.W., 1946, Physiographic divisions of the coterminous U.S., http://water.usgs.gov/GIS/metadata/usgswrd/XML/physio.xml, accessed: March 2005.

Finlayson, D.P., and Montgomery, D.R., 2003, Modeling large-scale fluvial erosion in geographic information systems: Geomorphology, v. 53, p. 147-164.

Fournier, F., 1949, Climatic factors in soil erosion (Les facteurs climatiques de l'érosion du sol), *in* Laronne, J.B., and Mosley, M.P., eds., 1982, Benchmark papers in geology/63: Erosion and sediment yield: Stroudsburg, Pennsylvania, Hutchinson Ross Publishing Company, p. 175-180.

Gabet, E.J., Pratt-Sitaula, B.A., and Burbank, D.W., 2004, Climatic controls on hillslope angle and relief in the Himalayas: Geology, v. 32, p. 629-632.

Gardner, T.W., 1989, Neotectonism along the Atlantic passive continental margin: A review: Geomorphology, v. 2, p. 71-97.

Gellis, A.C., Banks, W.S.L., Langland, M.J., and Martucci, S.K., 2004a, Summary of suspended-sediment data for streams draining the Chesapeake Bay watershed, water years 1952-2002, USGS Scientific Investigations Report 2004-5056, 59 p.

Gellis, A.C., Pavich, M.J., Bierman, P.R., Clapp, E.M., Ellevein, A., and Aby, S., 2004b, Modern sediment yield compared to geologic rates of sediment production in a

semi-arid basin, New Mexico: assessing the human impact: Earth Surface Processes and Landforms, v. 29, p. 1359-1372.

Giardini, D., Grünthal, G., Shedlock, K.M., and Zhang, P., 1999, The GSHAP global seismic hazard map: Annali di Geofisica, v. 42, p. 1225-1228.

Granger, D.E., Fabel, D., and Palmer, A.N., 2001, Pliocene-Pleistocene incision of the Green River, Kentucky, determined from radioactive decay of cosmogenic [26]Al and [10]Be in Mammoth Cave sediments: Geological Society of America Bulletin, v. 113, p. 825-836.

Granger, D.E., Kirchner, J.W., and Finkel, R., 1996, Spatially averaged long-term erosion rates measured from in situ-produced cosmogenic nuclides in alluvial sediments: Journal of Geology, v. 104, p. 249-257.

Hack, J.T., 1960, Interpretation of erosional topography in humid temperate regions: American Journal of Science, v. 258-A, p. 80-97.

—, 1982, Physiographic divisions and differential uplift in the Piedmont and Blue-Ridge, USGS Professional Paper 1265, 49 p.

Hasbargen, L.E., and Paola, C., 2000, Landscape instability in an experimental drainage basin: Geology, v. 28, p. 1067-1070.

Heimsath, A.M., Chappell, J., Dietrich, W.E., Nishiizumi, K., and Finkel, R.C., 2000, Soil production on a retreating escarpment in southeastern Australia: Geology, v. 28, p. 787-790.

Heimsath, A.M., Chappell, J., Spooner, N.A., and Questiaux, D.G., 2002, Creeping soil: Geology, v. 30, p. 111-114.

Heimsath, A.M., Dietrich, W.E., Nishiizumi, K., and Finkel, R.C., 1997, The soil production function and landscape equilibrium: Nature, v. 388, p. 358-361.

—, 1999, Cosmogenic nuclides, topography, and the spatial variation of soil depth: Geomorphology, v. 27, p. 151-172.

—, 2001, Stochastic processes of soil production and transport: erosion rates, topographic variation and cosmogenic nuclides in the Oregon Coast Range: Earth Surface Processes and Landforms, v. 26, p. 531-552.

Hewawasam, T., von Blanckenburg, F., Schaller, M., and Kubik, P., 2003, Increase of human over natural erosion rates in tropical highlands constrained by cosmogenic nuclides: Geology, v. 31, p. 597-600.

Hicks, D.M., Hill, J., and Shankar, U., 1996, Variation of suspended sediment yields around New Zealand: the relative importance of rainfall and geology, *in* Walling,

D.E., and Webb, B.W., eds., Erosion and sediment yield: global and regional perspectives: Wallingford, UK, International Association of Hydrological Sciences, p. 149-156.

Hitchcock, E., 1841, Final report on the geology of Massachusetts: Amherst, MA, J. S. and C. Adams, 831 p.

Jansen, J.M.L., and Painter, R.B., 1974, Predicting sediment yield from climate and topography: Journal of Hydrology, v. 21, p. 371-380.

Judson, S., and Ritter, D.F., 1964, Rates of regional denudation in the United States: Journal of Geophysical Research, v. 69, p. 3395-3401.

Kirchner, J.W., Finkel, R.C., Riebe, C.S., Granger, D.E., Clayton, J.L., King, J.G., and Megahan, W.F., 2001, Mountain erosion over 10 yr, 10 k.y., and 10 m.y. time scales: Geology, v. 29, p. 591-594.

Knighton, D., 1998, Fluvial forms and processes: a new perspective: New York, Oxford University Press Inc., 383 p.

Kohl, C.P., and Nishiizumi, K., 1992, Chemical isolation of quartz for measurement of *in-situ* -produced cosmogenic nuclides: Geochimica et Cosmochimica Acta, v. 56, p. 3583-3587.

Lal, D., 1991, Cosmic ray labeling of erosion surfaces: *in situ* nuclide production rates and erosion models: Earth and Planetary Science Letters, v. 104, p. 424-439.

Lal, D., and Peters, B., 1967, Cosmic ray produced radioactivity on the earth, *in* Sitte, K., ed., Handbuch der Physik: New York, Springer-Verlag, p. 551-612.

Langbein, W.B., and Schumm, S.A., 1958, Yield of sediment in relation to mean annual precipitation: American Geophysical Union Transactions, v. 39, p. 1076-1084.

Langland, M., and Cronin, T., 2003, A summary report of sediment processes in Chesapeake Bay and watershed: New Cumberland, Pennsylvania, USGS Water-Resources Investigations Report 03-4123, 109 p.

Langland, M.J., and Hainly, R.A., 1997, Changes in bottom surface-elevations in three reservoirs on the lower Susquehanna River, Pennsylvania and Maryland, following the January 1996 flood--Implications for nutrient and sediment loads to Chesapeake Bay, USGS Water-Resources Investigations Report 97-4138, 34 p.

Leemans, R., and Cramer, W.P., 1991, The IIASA database for mean monthly values of temperature, precipitation and cloudiness of a global terrestrial grid., Research Report RR-91-18, International Institute of Applied Systems Analyses, 61 p.

Ludwig, W., and Probst, J., 1998, River sediment discharges to the oceans: present-day controls and global budgets: American Journal of Science, v. 298, p. 265-295.

Matmon, A., Bierman, P.R., Larsen, J., Southworth, S., Pavich, M., and Caffee, M., 2003a, Temporally and spatially uniform rates of erosion in the southern Appalachian Great Smoky Mountains: Geology, v. 31, p. 155–158.

Matmon, A., Bierman, P.R., Larsen, J., Southworth, S., Pavich, M., Finkel, R., and Caffee, M., 2003b, Erosion of an ancient mountain range, the Great Smoky Mountains, North Carolina and Tennessee: American Journal of Science, v. 303, p. 817-855.

Meade, R.H., 1969, Errors in using modern stream-load data to estimate natural rates of denudation: Geological Society of America Bulletin, v. 80, p. 1265-1274.

Merritts, D., and Walter, R., 2003, Colonial mill ponds of Lancaster County Pennsylvania as a major source of sediment pollution to the Susquehanna River and Chesapeake Bay, *in* Merritts, D., Walter, R., and de Wet, A., eds., Channeling through time: landscape evolution, land use change, and stream restoration in the lower Susquehanna River Basin: Southeast Friends of the Pleistocene Fall 2003 Fieldtrip Guidebook, p. 56-65.

Miller, D.S., and Duddy, I.R., 1989, Early Cretaceous uplift and erosion of the northern Appalachian Basin, New York, based on apatite fission track analysis: Earth and Planetary Science Letters, v. 93, p. 35-49.

Mills, H.H., Brakenridge, G.R., Jacobson, R.B., Newell, W.L., Pavich, M.J., and Pomeroy, J.S., 1987, Appalachian mountains and plateaus, *in* Graf, W.L., ed., Geomorphic systems of North America, Centennial Special Volume 2: Boulder, Colorado, Geological Society of America, p. 5-50.

Molnar, P., 2003, Nature, nurture and landscape: Nature, v. 426, p. 612-614.

Montgomery, D.R., Balco, G., and Willett, S.D., 2001, Climate, tectonics, and the morphology of the Andes: Geology, v. 29, p. 579-582.

Morel, P., von Blanckenburg, F., Schaller, M., Kubik, P.W., and Hinderer, M., 2003, Lithology, landscape dissection and glaciation controls on catchment erosion as determined by cosmogenic nuclides in river sediment (the Wutach Gorge, Black Forest): Terra Nova, v. 15, p. 398-404.

Naeser, C.W., Naeser, N.D., Newell, W.L., Southworth, C.S., Weems, R.E., and Edwards, L.E., 2004, Provenance studies in the Atlantic Coastal Plain: what fission-track ages of detrital zircons can tell us about the source of sediment: Geological Society of America Abstracts with Programs, v. 36, p. 114.

NASA, National Imagery and Mapping Agency (NIMA), German space agency (DLR), and Italian space agency (ASI), 2004, Shuttle Radar Topography Mission elevation data sets (SRTM-3), ftp://e0mss21u.ecs.nasa.gov/srtm/, accessed: March 2005.

New, M., Lister, D., Hulme, M., and Makin, I., 2002, A high-resolution data set of surface climate over global land areas: Climate Research, v. 21, p. 1-25.

Nichols, K., Bierman, P., Finkel, R., and Larsen, J., in press, Long term sediment generation rates for the upper Rio Chagres Basin: evidence from cosmogenic [10]Be, *in* Harmon, R.S., ed., The Rio Chagres, Panama: a multidisciplinary profile of a tropical watershed, Springer.

Niemi, N., Oskin, M., and Burbank, D., 2004, A numerical simulation of the effects of mass-wasting on cosmogenically determined erosion rates: Eos Transactions American Geophysical Union, Fall Meeting Supplement, Abstract H51C-1157, v. 85.

NYS Museum/NYS Geological Survey, 1999, Statewide bedrock geology, http://www.nysm.nysed.gov/gis.html, accessed: March 2005.

Pazzaglia, F.J., and Brandon, M.T., 1996, Macrogeomorphic evolution of the post-Triassic Appalachian mountains determined by deconvolution of the offshore basin sedimentary record: Basin Research, v. 8, p. 255-278.

Pazzaglia, F.J., and Gardner, T.W., 1993, Fluvial terraces of the lower Susquehanna River: Geomorphology, v. 8, p. 83-113.

Pennsylvania Bureau of Topographic and Geologic Survey, Department of Conservation and Natural Resources, 1995a, Late Wisconsinan glacial border 1:100,000, http://www.pasda.psu.edu/documents.cgi/dcnr/pags/pags_glacier1k.xml, accessed: March 2005.

—, 1995b, Physiographic provinces 1:100,000, http://www.pasda.psu.edu/documents.cgi/dcnr/pags/pags_physprov1k.xml, accessed: March 2005.

—, 2001, Digital bedrock geology of Pennsylvania, http://www.dcnr.state.pa.us/topogeo/map1/bedmap.aspx, accessed: March 2005.

Phillips, J., 2003, Alluvial storage and the long-term stability of sediment yields: Basin Research, v. 15, p. 153-163.

Phillips, W.M., McDonald, E.V., Reneau, S.L., and Poths, J., 1998, Dating soils and alluvium with cosmogenic [21]Ne depth profiles: case studies from the Pajarito Plateau, New Mexico, USA: Earth and Planetary Science Letters, v. 160, p. 209-223.

121

Pinet, P., and Souriau, M., 1988, Continental erosion and large-scale relief: Tectonics, v. 7, p. 563-582.

Poag, C.W., and Sevon, W.D., 1989, A record of Appalachian denudation in postrift Mesozoic and Cenozoic sedimentary deposits of the U.S. middle Atlantic continental margin: Geomorphology, v. 2, p. 119-157.

Reusser, L.J., Bierman, P.R., Pavich, M.J., Zen, E., Larsen, J., and Finkel, R., 2004, Rapid late Pleistocene incision of Atlantic passive-margin river gorges: Science, v. 305, p. 499-502.

Reuter, J.M., Bierman, P.R., Pavich, M.J., Larsen, J., and Finkel, R.C., 2004, Linking [10]Be estimates of erosion rates with landscape variables: compilation and consideration of multiple data sets from around the world, 32nd International Geological Conference: Florence.

—, in preparation, Testing models of Appalachian Mountain geomorphology with erosion rates inferred from cosmogenic [10]Be.

Riebe, C.S., Kirchner, J.W., and Finkel, R.C., 2003, Long-term rates of chemical weathering and physical erosion from cosmogenic nuclides and geochemical mass balance: Geochimica et Cosmochimica Acta, v. 67, p. 4411-4427.

Riebe, C.S., Kirchner, J.W., and Granger, D.E., 2001a, Quantifying quartz enrichment and its consequences for cosmogenic measurements of erosion rates from alluvial sediment and regolith: Geomorphology, v. 40, p. 15-19.

Riebe, C.S., Kirchner, J.W., Granger, D.E., and Finkel, R.C., 2000, Erosional equilibrium and disequilibrium in the Sierra Nevada, inferred from cosmogenic [26]Al and [10]Be in alluvial sediment: Geology, v. 28, p. 803-806.

—, 2001b, Minimal climatic control on erosion rates in the Sierra Nevada, California: Geology, v. 29, p. 447-450.

Roden, M.K., and Miller, D.S., 1989, Apatite fission-track thermochronology of the Pennsylvania Appalachian Basin: Geomorphology, v. 2, p. 39-51.

Ruxton, R.P., and McDougall, I., 1967, Denudation rates in northeast Papua from potassium-argon dating of lavas: American Journal of Science, v. 265, p. 545-561.

Safran, E.B., Bierman, P.R., Aalto, R., Dunne, T., Whipple, K.X., and Caffee, M., in press, Erosion rates driven by channel network incision in the Bolivian Andes: Earth Surface Processes and Landforms.

Schaller, M., von Blanckenburg, F., Hovius, N., and Kubik, P.W., 2001, Large-scale erosion rates from in situ-produced cosmogenic nuclides in European river sediments: Earth and Planetary Science Letters, v. 188, p. 441-458.

Schildgen, T.F., Phillips, W.M., and Purves, R.S., 2005, Simulation of snow shielding corrections for cosmogenic nuclide surface exposure studies: Geomorphology, v. 64, p. 67-85.

Schumm, S.A., 1963, The disparity between present rates of denudation and orogeny, USGS Professional Paper 454-H, 13 p.

Shultz, A.P., editor, 1999, The geology of Pennsylvania: Harrisburg, PA, Pennsylvania Geological Survey, 888 p.

Stranahan, S.Q., 1993, Susquehanna, river of dreams: Baltimore, The Johns Hopkins University Press, 322 p.

Summerfield, M.A., and Hulton, N.J., 1994, Natural controls of fluvial denudation rates in major world drainage basins: Journal of Geophysical Research, v. 99, p. 13871-13883.

Syvitski, J.P.M., Peckham, S.D., Hilberman, R., and Mulder, T., 2003, Predicting the terrestrial flux of sediment to the global ocean: a planetary perspective: Sedimentary Geology, v. 162, p. 5-24.

Trimble, S.W., 1977, The fallacy of stream equilibrium in contemporary denudation studies: American Journal of Science, v. 277, p. 876-887.

—, 1997, Contribution of stream channel erosion to sediment yield from an urbanizing watershed: Science, v. 278, p. 1442-1444.

Tully, J., 2001, Coal fields of the United States, http://www.nationalatlas.gov/metadata/coalfdp050.html, accessed: March 2005.

United States Census Bureau, 2004, U.S. Census Database, 2000, http://nationalatlas.gov/atlasftp.html, accessed: March 2005.

USGS, 1997, New York land cover data set, http://landcover.usgs.gov/nlcd/show_data.asp?code=NY&state=New_York, accessed: April 2005.

—, 1999a, Major dams of the United States, http://nationalatlas.gov/atlasftp.html, accessed: June 2003.

—, 1999b, Maryland land cover data set, http://landcover.usgs.gov/nlcd/show_data.asp?code=MD&state=Maryland, accessed: April 2005.

—, 1999c, Pennsylvania land cover data set, http://landcover.usgs.gov/nlcd/show_data.asp?code=PA&state=Pennsylvania, accessed: April 2005.

—, 2002, Cities and towns of the United States, http://nationalatlas.gov/atlasftp.html, accessed: April 2005.

USGS, E.D.C., 1999d, National elevation dataset, http://gisdata.usgs.net/ned/, accessed: April 2005.

Vance, D., Bickle, M., Ivy-Ochs, S., and Kubik, P.W., 2003, Erosion and exhumation in the Himalaya from cosmogenic isotope inventories of river sediments: Earth and Planetary Science Letters, v. 206, p. 273-288.

von Blanckenburg, F., Hewawasam, T., and Kubik, P.W., 2004, Cosmogenic nuclide evidence for low weathering and denudation in the wet, tropical highlands of Sri Lanka: Journal of Geophysical Research, v. 109, p. 1-22.

Walling, D.E., and Webb, B.W., 1983, Patterns of sediment yield, *in* Gregory, K.J., ed., Background to palaeohydrology, John Wiley & Sons Ltd., p. 69-100.

Way, J.H., 1999, Appalachian Mountain section of the Ridge and Valley province, *in* Shultz, C.H., ed., The geology of Pennsylvania: Harrisburg, Pennsylvania Geological Survey, p. 353-361.

Willett, S.D., and Brandon, M.T., 2002, On steady states in mountain belts: Geology, v. 30, p. 175-178.

Williams, D.F., and Reed, L.A., 1972, Appraisal of stream sedimentation in the Susquehanna River Basin, USGS Water-Supply Paper 1532-F, 24 p.

Wolman, G.M., 1967, A cycle of sedimentation and erosion in urban river channels: Geografiska Annaler, v. 49A, p. 385-395.

Young, A., 1960, Soil movement by denudational processes on slopes: Nature, v. 188, p. 120-122.

### *Purpose and scope of this section*

The purpose of this section is to provide documentation regarding the mechanics of GIS analysis that I completed, including information about the GIS data sets that I used and the processing steps that I applied. The level of detail included in this section should be adequate to allow a user who is familiar with GIS software to duplicate the work. I have also inserted bits of advice that may be useful for anyone who would like to perform similar analyses.

I used ESRI software for all of the GIS analysis. Although ArcGIS 8.x has been available through the duration of my thesis work, I utilized both ArcView 3.x (hereafter referred to simply as ArcView) and ArcGIS 8.x (including ArcInfo Workstation). ArcGIS offers new features relative to ArcView, but ArcView provides stability and predictable behavior that I often prefer. Furthermore, each version offers different options for batch processing and programming; my knowledge of these features influenced my decisions regarding which version I should use for any given task.

In the following sections, I occasionally provide examples of syntax, particularly for grid operations; in those instances, I have specified which version of ESRI software I used. Most commands have equivalents in other versions of the software, even if the syntax is slightly different.

### *Flow chart of GIS procedures*

A flow chart that summarizes the procedures is included in on the data CD (Appendix B). The flow chart also appears on the following pages, at a reduced size and

split into two pieces. This flow chart is intended to be a comprehensive overview of the data processing that I did for both the Susquehanna project and the global data compilation. This methods section contains further explanation, and the section headings used in this document are referenced on the flow chart. A few points of explanation about the flow chart:

- In order to conserve space on the flow chart, I did not include data sets that are created as intermediate steps and that are unlikely to be used again; the data sets shown in parallelograms on the flow chart roughly correspond to the ones that I maintained on the hard drive.

- I did not do all steps for all regions; for example, I generated longitudinal profiles only for the Susquehanna.

- The flow chart does not fully reflect automation that I implemented to streamline certain steps. The end of this appendix contains further information on some of the custom automation that I used.

- Different line types/weights between boxes have no particular meaning; they are simply used to enhance the ability to keep track of each individual line amongst the complexity.

**Flow Chart of
GIS and Data Processing Methods**

**DEMs: Hypsometry**

convert DEM to integer grid → tabulate areas → dbf file hypsometry of basins

query flowacc— threshold stream

reclass—not on stream = NoData

**DEMs: Stream networks**

streamorder → streamshape → vector stream network shp

**DEMs: Long profiles and channel gradients**

LP work (look for details elsewhere) → channel gradient & other LP stuff

clip and intersect network with basins → dbf summary of stream length by order

**Approach to data compilation**

Approach database— joined tables → export to dbf

**Existing data: Determining sample locations**

position sample sites on flow accumulation

assign nest level → by nest level, convert points on flowacc to grid → delineate basins → convert to shapefile → merge shapefiles from each nest level → all sample basins shapefile

**Existing data: Delineating basins**

**Excel work**

open dbf in Excel and save as txt

open txt in Excel and save as xls

calculate $^{10}Be$

sort/filter data

Excel workbook

data checking and quality control

visualize data

summarize zones

dbf files (one file per region per data type)

text files (one file per region per data type)

**Combining tables**

combine tables perl script

combine files manually → one text file per data type

LD rid

dbf files (one file per region per data type) → text files (one file per region per data type)

Statistical package (JMP)

Graphing program (Sigma Plot, etc.)

128

*Advice*

**File management and organization**

Spending some time strategizing about data organization up front can save countless hours and headaches later. A directory structure with a fair amount of logical structure that also allows for growth in unanticipated directions is really important. The hierarchy of file organization that I used had region at the highest level, followed by datum/coordinate system, and finally directories according to data type (DEM, basins, political, etc.). I make file names as descriptive as possible without making them excessively long.

**It is absolutely critical to keep track of where files are being stored at all times**, and it is important to clean up unnecessary files along the way.

**Projection and datum issues**

Selecting an appropriate projection is important to minimize distortion of spatial data (Finlayson and Montgomery, 2003). Because I used ArcView extensively, and because ArcView has limited on-the-fly projection capabilities, I converted all data to UTM for analysis. No single drainage basin in the global compilation extended unreasonably beyond UTM zone boundaries.

Use of a suitable method of resampling of grids is important to maintain the integrity of grids during projections. I used nearest neighbor for discrete value grids in which each value represents a particular class of something (such as land use). I used bilinear or cubic when the values were part of a continuous range (such as elevation or precipitation). Cubic resampling results in more smoothing and tends to produce more

severe extreme values near edges than bilinear resampling. (See ArcInfo Workstation help for more information on resampling.) Therefore, particularly for SRTM data, I preferred the bilinear algorithm to resample the digital elevation data.

For each region, I chose a working datum that matched the digital elevation data, and I shifted other data as necessary to match this. For the United States, this datum is NAD83, except in Alaska, which uses NAD27. I used WGS84 for global data outside of the U.S.

### Running an AML

ArcInfo Workstation AMLs are well suited to automating tasks. I wrote only the simplest AMLs--lists of Grid commands to be run successively; these are saved in text format with an AML extension on the file name. One limitation is that the input and output files will all end up in a single directory.

This is just a reminder on how to run an AML:

Open ArcInfo Workstation. This will bring up the Arc prompt:

Arc:

First set the workspace; this is the directory where both the data and the AML reside:

Arc: workspace c:\_data\

If the AML requires Grid, then bring up the grid prompt by typing "grid":

Arc: grid

At the grid prompt, run the aml:

Grid: &run hydro_grids.aml

130

### *Digital data sources*

Many digital spatial data sets are available free of charge from the internet. Table 1 provides a listing of primary data layers that I used for analysis. Although GIS data can often be found with a web search, there are a few really noteworthy sources that have excellent collections of data. Here is a listing of a few that I found particularly useful:

- With the USGS seamless data server (http://seamless.usgs.gov; accessed March 2005), the days of mosaicing 7.5 minute DEMs are happily in the past. NED and NLCD are among the data sets that are available here. International data (including SRTM data) are also available (or becoming available).

- The National Atlas (http://www.nationalatlas.gov/; accessed March 2005) is another good source for a variety of U.S. data (for example, roads, stream networks, census data), though not at particularly high resolution.

- The Global Land Cover Facility (http://glcf.umiacs.umd.edu/index.shtml; accessed March 2005) provides a variety of data sets, primarily remote sensing and related raster data sets, including Landsat data.

- Global GIS (http://webgis.wr.usgs.gov/globalgis/; accessed March 2005) is a collection of global data available on a set of CDs (or a DVD). This collection includes a variety of data types, but most are at a relatively coarse resolution.

- The USDA Geospatial Data Gateway (http://datagateway.nrcs.usda.gov/; accessed March 2005) also has a collection of data sets, including PRISM precipitation data.

- The Pennsylvania Spatial Data Access site (http://www.pasda.psu.edu/; accessed March 2005) is a good source for statewide data.

TABLE 1. SOURCES FOR GIS DATA

| GIS data set name | Web link | Scale or resolution | Reference |
|---|---|---|---|
| SRTM (Shuttle Radar Topography Mission) | ftp://e0mss21u.ecs.nasa.gov/srtm/ | 3 arc second | (NASA et al., 2004) |
| GTOPO30 | http://edcdaac.usgs.gov/gtopo30/gtopo30.asp | 30 arc sec (approx. 1 km) | |
| Climate: New et al. | http://www.cru.uea.ac.uk/cru/data/hrg.htm | 10 min | (New et al., 2002) |
| Precipitation and temperature: Leemans and Cramer | http://www.pik-potsdam.de/~cramer/climate.htm | 0.5 degrees | (Leemans and Cramer, 1991) |
| Global Seismic Hazard Map | http://www.seismo.ethz.ch/GSHAP/index.html | 0.1 degrees | (Giardini et al., 1999) |
| WWF Ecoregions | http://www.worldwildlife.org/science/ecoregions/terrestrial.cfm | | |
| AVHRR Continuous fields tree cover project | http://glcf.umiacs.umd.edu/data/treecover/ | 1 km | (DeFries et al., 2000) |
| Global glacial extent | | | (Ehlers and Gibbard, 2004b, 2004a, 2004c) |
| NED (National Elevation Dataset) | http://ned.usgs.gov | 1 arc sec (approx. 30 m) | (USGS, 1999d) |
| NLCD (National Land Cover Database) | http://landcover.usgs.gov/natllandcover.asp | 1 arc sec | (USGS, 1999c) |
| Physiographic provinces | http://water.usgs.gov/GIS/metadata/usgswrd/XML/physio.xml | 1:7,000,000 | (Fenneman and Johnson, 1946) |
| PRISM Precipitation | http://www.ocs.orst.edu/prism/ | 150 arc sec | (Daly and Taylor, 1998) |
| Dams | http://www.nationalatlas.gov/mld/dams00x.html | | (USGS, 1999a) |
| Digital bedrock geology of Pennsylvania | http://www.dcnr.state.pa.us/topogeo/map1/bedmap.aspx | 1:250,000 | (Pennsylvania Bureau of Topographic and Geologic Survey, 2001) |
| Late Wisconsinan Glacial Border 1:100,000 | http://www.pasda.psu.edu/summary.cgi/dcnr/pags/pags_glacier1k.xml | 1:100,000 | (Pennsylvania Bureau of Topographic and Geologic Survey, 1995a) |
| DRG (Digital Raster Graphics) | ftp://www.pasda.psu.edu/pub/pasda/drg24k-cu/ | 1:24,000 | |
| Pennsylvania Physiographic provinces | | 1:100,000 | (Pennsylvania Bureau of Topographic and Geologic Survey, 1995b) |

***Description of GIS and data processing methods, keyed to the flow chart***

***Digital elevation models***

<u>Overview</u>

Digital elevation models (DEMs) are of particular importance in executing data analysis because they are the basis from which stream networks and drainage basins are delineated. The release of the SRTM digital elevation data at a 3 arc second (approximately 90 m) resolution enables a new level of analysis for the ever-growing set of samples which have been analyzed for [10]Be in sediment. The Australian data set, released in July 2004, was the final SRTM region to be made publicly available at the 3 arc second resolution. Prior to SRTM, the highest resolution digital elevation model which covered all regions with [10]Be sediment samples was the 30 arc second (approximately 1 kilometer) GTOPO30, which is not fine enough resolution for automated delineation of basins at the scale that most [10]Be sediment samples represent. The SRTM data set greatly expands the range of basin sizes that can be delineated and analyzed. However, even the SRTM data are not fine enough to allow for the delineation of the smallest basins that have been sampled for sediment. I set a minimum basin size cutoff at approximately 0.5 km$^2$ for basins that I included in the global compilation.

DEM data are available for all of the contiguous U.S. at a 1 arc second (approximately 30 meter) or finer resolution through the seamless National Elevation Database (NED). I did the basin delineations for the U.S. based on 30 m NED. For Alaska, no SRTM data are available, but the NED data are available at a 90 m resolution, so I used NED in lieu of SRTM for Alaska.

The NED and SRTM files from the USGS seamless data server

(http://seamless.usgs.gov; accessed March 2005) unzip directly to ESRI grid format.

However, the seamless data server had SRTM only for North and South America as of

June 2004.

For other regions, files are available for download in one degree blocks from the

NASA SRTM FTP site (ftp://e0mss21u.ecs.nasa.gov/srtm/; accessed March 2005). After

unzipping the files, they can be converted to an ESRI grid format by running

srtmgrid.aml, which is also available on the FTP site. Here are a few notes on how to do

this:

In ArcInfo Workstation, set the workspace:

Arc: workspace c:\data\

Run srtmgrid.aml (from either Arc or Grid):

Arc: &run srtmgrid.aml n45e001.hgt n45e001

If necessary, mosaic the grids together to obtain complete coverage of the region of

interest. Then, project to an appropriate coordinate system using bilinear interpolation.

Finally, fill data gaps, as addressed in the next section.

*Filling gaps in SRTM data*

SRTM grids commonly contain cells or clusters of cells with no data, both in

areas of very rugged topography as well as in flat areas, particularly in association with

bodies of water. These gaps must be filled with data values in order to perform

hydrologic operations and to delineate watersheds. Driven by this practical necessity, I

took two approaches to filling the gaps, depending on the size of the gaps.

In the Himalayas, the data gaps are substantial, in cases exceeding 10 km across. These cannot be estimated reasonably based on nearby data. I used the next-highest resolution data available--the GTOPO30 data--to fill in the gaps. This solution was adequate for determining stream networks and drainage boundaries, particularly since most of the missing data are internal to the sampled basins, not along basin boundaries. The following conditional statement, applied in Grid of ArcInfo Workstation, fills the SRTM gaps with GTOPO data:

```
filledgrid = CON(ISNULL(ORIGSRTM), GTOPO, ORIGSRTM)
```

In regions where the data gaps were not as substantial, I filled in values based on the surrounding cells. I iteratively applied the following ArcInfo Grid command until the no data cells had been filled:

```
outgrid = con(isnull(INGRID), focalmean(INGRID, rectangle,5,5), INGRID)
```

Neither approach is adequate to construct realistic topography at a level to match the good sections of SRTM data. As a result, I used the original data sets--not the filled ones--in the calculation of slope, aspect, and curvature; these derived grids would be sensitive to artifacts introduced during the gap-filling process. (In conjunction with this, I also calculated the extent of missing data values; see the section on "Keeping track of SRTM gaps.") I did, however, use the filled data sets for the delineation of drainage basin boundaries, for the calculation of relief, and for the calculation of production rate.

*Keeping track of SRTM gaps*

In order to quantify the amount of missing SRTM data, I reclassified the grids so that NoData values were 0 and data values were 1. Summarizing Zones of this grid within the basins allows for the determination of the percent of missing data.

Slope, aspect, and curvature (total, plan, and profile) can all be derived through a single command in Grid of ArcInfo Workstation. Here is an example:

```
ll_curv = CURVATURE(ll_ned,ll_profc,ll_planc,ll_slope,ll_aspct)
```

"ll_ned" is the input grid, and the others are the derived grids. I typically combined this command with the commands for hydro operations into a quick and simple AML. (Although these lines can be entered singly at the grid prompt, for large grids, it is convenient to put them together in an aml so that they can be left to run unattended.)

*Hydro operations*

Performing hydrologic operations on a DEM makes possible the automated delineation of drainage basins. The necessary steps include filling sinks, calculating flow direction, and calculating flow accumulation. I used ArcInfo Workstation to perform the hydro operations, as it was easily streamlined as part of an AML, in which I also included the CURVATURE command (see "Standard derived grids"). Thus, these sometimes time consuming calculations would be completed without my constant attention. Here are the Workstation commands, to be run at the Grid prompt:

```
FILL ll_ned_c ll_fill sink # ll_dir
ll_acc = FLOWACCUMULATION(ll_dir,#)
```

Other alternatives exist, including extensions that calculate the derived grids at the click of a mouse button. I also tinkered with TauDEM, which uses a more sophisticated method of determining flow paths on hill slopes, but I determined that it would not sufficiently enhance the work that I am doing to merit the extra effort involved in using it.

*Relief*

A common method of calculating drainage-basin relief is to first calculate the

relief of coarse grid cells (usually on the order of kilometers on a side), then to average

the values of the grid cells within the basin of interest. For example, Ahnert (1970)

subtracted the minimum from the maximum elevation in grid cells that were 20 km by 20

km. Vance et al. (2003) subtracted the minimum elevation from the mean elevation in

grid cells that were 9 km by 9 km.

The AGGREGATE command can be used to convert the SRTM into a grid with a

coarse cell size. I saved the following commands as an AML, which I ran at the grid

prompt in ArcInfo Workstation:

```
sq5km_mean = aggregate(sq_srtm_b , 56, mean, truncate, data)
sq5km_min = aggregate(sq_srtm_b , 56, min, truncate, data)
sq5km_max = aggregate(sq_srtm_b , 56, max, truncate, data)
sq5m_max-min = sq5km_max – sq5km_min
sq5m_mean-min = sq5km_mean – sq5km_min
sq20km_mean = aggregate(sq_srtm_b , 222, mean, truncate, data)
sq20km_min = aggregate(sq_srtm_b , 222, min, truncate, data)
sq20km_max = aggregate(sq_srtm_b , 222, max, truncate, data)
sq20_max-min = sq20km_max – sq20km_min
sq20_mean-min = sq20km_mean – sq20km_min
```

This particular example uses the grid names for the Susquehanna; I used Find and

Replace in a text editor to alter the grid names for each regions.

These commands calculate relief on two scales. The first uses a 5 km grid cell

size, and the second uses a 20 km grid cell size. I calculated both maximum minus

minimum and mean minus minimum for each scale.

Because of the coarse grid cell size, these relief measures are most appropriate for

large basins. However, I still wanted to summarize the data for all basins, regardless of

size. This required resampling the relief grids at a higher resolution. (I used RESAMPLE

in ArcView, and I built it into a modified version of the Summarize Zones Avenue script

that appears later in this document.)

*Hypsometry*

To calculate hypsometry, I converted the DEM to an integer grid, which can be

accomplished by applying the Int request in the Map Calculator of ArcView 3.x.

Tabulate Areas can then be used to determine the amount of area at each 1 meter

increment of elevation. The resulting dbf file can be opened in Excel, where the data can

be manipulated to produce the desired hypsometric plots or to calculate hypsometric

integrals.

*Summarizing aspect*

Although aspect is a continuous value grid, simply taking the average of the

aspect does not produce a useful value. I reclassified the grid into eight dominant

compass directions, so that I could treat aspect as a discrete value grid rather than a

continuous value grid. The classes that I used are as follows:

TABLE 2. RECLASSIFICATION VALUES FOR ASPECT

| Orientation | Old values (compass directions) | New value |
|---|---|---|
| N | -5 - 22.5 | 1 |
| NE | 22.5 - 67.5 | 2 |
| E | 67.5 - 112.5 | 3 |
| SE | 112.5 - 157.5 | 4 |
| S | 157.5 - 202.5 | 5 |
| SW | 202.5 - 247.5 | 6 |
| W | 247.5 - 292.5 | 7 |
| NW | 292.5 - 337.5 | 8 |
| N | 337.5 - 360 | 1 |

When summarizing the aspect data, I used both Tabulate Areas and Summarize

Zones. Tabulate Areas is the usual method of summarizing data for a discrete value grid,

but Summarize Zones also reports which value is the Majority (because this is an integer grid). (One could also skip Summarize Zones and determine the majority direction in Excel based on the results from Tabulate Areas.)

Using the summarized data, I considered how dominant the majority direction is by calculating ratios of the pixels in the majority direction to pixels in the total basin. Big basins, of course have, more uniform aspect distributions, while small basins tend to have a dominant aspect direction. Ultimately, aspect showed little promise of explaining the scatter in the data for the Susquehanna River Basin, and I did not calculate summary statistics for aspect for all of the international basins.

*Stream networks*

This section addresses creating a vector stream network from the flow accumulation grid. Determining channel networks in a geomorphically meaningful way based on digital elevation data can be an involved task. For simplicity, I used a simple basin-area threshold to generate channel networks. The resulting channel networks are not particularly useful for comparing stream length between regions. However, stream networks generated in this simple manner are useful for display and presentation of data, and they can be utilized for generating longitudinal profiles.

The first step in creating a vector network is to select a threshold value to determine which cells of the flow accumulation grid will be considered to be part of the stream network. I desired a channel network that would extend into the smallest sample basins (that were large enough to analyze), so I used a flow accumulation threshold of 0.1 km$^2$.

The next step is to query the flow accumulation grid to identify cells with values greater than or equal to the desired flow accumulation threshold. Because the flow accumulation grid is, by default, measured in cells, the threshold area should be converted to number of cells in order to perform the query.

In ArcView, the output queried grid contains values of 1 which correspond to streams (according to the query) and values of 0 which are off of the stream network. This should be reclassified so that the values off of the stream network have a NoData value.

Sometimes it is useful to classify the streams by order. The ArcInfo Workstation Grid command for this is as follows:

sorder = streamorder(netgrid, dirgrid, strahler)

Here, the netgrid is the grid with values on the network and NoData off of the network.

To convert the grid to a vector network, use STREAMSHAPE in Grid as follows:

strm_net.shp = STREAMSHAPE(netgrid, dirgrid, noweed)

The arbitrary threshold method of network delineation makes summarized characteristics (such as stream length or density) less meaningful. In the interest of completeness, however, here is a brief outline of how to summarize stream length for each basin. First, in ArcView, clip the stream shapefile with the basin boundaries. Then, take the clipped file and intersect it with the basin boundaries. Open the attribute table of the stream network that has been clipped and intersected. Highlight the column heading of the column that contains the unique basin IDs (probably called Gridcode). Summarize this column based on the length Field, and summarize by Sum (and other values, if desired). The resulting output table will have the total stream length in each basin.

140

It is also possible to summarize the stream length by stream order within each basin; this would give the length of first order streams, the length of second order streams, and so forth for each basin. I did this with a custom Perl script for a few regions. There are two reasons why this really was not worth doing everywhere. First, the stream networks that I delineated were based on arbitrary basin area thresholds. Second, for the regions in which I did consider stream order, the length of first order streams was very strongly correlated with total stream length.

One particularly big advance in ArcGIS is the ability to create network connectivity in a geodatabase. I used geodatabases for the task of generating maps of stream networks for only sample basins. This can be done by flagging a stream in the headwaters of each sample basin and using the trace downstream function. The selected segments can be used to create a new shapefile for display of the streams from their origins in each sample basin to the mouth.

## Long profiles and channel gradients

I did not find any pre-made tools that did the full range of things that I wanted to do with longitudinal profiles and channel gradients, so I wrote my own. They are not pretty, nor are they well documented, so I am going to include only an outline. I would suggest that anyone who wants to deal with long profiles in a more meaningful and substantial way should get in touch with Kelin Whipple.

Here is an outline of my approach:

--I started with a stream network created using StreamShape in either Arc/INFO or ArcGIS.

141

--I took the attribute table for the StreamShape shapefile and ran it through a Perl script to group streams together according to connectivity.

--I converted StreamShape shapefile to spaced points--point spacing should be less than the size of a grid cell (so there is at least one point on every stream segment generated by StreamShape).

--I obtained the elevations for each of the points from the DEM.

--I used an Avenue script in ArcView 3.x to determine location of each point along each stream segment; I also used a spatial join to copy some key information from the stream segment.

--I ran another Perl script which reorders the points to correspond to the groups from the StreamShape script. This also calculates distance to the mouth.

--I ran a final Perl script which calculates the slope.

--I brought the data back into ArcView and Excel to view in various ways.

### *Using GIS to develop a sampling strategy*

For the Susquehanna River system, I sought to investigate the characteristics of a wide variety of drainage basins to assist with the development of a sampling strategy. My approach to delineating numerous candidate basins was to query the flow accumulation grid for a series of desired basin size ranges; the query identifies positions on the flow accumulation grid that correspond to the desired basin size, and these positions are used as basin outlets for watershed delineation. I summarized basin characteristics (slope, lithology, physiography, land use, etc.) for all of the candidate basins. Based on

142

exploration of the characteristics of available basins, I selected a series of candidate

sample sites that represented gradients in the variables I wanted to consider.

There are several considerations to take into account when deciding what range of

basin sizes to use for querying the flow accumulation. Because basin area increases in a

stepwise fashion as tributaries enter the mainstem, querying the flow accumulation for a

single basin area is inefficient. For example, a query for all basins that are 10 km$^2$ will

miss a case in which a stream draining 9 km$^2$ joins a tributary that drains 2 km$^2$ to become

an 11 km$^2$ basin. Thus, I found it best to query for a range of sizes. If the size range is too

large, a problem develops related to nesting. Selecting a range such that the maximum

basin size is less than twice the minimum basin size will prevent nesting problems. I used

increments that corresponded to a quarter of a log scale; for example, in square

kilometers, 0.1 - 0.18, 0.18 - 0.31, 0.31 - 0.56, 0.56 - 1, etc. I iteratively delineated basins

for each of the size ranges.

Once a size range (or a series of them) has been chosen, the flow accumulation

can be queried to match that range. (It is important to remember to convert area from

square kilometers to number of cells for use in the query.) After querying, apply the

StreamLink function in ArcView's Map Calculator:

streamID = [MapQuery].StreamLink([FlowDirection])

Next, use the Watershed function in Map Calculator:

basingrid = [FlowDirection].Watershed([StreamID])

Convert the resulting grid into a shapefile; this contains the basin polygons.

If using multiple size ranges, these steps will need to be repeated for each size

range of interest. The resulting basin polygon shapefiles can be merged together so that

data need be summarized for only a single shapefile; ArcView has no trouble handling overlapping polygons in shapefile format. After merging the files, it is important to add a new unique ID field to keep track of the basins during further work. (A script called addautonumbers.ave, which is available from the ESRI ArcScripts page, will do this.)

After basins are delineated, the methods for summarizing data as outlined in the rest of this document and on the flow chart can be used. Analysis of the summarized characteristics will vary on a case-by-case basis.

### *Working with existing cosmogenic data*

The first step in working with existing cosmogenic data was to assign a unique numeric ID to each drainage basin. I called this the "CosID." (Given the way this numeric ID evolved, I later realized that "BasinID" would have been a more appropriate name, because the ID is unique to the drainage basin, not to the cosmogenic measurement.) Attaching the CosID to the data at the beginning was important because the location data and the cosmogenic data go off in different directions and need to be brought back together again eventually in a database.

In order to keep track of replicate cosmogenic samples for a single drainage basin, I also assigned a value in a "Replct" (replicate) field. If there is only one measurement for the site, this value is 0. If there is more than one measurement (for whatever reason), each measurement is numbered 1, 2, ...n.. In the case of replicates, I also created a record with the Replct = 99, and I used the available data to come up with the best, most usable, value for that sample. So, for example, if the replicates represent multiple grain sizes, I would select the sample with the sand sized fraction to be used in the record with Replct = 99

for that CosID. If there were quality control replicates for the same grain size fraction, I would simply average the $^{10}$Be values to generate the values for "Replct" = 99, unless there was a reason to discard one of the measurements (for example, if there was particularly high measurement uncertainty).

*Existing data: Determining sample locations*

After the CosID has been assigned for each basin, the next task was to pinpoint the sample site locations on the flow accumulation grid so that basins could be delineated automatically. Positioning sample locations was a manual and typically time-consuming step. The flow accumulation grid sometimes deviates from the actual stream network; sometimes this is due to poor quality DEM data, and sometimes it is due to actual changes in the channel network. In any case, even high quality GPS locations must be individually confirmed to ensure that they fall in the correct location with respect to tributaries on the flow accumulation grid.

On rare occasions, the flow accumulation grid deviates substantially enough from reality that it cannot be used for basin delineation "as is." This may happen, for example, in a wide floodplain where the flow accumulations that represent tributaries do not join the mainstem flow accumulation in a reasonable location. If the discrepancy is deemed to be problematic enough to warrant modification, there are a several options. One option is to force the flow accumulation into a different position by modifying the DEM. This may involve creating a new grid that has cells in the problem area which, when added to the original DEM, will force the flow accumulation to behave as desired. This, of course, requires calculating new flow direction and flow accumulation grids. Alternatively, and

145

probably easier in most cases, basin boundaries can be drawn from scratch or modified manually in shapefile form.

I used all available resources to pinpoint the location of each sample. For published data, these resources include coordinates, maps, basin areas, and elevations of sample sites. For unpublished data, field notes and original field maps also proved valuable. Sometimes, one or more of these sources of information were in conflict. If I felt highly uncertain about the location of a point given the information available to me, I did not use that point. If I felt moderately confident in the location, I used the point but recorded it as having uncertainty in its location, so that these points could be identified and specially assessed in the analysis phase. See Appendix B for a table of the problem sites and errors in published papers.

### *Existing data: Delineating basins*

The hard part is over once the positions of basin outlets have been determined. However, there is still some work to be done, largely to avoid problems with nested basins. The goal is to have a single shapefile with all of the basins as whole polygons.

My preferred approach for handling nested basins for existing samples was to add a field to the point shapefile for "NestLevel." In this field, I assigned a value of 0 for basins that are not nested, a value of 1 for basins that contain only un-nested basins, a value of 2 for basins that contain basins of NestLevel no greater than 1, etc. Then, when delineating basins, I worked only on a single nest level at a time.

Here is an outline of the steps that I performed for each NestLevel in ArcView:
--Select the points in the shapefile which have the NestLevel of current interest.

146

--Convert these points to a grid with cell size and extent equal to the flow direction or flow accumulation grid.

--Use the Watershed function in Map Calculator to create a grid of the basins:

 [FlowDirection].Watershed([SampleSites])

--Convert the grid to a polygon. Open and start editing the attribute table of the polygon shapefile. Add a new field called "Area." Use Shape.ReturnArea/1000000 in the field calculator to calculate area in square kilometers in this new field. Check to see if there are any polygon fragments by inspecting the Area field for very small values; delete these.

--Clean up any extraneous grids that will not be used again.

After doing this for each nest level, merge the polygons for each nest level together into a single shapefile with all of the basins for the region of interest. A little tip: To prepare for the merge, list the basin shapefiles in the table of contents with the smallest basins at the bottom and increasingly bigger ones on top; yes, this is counterintuitive. When merged, the biggest ones will be on the bottom, with successively smaller ones on top, which aids in displaying the basins.

### *Production rates*

Nuclide production rates must be calculated in order to estimate erosion rates. Table 2 of Lal (1991) has values for coefficients (that vary with latitude) for a third degree polynomial incorporating elevation.

$$s = a1 + a2*y + a3*y^2 + a4*y^3$$

y is elevation in kilometers, and s is nuclear disintegration rate in the atmosphere. Coefficients in the table are given for latitudes in 10 degree increments.

The overall approach that I took was to make grids of the coefficients (varying as a function of latitude and linearly interpolated between the values in Lal's table) so that they can be used with the DEM to calculate production rate on a pixel-by-pixel basis.

I first made a series of point shapefiles, one for each coefficient. These are in geographic coordinates with points spaced 0.5 degrees apart, and I used linear interpolation to determine the coefficient values between the 10º latitude intervals that Lal provides. The point files can easily be converted to grids in regions of interest as follows:

I opened the point themes, selected the points in the region of interest, and converted to a new shapefile (in the coordinate system that I used for the region of interest).

More detail:

--The easiest way to do this is to start with an ArcMap data frame that has data of the region of interest. The coordinate system should be set so it matches the regional data.

--Then add the a1, a2, a3, and a4 shp files.

--Click on the Select Features toolbar button, then highlight points in the a# layers that cover the entire region of interest. (ArcMap seems to select features from all layers at once by default...this is fine.)

--One by one, go through the a# shp files, and do the following: right click>Data>Export

--Data. Export: Selected features (the default). Select Use the same Coordinate System as the data frame. Change the directory and give a name in the style of:

d:\smokies\utm1783\prod_rate\a1crop.shp

I then converted the point themes to TINs (using the coefficient value as the height source), and converted the resulting tins to grids. (Using a TIN essentially allows for a simple linear interpolation between points; I ended up with some ugly artifacts from the interpolation methods that were available when I attempted to go straight from points to a grid.) For the final coefficient grids, I ended up using a 3 km cell size. In general, this is probably finer than it needs to be, but the file size of the grid is trivial relative to the elevation grid.

Here's some additional detail:

--I did the TIN conversion in ArcView 3.x. So, add a1crop.shp et al. to a new view.

--It's a good idea to set the working directory.

--Turn on the 3d analyst extension.

--Then, Surface>Create TIN from Features. Change Height source to Value. OK. Put it in the same directory as before, with names such as a1tin etc. Repeat for the others.

--Then for each TIN, Theme>Convert to Grid... Select appropriate cell size & file name.

Once the grids are made, it's just a matter of using Map Calculator/Raster Calculator to compute the production rate.

Elevation should be in KILOMETERS, so convert it (or appropriately modify the input expression for the raster calculator below).

Also make sure the output cell size will match that of the elevation input grid and not the coefficient input grids.

ELD = (a1grd + (a2grd * ned) + (a3grd * ned^2) + (a4grd * ned^3))/563.4

For copying and pasting purposes, here is exactly what the expression should look like in ArcView's Map Calculator if the elevation in kilometers is [Map Calculation 1]:

149

ELD = ( [A1grid] + ([A2grid] * [Map Calculation 1]) + ([A3grid] * [Map Calculation 1]

* [Map Calculation 1]) +([A4grid] * [Map Calculation 1] * [Map Calculation 1] * [Map

Calculation 1]) )/563.4

ELD (which stands for Elevation, Latitude, and Depth) is the ratio of nuclide production

for each pixel relative to production at sea level and high latitude. ELD is 1 at sea level

high latitude.

production rate (atoms gram$^{-1}$ year$^{-1}$) = ELD * 5.2

Because the conversion of the production rate coefficients into several different

forms (shapefiles, tins, grids) opens up opportunity for mistakes, it is a good idea to

identify the ELD for a few pixels and check that the values match the ones calculated in a

traditional way (coded into an Excel spreadsheet, for example).

To get the elevation-weighted ELD (or production rate), Summarize Zones (in

ArcView), using the basins as zones. The mean value should be essentially the same as

the value calculated from hypsometry.

The next step is to account for different lithologies. If one assumes that the basin

is eroding uniformly, then one can weight pixels based on estimated quartz content to

calculate the ELD/production rate.

***Summarizing data***

<u>*Continuous value grids*</u>

In ArcView, Summarize Zones (Analysis menu) calculates summary statistics

(minimum, maximum, mean, etc.) for the values of a grid within each polygon (basin) of

an input shapefile. (The equivalent in ArcGIS/ArcInfo is ZonalStats.)

In order to expedite the processing of multiple data sets (for the international basins), I modified the system script called Spatial.SummarizeZones so that I could summarize the zones for data from each view in a project with just a few clicks of the mouse button. (See content of the script below in "Summarize zones for multiple regions and export as text Avenue script.") The modified script also exports a text version of each file, as the text files are easier to manipulate; see "Combining tables" for more information about that.

*Discrete value grids*

Grids that are composed of discrete values, including lithology and land cover grids such as NLCD, can be summarized using Tabulate Areas in ArcView. Select options to create an output table with one row for each basin and one column for each class of the discrete value grid.

**Combining tables**

After Summarizing Zones and Tabulating Areas, I had one text file for each region for each data type. The files were grouped according to data type, such that the files from all regions for a given data type were in a single directory.

For tables produced by Summarize Zones, the column headings generated by ArcView are identical from file to file, for all practical purposes. (Tables produced by Summarize Zones for integer grids have some data that the equivalent tables from non-integer grids do not contain; however, as these are at the end of the table, and none were of interest to me, it did not matter if they came along for the ride from some regional tables but not from others. Depending on processing methods, some SRTM grids were

integer, although others were not.) Thus, I wrote a simple Perl script that would read all of the files from a directory and print out the data into a new file. (See "Combine_Tables.pl" in the section "Scripts and code for the automation of tasks.") I also designed the script to add a prefix to the header of each column, so that the data type would be readily identifiable in further processing.

Here are a few details about using the script: In summarizing the international data, I put all of the data tables from all regions for a given data type (say, SRTM slope) into a single directory (using the script in the section below--"Summarize zones for multiple regions and export as text Avenue script"). The script puts both dbf files and the txt files into a single directory. I deleted everything except the text files from the ArcView project, then from the directory. Next I ran the script combine_tables.pl. The result is a single text file that contains all of the data for the given data type.

Tables produced by Tabulate Areas are not as simple to combine as for Summarize Zones, because the columns do not always line up from regional table to regional table. This is because columns are only present for data that exist in the grid that was summarized. Because I dealt with only a few types of discrete value data, I manually compiled the tables from each region to produce a single table for the data type of interest. I did this by opening the tables in Excel, copying them all to a single worksheet, and manually aligning the columns. Alternatively, for about the same amount of work, the tables could be imported one by one into a dbf in Approach. I utilized this feature on occasion when bringing in a "straggler" data set, but on a large scale it is somewhat tedious and prone to error.

152

*Approach to data compilation*

Summarizing data in ArcView produces many different files, and, by default, they are generally not labeled very well in terms of either the file names or the column headings. The task of compiling these can be daunting. I used methods described in "Combining tables" in conjunction with Lotus Approach (a database program) as a way to bring data together from a variety of sources.

The use of a database allows multiple files to be joined together. The "CosID" (a unique ID for each basin) is the value that I used to join the tables. I created a master file which contains, for each sample sediment sample, the CosID, original sample name, nuclide data, grain size data, and other pertinent information. I could then bring in additional data tables and join them to the master data files.

Approach does its work with dbf files. Simply opening a text file in Approach will generate a dbf from the table.

Once a dbf exists with data for the region(s) of interest, the table can be joined to the master dbf. Joins are saved as a part of an Approach apr file (not to be confused with an ArcView apr file). At this point, the data can be exported from Approach.

*Excel work*

After the export from Approach, I worked with the data in Excel. The dbf file behaved strangely when opened directly in Excel. (There seems to be coding regarding how the dbf deals with scientific notation or decimal locations that Excel does not interpret properly.) As a workaround, I opened the dbf in Excel, saved it as a txt file, then opened the txt file again in Excel and saved it as an xls file.

The first step in Excel is to calculate the $^{10}$Be erosion rate using the following formula:

=(165/2.7)*((5.2/($G2*10^6/$AD2))-(4.62*10^-7))/100*10^6

$G2 contains $^{10}$Be in $10^6$ atoms/gram. $AD2 contains the mean ELD for the basin.

I also used Excel to filter out samples with less desirable characteristics (such as basins that were glaciated or samples for which more than just the sand fraction was analyzed).

## Data checking and quality control

For quality control, I looked at relationships between published erosion rates and the rates that I had calculated. This raised several red flags that led me to track down mistakes. I also checked published values for basin areas against the basin areas that I calculated, as well as published elevation against the elevation I determined.

I also printed a full database of the cosmogenic data and I did data quality checking against the original published data or against original data tables (for unpublished studies).

## Making Excel plot data efficiently

At this point, I faced the option of going to yet another program--some sort of graphing program, or sticking with Excel and forcing it to do what I wanted. (Eliminating Excel completely from the chain is not feasible given the calculations that need to be done.) I decided to force Excel to cooperate. See the Excel spreadsheet with the global data compilation on the data CD (Appendix B) for the outcome. This section contains some tips and tricks that I learned along the way.

Excel Help is not very helpful. It is much easier to find general answers about Excel through Google than through the built in Help (though I found that I used a combination of both). There are a number of Excel consulting businesses out there that have free online discussion forums. Some of them also have example worksheets which showcase various interesting features and tricks.

I wanted to be able to create scatter plots with a wide assortment of fields, and I wanted each regional data set to be a single series with the same color scheme on each plot. I did not want to manually select the ranges for each series each time. I stumbled across some websites that spoke of dynamic ranges--essentially, ranges that updated based on changes or additions to cells.

The systems that I eventually came up with allows me to look at a list of column headings and enter the number of the column heading that I want on each axis. Then, a chart instantly updates with the data from the desired columns.

The first step is to build expressions for dynamic references to blocks of cells. In this example, the data are in a worksheet named "export." The first column of the worksheet "export" contains names that indicate which data go together as series--so these are region names (for example, Rio Puerco, Oregon Coast Range, Susquehanna). These must be sorted such that all like names are in a single block. There is a second worksheet (which I have named and will refer to as "forplot") that contains the formulas that dynamically reference the cells of interest. Here is an example of an expression that creates a cell reference in text format:

=$C$3&"!"&ADDRESS(MATCH($B8,OFFSET(export!$A$2,0,0,COUNTA(export!$A$2:$A$10000),1),0)+1,$C$1)&":"&ADDRESS(MATCH($B8,OFFSET(export!$A$2,0,0

,COUNTA(export!$A$2:$A$10000),1),0)+COUNTIF(OFFSET(export!$A$2,0,0,COUN

TA(export!$A$2:$A$10000),1),$B8),$C$1)

The contents of the cells that this refers to are as follows:

$C$3: gives the name of the worksheet where the data are located

$B8: gives the name of the series of interest (Rio Puerco, for example)

export$A$2:$A$10000: the range of cells in which to look for the value in $B8

$C$1: a cell that contains the number of the column which should be plotted on the x axis

And the results of the formula are as follows:

export!$EK$2:$EK$38

These results are text. In order for Excel to recognize that they are a cell

reference, the INDIRECT function must be applied. In order to do this, go to Insert >

Name > Define...

Enter a name, including a worksheet name (even though Excel does not indicate that a

worksheet name might be a good idea). So, for example, enter forplot!RP_x in the

"Names in workbook..." box, and in the "Refers to:" box, enter

=INDIRECT(forplot!$C$8), where $C$8 is the cell that contains the cell reference as

text. Entering all of these is a rather annoying step, but once done, the workbook can be

used as a template and the data in the "export" worksheet can be reused.

A dynamic range should be set up for each x column and each y column that will

work together as a series.

Once the names are defined, they can be utilized to make plots. The best way to

do this is to create a scatter plot with a blank series. Click on the point that shows up at x

= 1, y = 1. The formula bar at the top of the screen will have something that looks like:

=SERIES(,,{1},1). Edit the values so that it looks something like this:

=SERIES("HM",forplot!HM_x,forplot!HM_y,23). The data points should appear on the

plot.

### *Scripts and code for the automation of tasks*

#### *Automation of projections for global compilation: clipprj.aml*

For global coverages that needed to be summarized for all international basins, I

used the AML that follows to clip to the region of interest and to project to UTM. This

requires that projection files be present in the same directory; an example of a projection

file follows the aml. (The projection files need be created only once.)

I coded Excel to build the commands based on a few cells in which I insert the

input file name, the type of resampling, and the output cell size. (This involves extensive

use of Excel's concatenate function.) Excel automatically updates all of the commands,

which I copy and paste as text into a file that I save with an aml extension.

So, why did I do all this clipping and resampling? I resampled grids at a finer

resolution than the original data. The need to do this was driven by ArcView's inability to

Summarize Zones when the grid cell sizes are very large relative to the basin sizes.

Resampling at a finer cell size results in larger file sizes, which is why it was necessary to

clip each grid.

```
GRIDCLIP seishazgrid2 ll_AK06_xx BOX -150.4 67.9 -146 70.4
GRIDCLIP seishazgrid2 ll_OC10_xx BOX -124.4 43.2 -123.5 44.8
GRIDCLIP seishazgrid2 ll_SR10_xx BOX -121.6 39.4 -119.8 40.4
GRIDCLIP seishazgrid2 ll_CA10_xx BOX -122.8 37.6 -122.3 38.1
GRIDCLIP seishazgrid2 ll_ID11_xx BOX -116.8 43.5 -112.6 47
GRIDCLIP seishazgrid2 ll_YU11_xx BOX -114.8 32.8 -114.2 33.5
GRIDCLIP seishazgrid2 ll_RP13_xx BOX -108.7 34.1 -106.5 36.5
```

```
GRIDCLIP seishazgrid2 ll_LL14_xx BOX -99.3 30.1 -98.4 30.9
GRIDCLIP seishazgrid2 ll_SM17_xx BOX -84.2 35.2 -82.8 36
GRIDCLIP seishazgrid2 ll_SQ18_xx BOX -79.3 39.4 -74.3 43.2
GRIDCLIP seishazgrid2 ll_PR20_xx BOX -66.2 17.8 -65.5 18.5
GRIDCLIP seishazgrid2 ll_PN17_xx BOX -79.8 9 -79 9.7
GRIDCLIP seishazgrid2 ll_VZ19_xx BOX -72.7 6.7 -66 10.7
GRIDCLIP seishazgrid2 ll_EU31_xx BOX 0.5 44.3 7 51.8
GRIDCLIP seishazgrid2 ll_EU32_xx BOX 7.7 47.6 10.6 49.9
GRIDCLIP seishazgrid2 ll_EU33_xx BOX 11.8 48.6 13.7 49.7
GRIDCLIP seishazgrid2 ll_NM33_xx BOX 13.4 -23.7 17.6 -19.4
GRIDCLIP seishazgrid2 ll_HM44_xx BOX 77.9 29.5 80.5 31.7
GRIDCLIP seishazgrid2 ll_BH45_xx BOX 89.1 26.8 90.7 28.5
GRIDCLIP seishazgrid2 ll_SL44_xx BOX 80.2 6.5 81.3 7.7
GRIDCLIP seishazgrid2 ll_NY36_xx BOX 34.7 29.3 35.2 29.8


z06NAK_seis = PROJECT(ll_AK06_xx, z06N_NAD27.prj, BILINEAR, 500, #)
z10NOC_seis = PROJECT(ll_OC10_xx, z10N_NAD83.prj, BILINEAR, 500, #)
z10NSR_seis = PROJECT(ll_SR10_xx, z10N_NAD83.prj, BILINEAR, 500, #)
z10NCA_seis = PROJECT(ll_CA10_xx, z10N_NAD83.prj, BILINEAR, 500, #)
z11NID_seis = PROJECT(ll_ID11_xx, z11N_NAD83.prj, BILINEAR, 500, #)
z11NYU_seis = PROJECT(ll_YU11_xx, z11N_NAD83.prj, BILINEAR, 500, #)
z13NRP_seis = PROJECT(ll_RP13_xx, z13N_NAD83.prj, BILINEAR, 500, #)
z14NLL_seis = PROJECT(ll_LL14_xx, z14N_NAD83.prj, BILINEAR, 500, #)
z17NSM_seis = PROJECT(ll_SM17_xx, z17N_NAD83.prj, BILINEAR, 500, #)
z18NSQ_seis = PROJECT(ll_SQ18_xx, z18N_NAD83.prj, BILINEAR, 500, #)
z20NPR_seis = PROJECT(ll_PR20_xx, z20N_NAD83.prj, BILINEAR, 500, #)
z17NPN_seis = PROJECT(ll_PN17_xx, z17N_WGS84.prj, BILINEAR, 500, #)
z19NVZ_seis = PROJECT(ll_VZ19_xx, z19N_WGS84.prj, BILINEAR, 500, #)
z31NEU_seis = PROJECT(ll_EU31_xx, z31N_WGS84.prj, BILINEAR, 500, #)
z32NEU_seis = PROJECT(ll_EU32_xx, z32N_WGS84.prj, BILINEAR, 500, #)
z33NEU_seis = PROJECT(ll_EU33_xx, z33N_WGS84.prj, BILINEAR, 500, #)
z33SNM_seis = PROJECT(ll_NM33_xx, z33S_WGS84.prj, BILINEAR, 500, #)
z44NHM_seis = PROJECT(ll_HM44_xx, z44N_WGS84.prj, BILINEAR, 500, #)
z45NBH_seis = PROJECT(ll_BH45_xx, z45N_WGS84.prj, BILINEAR, 500, #)
z44NSL_seis = PROJECT(ll_SL44_xx, z44N_WGS84.prj, BILINEAR, 500, #)
z36NNY_seis = PROJECT(ll_NY36_xx, z36N_WGS84.prj, BILINEAR, 500, #)
```

Contents of an example projection file (named z10n_NAD83.prj):

```
INPUT
Projection Geographic
Units DD
Datum WGS84
Parameters
OUTPUT
Projection UTM
Zone 10
Datum NAR_C
Units METERS
Parameters
END
```

***Summarize zones for multiple regions and export as text Avenue script***

An Avenue (ArcView) script is included on the data CD (Appendix B) that streamlines the process of summarizing data for multiple regions. If an ArcView project has multiple views, all containing polygon themes as well as themes to be summarized, this script can be used to summarize the data for multiple data sets simultaneously. To do so, in each view, make the polygon theme active for which data are to be summarized. Then, go to the project window and highlight the views with data to be summarized. Run the script.

***Combine_Tables.pl***

A script is included on the data CD (Appendix B) that automates the process of combining data tables (in particular, those generated by summarizing zones) from multiple regions into one master table.

Perl is a programming language that I have found to be really useful for manipulating data in text format. Plus, it is free. To download Perl, go to http://www.perl.com (accessed April 2005). Perl scripts are just text files with a ".pl" extension, and they can be run from the command prompt by navigating to the directory that contains the script and then typing:

perl combine_tables.pl

A data CD accompanies this thesis. See the "readme.txt" file on the CD for more information. Contents of the CD include:

- field sample sheets from the Susquehanna River Basin;

- photos of sample sites in the Susquehanna River Basin;

- a data table for the Susquehanna River Basin (as an Excel file and as delimited text);

- a data table for the global data compilation (as an Excel file and as delimited text);

- a list of sites identified as problematic in the global data compilation and a list of errors from papers;

- GIS shapefiles (point sample location and polygon drainage basins) for the Susquehanna River Basin and the global data compilation;

- a digital version of the flow chart of GIS and data processing methods (fig. 1 of Appendix A);

- the scripts mentioned in Appendix A;

- GIS shapefiles that I developed for utilization in production rate calculations.